Diplomarbeit

The cannabinoid receptor agonist WIN-55,212-2 inhibits proliferation, angiogenesis and invasiveness, and induces apoptosis in small intestine neuroendocrine cancer

zur Erlangung des akademischen Grades

Doktor der gesamten Heilkunde

(Dr. med. univ.)

eingereicht an der

Medizinischen Universität Graz

von Ruben Errampalli

ausgeführt am

Institut für Pathophysiologie und Immunologie

unter der Anleitung von

Univ.-Ass. Mag. Dr. rer. nat. Nassim Ghaffari Tabrizi-Wizsy

Graz, am 24.05.2016

EIDESSTATTLICHE ERKLÄRUNG

Ich erkläre ehrenwörtlich, dass ich die vorliegende Arbeit selbstständig und ohne fremde Hilfe verfasst habe, andere als die angegebenen Quellen nicht verwendet habe und die den benutzten Quellen wörtlich oder inhaltlich entnommenen Stellen als solche kenntlich gemacht habe.

Graz, am 24.05.2016 Ruben Errampalli eh.

Acknowledgements

First of all, I would like to thank my supervisor Dr. Nassim Ghaffari Tabrizi-Wizsy for giving me the opportunity to write my diploma thesis. Thank you for all the advice, guidance and also for your patience waiting for this thesis. You always pushed me further, and were very understanding and supportive during my work.

I would like to thank Roswita Pfragner and Gert Schwach for letting me work with their cell line and their advice regarding cell culture.

Carmen, thank you for all the help, and for organising the jogging and all the outings, it was a pleasure working with you.

Thanks to Nathalie, Anika, Waltraud, Karin and Robert for their technical support and advice.

I would like to thank Corinna, Christina, Florian and Izabela for sharing the office with me and enduring the spreading chaos originating from my desk.

Very special thanks to my lectors Emily, Nassim, Michele and my mum for correcting this thesis over and over again.

Also I would like to thank Emily for her support, patience and understanding during my work at the institute and while writing my thesis.

Last but not least, I would like to thank all the members and friends at the institute of pathophysiology for providing such a positive and familiar work environment, for all the nice times during and after work and for all the support I received from the people already mentioned and everyone at the institute.

Table of Contents

List of Figures

List of Tables

List of Equations

Abbreviations

2-AG 2-arachidonoylglycerol
4EBP1 ..... 4E binding protein 1
5-FU 5-fluorouracil
AC ..... adenylyl cyclase
AEA ..... arachidonoylethanolamine (anandamide)
AKT ..... protein kinase B
Alk ..... anaplastic lymphoma kinase
ARE ..... antioxidant responsive element
ATF3 ..... activating transcription factor 3
BAN 4-bromoanisole
Bax ..... BCL2-associated X protein
Bcl-2 ..... B cell lymphoma 2
Bcl-xl ..... B-cell lymphoma extra large
bFGF ..... basic fibroblast growth factor
bHLH ..... basic helix-loop-helix
BMP ..... bone morphogenic protein
Br-dUTP ..... bromolated deoxyuridine triphosphate nucleotides
cAMP ..... cyclic adenosine monophosphate
CB ..... cannabinoid receptor
CDK ..... cyclin-dependent kinase
cDNA ..... complementary deoxyribonucleic acid
CMF-/PBS ..... calcium-magnesium free -/phosphate-buffered saline
COX-2 ..... cyclooxygenase-2
Cq ..... quantification cycle
Ctrl ..... control
CXCL12 ..... CXC-Motiv-Chemokin 12
DAPI ..... 4′,6-Diamidin-2-phenylindol
ddH_2O ..... bidistilled water
DMSO ..... dimethyl sulfoxide
DNA ..... deoxyribonucleic acid
DNES ..... diffuse neuroendocrine system
E-box ..... enhancer box
EC ..... succinate-tetrazolium-reductase
EGR-1 ..... epithelial growth factor
ER ..... oestrogen receptor
ERK ..... extracellular-signal regulated kinase
F12 ..... cell culture medium
FAAH ..... fatty acid amide hydrolase

FBS ..... fetal bovine serum
Fwd ..... forward
GEP ..... gastroenteropancreatic
GFP ..... green fluorescent protein
GPR55 ..... G protein-coupled receptor 55
GTPase ..... guanosine triphosphatase
HPRT-1 ..... hypoxanthine phosphoribosyltransferase 1
ICAM-1 ..... intracellular adhesion molecule 1
Id ..... inhibitor of differentiation
Id-1 ..... Id-1 overexpressing P-STS cells
JunD ..... transcription factor junD
Ki67 ..... proliferation marker
L30 ..... ribosomal protein L30 gene
LCA ..... lens culinaris agglutinin
M199 ..... cell culture medium
MAP ..... mitogen activated protein
MAPK ..... mitogen activated protein kinases
MEK1/2 ..... MAPK/ERK kinase
MEM ..... minimal essential medium
MEN 1/2 ..... multiple endocrine neoplasia
MMP-2 ..... matrix metalloproteinase-2
mRNA ..... messenger ribonucleic acid
mTOR ..... mechanistic target of rapamycin
NET ..... neuroendocrine tumour
NfκB ..... nuclear factor “kappa-light-chain-enhancer” of activated B-cells
NGF ..... nerve growth factor
Nrf2 ..... nuclear factor erythroid 2-related factor
P16INK4a ..... cyclin-dependent kinase inhibitor 2A
P21WAF1 ..... cyclin-dependent kinase inhibitor 1
P27Kip1 ..... cyclin-dependent kinase inhibitor 1B
Pac ..... puromycin N-acetyltransferase
PAI-1 ..... plasminogen activator inhibitor-1
PFA ..... paraformaldehyde
PGE2 ..... prostaglandin E2
PPAR ..... peroxisome proliferator-activated receptors
PR ..... progesterone receptor
Raf1 ..... rapidly accelerated fibrosarcoma
Rb ..... retinoblastoma protein
REF ..... reference gene
Rev ..... reverse

RhoA ..... RAS homolog gene family, member A
RNA ..... ribonucleic acid
ROI ..... region of interest
ROS ..... reactive oxygen species
Rpm ..... rotations per minute
RT-qPCR ..... real time quantitative polymerase chain reaction
SBE ..... Smad binding elements
SEER ..... Surveillance Epidemiology and End Results database
SiA ..... Id-1 silencing clone variant A
SiB ..... Id-1 silencing clone variant B
Smad ..... TGF-β signal transducer
STZ ..... streptozotocin
T-25 ..... 25 mm^2 growth surface
T-BST ..... Tween 20-tris-buffered saline
TdT ..... deoxynucleotidyl transferase
TGF-β ..... tumour growth factor β
TIMP-1 ..... matrix metalloproteinase-1
TNF-α ..... tumour necrosis factor
TNM ..... classification of malignant tumours
TrpV1 ..... transient receptor potential cation channel subfamily V member 1
VEGF ..... vascular endothelial growth factor
Vps34 ..... phosphatidylinositol 3-kinase
WST ..... water soluble tetrazolium
Δ^9-THC ..... Δ^9-Tetrahydrocannabinol

Cell lines

4T1 ..... metastatic breast cancer cell line
EFM-19 ..... breast cancer cell line
LNCaP ..... prostate cancer cell line
MCF-7 ..... breast cancer cell line
MCF7-AR1 ..... breast cancer cell line
MDA-MB-231 ..... breast cancer cell line
P19 ..... embryonal carcinoma
P-STS ..... primary tumour-small intestine neuroendocrine tumour cell line

Cannabinnoids

ACEA arachidonyl-2-chloroethylamide
ACPA ..... arachidonylcyclopropylamide
CBC ..... cannabichromene
CBCV ..... cannabichromevarin
CBD ..... cannabidiol

CBDV ..... cannabidivarin
CBG ..... cannabigerol
CBGM ..... cannabigerol monoethyl ether
CBGV ..... cannabigerovarin
CBL ..... cannabicyclol
CBV ..... cannabivarin
HU210 ..... synthetic CB1 & CB2 agonist
JWH-015 ..... synthetic CB1 & CB2 agonist (high CB1 affinity)
JWH-133 ..... synthetic CB2 agonist
LYR-7&8 ..... synthetic CB1 & CB2 agonist
THCV ..... tetrahydrocannabivarin
WIN-55,212-2 ..... synthetic CB1 & CB2 agonist

Zusammenfassung

Einleitung

Inhaltsstoffe der Cannabis-Pflanze, sogenannte Cannabinoide, zeigen antitumorigene Eigenschaften auf. Die Anti-Krebs-Wirkung vollzieht sich über verschiedene Mechanismen. Unter anderem wird in Brustkrebs die Wirkung der Cannabinoide durch Id-1, einen helix-loop-helix Transkriptionsfaktorinhibitor, reguliert. In einer früheren Arbeit, konnte unsere Gruppe zeigen, dass Id-1 in der gastroentero-pankreatischen neureoendokrinen Tumor Zelllinie P-STS exprimiert wird und somit ein potentielles Target für Cannabinoide darstellt.

Zielsetzung

Ziel dieser Arbeit ist es, die Wirkung von WIN-55,212-2, einem synthetischen, nicht selektiven CB1 und CB2 Agonisten auf die Zelllinie P-STS und eine mögliche Beteiligung von Id-1 an dem Signalweg, aufzuzeigen.

Material und Methoden

P-STS Zellen wurden mit WIN-55,212-2 behandelt. Die Effekte auf Zellproliferation und Viabilität wurden mit dem CASY® Cell Counter, WST-1 Assay und Ki67 labelling index untersucht. Die Apoptose wurde mit Caspase-Glo® 3/7 Assay und TUNEL Assay nachgewiesen. Die *in vivo* Wirkung von WIN-55,212-2 (Tumorwachstum und Angiogenese) wurde mittels CAM Assays untersucht.

Resultate und Schlussfolgerung

WIN-55,212-2 hemmte sowohl *in vitro* als auch *in vivo* die Zellproliferation, wobei Id-1 überexprimierende Zellen weniger stark reagierten. Auch führte die Behandlung zu einer “downregulation” von Id-1 und löste in P-STS Zellen Apoptose aus. *In vivo* wurden unter WIN-55,212-2 Einfluss weniger solide Tumore gebildet. Mit WIN-55,212-2 behandelte Tumore waren auch weniger invasiv. Angiogenese wurde bei unseren Experimenten durch WIN-55,212-2 *in vitro* induziert, aber *in vivo* gehemmt. Diese antitumorigene Eigenschaften sollten in anderen Zelllinien der neuroendokrinen Tumoren bestätigt werden.

Abstract

Introduction

Extracts from Cannabis, cannabinoids, have been shown to exhibit anticarcinogenic properties. Cannabinoids inhibit several hallmarks of cancer through various molecular mechanisms. In breast cancer, the anticarcinogenic properties are regulated by Id-1, a helix-loop-helix transcription factor inhibitor. According to a previous study of our group, Id-1 is highly expressed in the small intestine neuroendocrine cancer cell line P-STS.

Aims of this study

In this study, we investigated the effect of the synthetic unselective CB1 and CB2 receptor agonist on the small intestine neuroendocrine cancer cell line P-STS.

Materials and Methods

P-STS cells were treated with the unselective CB1 and CB2 agonist WIN-55,212-2. The effects on proliferation and viability were assessed with the CASY® Cell Counter, WST-1 Assays and Ki67 labelling index. Apoptosis was analysed through Caspase-Glo® 3/7 activation and TUNEL Assays. The *in vivo* effect on angiogenesis and invasion was observed *via* CAM Assays.

Results and Conclusion

Treatment with WIN-55,212-2 induced a concentration-dependent inhibition of cell proliferation. This effect could be shown in terms of cell growth, cell viability and Ki67 expression and occurred under *in vitro* as well as under *in vivo* conditions. Additionally, the susceptibility to WIN-55,212-2 was increased in Id-1 silencing and decreased in Id-1 overexpressing P-STS cells. This indicates that Id-1 plays a protective role against WIN-55,212-2 induced inhibition of cell proliferation. Furthermore, Id-1 was downregulated by treatment with WIN-55,212-2, showing that the effects of WIN-55,212-2 on P-STS cells might be mediated by Id-1. Regarding apoptosis, we found that WIN-55,212-2 induces apoptosis under *in vitro* conditions, but no effect occurred *in vivo.* WIN-55,212-2 also decreased solid tumour formation and invasiveness. Angiogenesis was enhanced *in vitro* and inhibited *in vivo*.

1 Introduction

1.1 Neuroendocrine tumours

The diffuse neuroendocrine system (DNES) is a heterogeneous group of more than 40 distinct endocrine cell types, spread as single cells or as cell clusters throughout the gastrointestinal tract, the bronchopulmonary system, and the urogenital tract (Figure 1).(1) Characteristics of neuroendocrine cells are(2):

- The production of neurotransmitters, neuromodulators or neuropeptide hormones
- The storage of these substances in membrane-bound granules or vesicles, which are released by regulated exocytosis upon external stimulus
- The absence of axons and specialised nerve terminals
- The expression of several marker proteins such as: neuropeptides, chromogranins, neuropeptide processing enzymes SPC2 and SPC3(3)

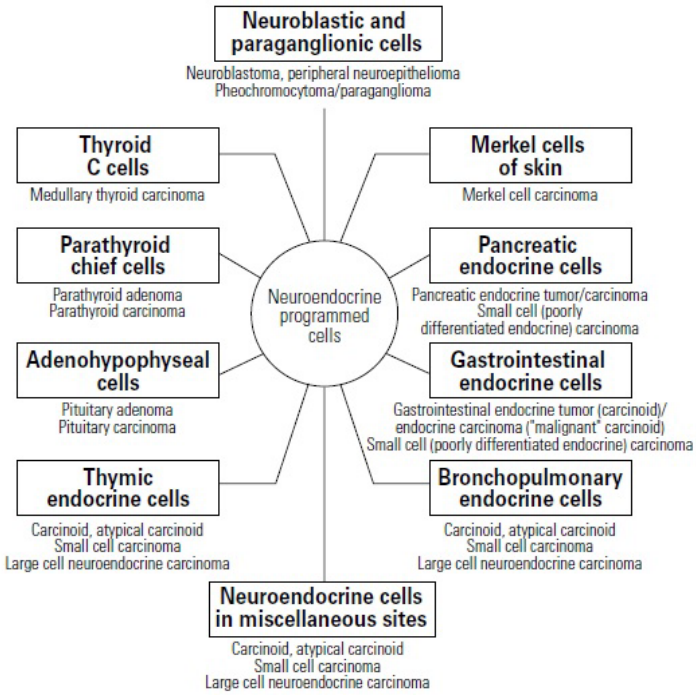

Figure 1: Distribution of neuroendocrine cells in the body(4)

The neuroendocrine tumours (NETs) developing from the DNES are a group of tumour entities, which are as heterogeneous as the cells they originate from. As a result of the diffuse distribution of neuroendocrine cells throughout the body, primary

NETs can originate from a variety of different organ systems. Historically, they were referred to as carcinoids, although today this term is used for well-differentiated NETs.

NETs represented 0.66% (462 NETs) of all malignancies in the Surveillance Epidemiology and End Results (SEER) database over the time period from 1973 to 2004. The incidence of NETs increased by 3–10% per year over this period.(1) The reason for this drastic increase in NETs is most likely an increased diagnostic sensitivity. This is supported by a Scandinavian autopsy study,(5) which performed 16,294 autopsies and found a total of 199 (1.2%) NETs. This indicates that the realistic incidence of NETs is higher than 0.66%. The most frequent location of NETs is the gastrointestinal tract (65%), followed by the bronchopulmonary system (31%) (Figure 2).(1)

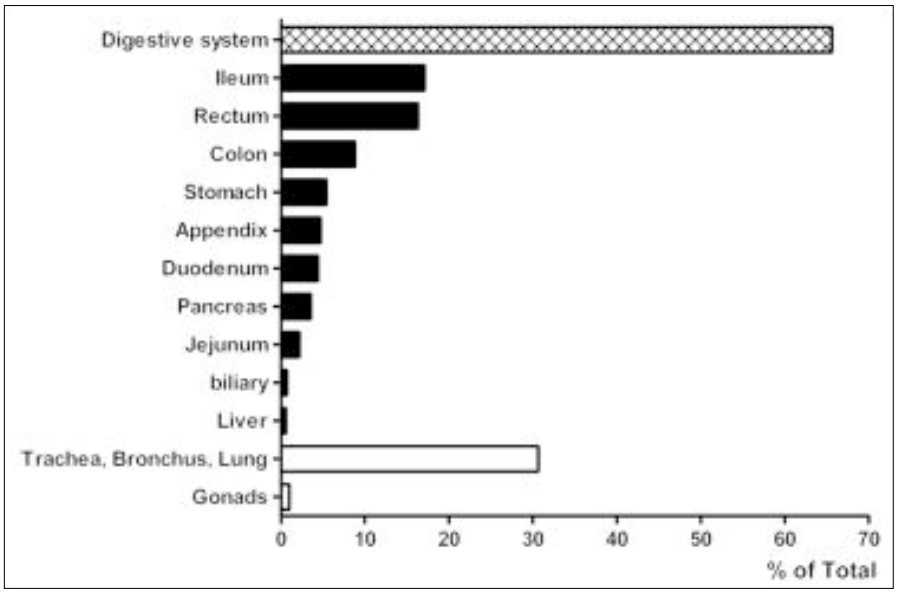

Figure 2: Topographic distribution of 20,436 neuroendocrine (classical carcinoid) tumours derived from the Surveillance Epidemiology and End Results database 1973–2004(1)

Neuroendocrine tumours can occur sporadically or as part of genetic syndromes such as multiple endocrine neoplasia (MEN1 and MEN2), von Hippel-Lindau syndrome and neurofibromatosis.(6)

NETs tend to have a slow growth rate and most patients only exhibit scarce clinical symptoms. This represents a difficult diagnostic and therapeutic challenge, since clinical symptoms are often absent until the primary tumour has already metastasised. If patients do present clinical symptoms, they are often unspecific

because NETs cause a broad spectrum of clinical symptoms, depending on the phenotype and the endocrine activity of the tumour. Hormonally active tumours cause varying symptoms, depending on the bioactive substances secreted (serotonin, cathecholamines, dopamine, histamine, etc.). The classical carcinoid syndrome, typically consisting of diarrhoea, cutaneous flushing, broncho-constriction and right-sided heart failure is, however, relatively uncommon (~20% of small intestine NETs, <5% for NETs of other locations).(1) NETs are classified according to the WHO classification released in 2010, which is based on tumour origin, clinical presentation and differentiation.(7)

1.2 Gastroenteropancreatic neuroendocrine tumours – GEP-NETs

GEP-NETs are a number of tumour entities originating from cells of the gastrointestinal mucosa and the pancreas. The GEP-NET classification includes carcinoids, insulinomas, gastrinomas, tumours that secrete vasoactive intestinal peptides, glucagonomas, somatostatinomas, and non-functional pancreatic endocrine tumours (PETs).(6) Most GEP-NETs have slow growth rates, although aggressive tumours with faster growth rates exist. Patients are mostly asymptomatic, but if they do present clinical symptoms, they are most frequently endocrine syndromes caused by hypersecretion of functional hormones, common in GEP-NETs (Figure 3).(8)

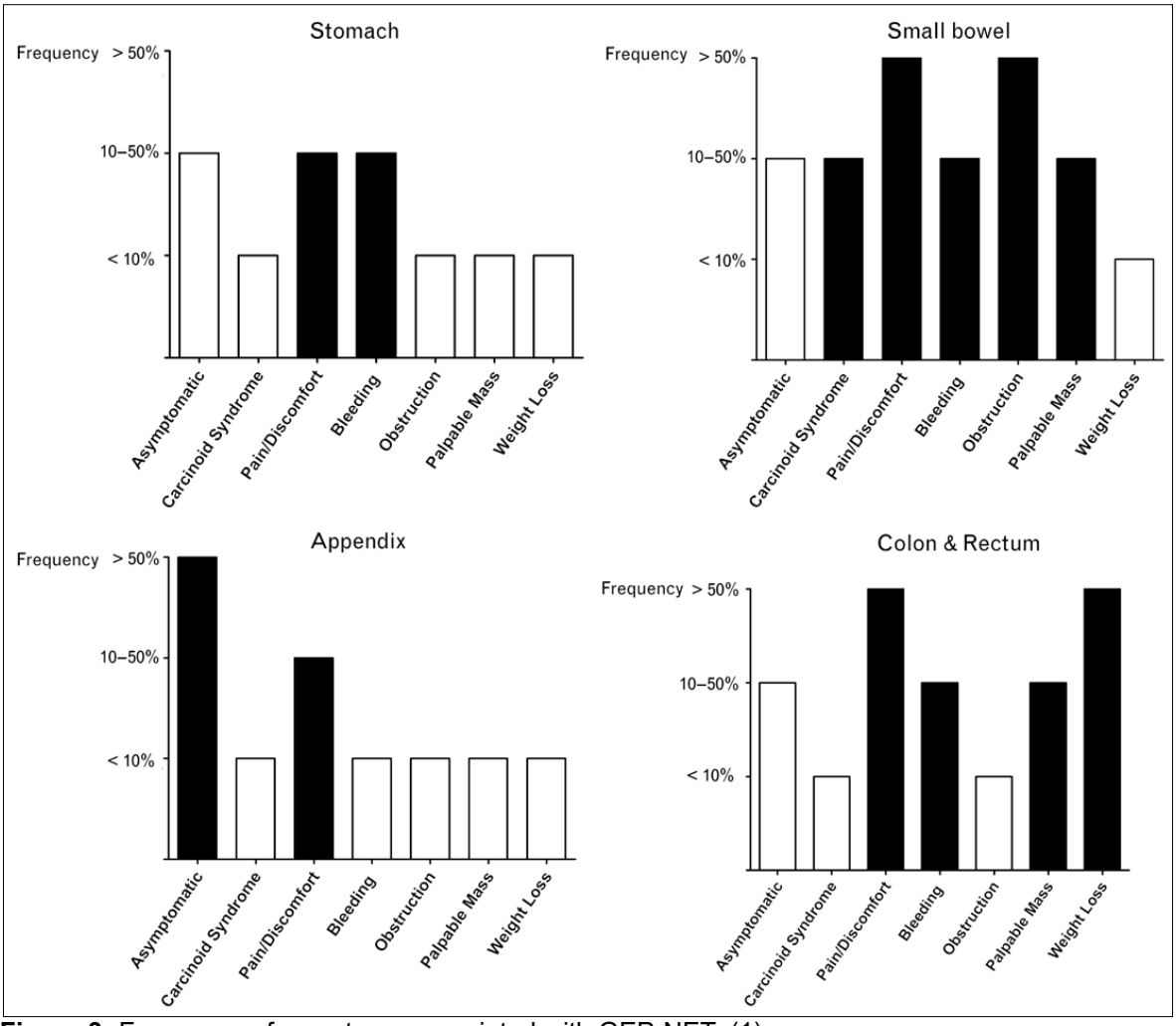

Figure 3: Frequency of symptoms associated with GEP-NETs(1)

1.3 Small intestine GEP-NETs

Small intestine NETs comprise 24.3% of all NETs and present additional diagnostic difficulties due to the inaccessibility through endoscopy. Upper gastrointestinal endoscopy can identify lesions to the level of the ligament of Treitz, whereas colonoscopy can detect terminal ileal tumours as well as colon and rectal NETs. Most of the small intestine is therefore inaccessible to non-invasive diagnostic tools.(1) Classification and staging of small intestine GEP-NETs are based on the TNM classification (Figure 4).

a TNM classification of Si-NENs

T – Primary tumor	
x	Primary tumor cannot be assessed
0	No evidence of primary tumor
1	Tumor invades mucosa or submucosa and size ≤1 cm
2	Tumor invades muscularis propria or size >1 cm
3	Tumor invades subserosa
4	Tumor invades peritoneum/other organs
	for any T add (m) for multiple tumors
N – Regional lymph node metastasis	
x	Regional lymph nodes cannot be assessed
0	No regional lymph node metastasis
1	Regional lymph node metastasis
M – Distant metastasis	
x	Distant metastasis cannot be assessed
0	No distant metastasis
1	Distant metastasis

b Staging of Si-NENs

Stage		TNM			Disease
0		Tis (Stage 0: ENETS only)	N0	M0	localized
I		T1	N0	M0	
II	a	T2	N0	M0	
	b	T3	N0	M0	
III	a	T4	N0	M0	
	b	any T	N1	M0	regional
IV		any T	any N	M1	distant

c Grading of Si-NENs

Grade	Ki-67 index (%)	Mitotic index (mitoses/10 HPF)
G1	≤2	<2
G2	3–20	2–20
G3	>20	>20

Figure 4: TNM classification and staging of small intestine NETs(9)

1.4 Therapy

1.4.1 Surgical treatment

Because of the scarcity of clinical symptoms and the inaccessibility to non-invasive diagnostic tools such as endoscopy, the majority of small intestine GEP-NETs are diagnosed at an advanced tumour stage with multiple metastases. A curative

approach with radical resection of the primary tumour together with a lymph node dissection along the superior mesenteric root is indicated for tumour stages I-III. At stage IV, the surgeon must decide between curative resection, palliative resection and no operation.(9)

1.4.2 Biotherapy

Apart from surgical treatment, the best therapeutic approach is somatostatin analogues. The expression of all 5 somatostatin receptors is quite common in GEP-NETs, making them susceptible to treatment with somatostatin analogues, such as octreotide, pasireotide and lanreotide.(10) The somatostatin receptor 2, in particular, is widely expressed in GEP-NETs.(8) Although somatostatin analogues rarely decrease the volume of the tumour,(11) they are the best therapeutic option for inducing a biochemical response and thus allow management of the patients' clinical symptoms.(1) Interferon therapy is an alternative treatment option, but the increased adverse effects and the delayed response make somatostatin analogues the better choice.

1.4.3 Chemotherapy

Several different chemotherapy regimens exist for NETs. Treatment consists of combinations of streptozotocin (STZ), doxorubicin, 5-fluorouracil (5-FU), cisplatin, etoposide, dacarbacine, oxaliplatin, temozolomide and capecitabine. The main indications for chemotherapy are poorly differentiated and inoperable NETs.(12)

1.4.4 Radiotherapy

External-beam radiation therapy has no effect on NET progression. However, it might be viable in palliative treatment of bone and brain metastases, as well as spinal cord compression.(13) Recently, peptide receptor radiotherapy has been introduced with promising results.(14) By using different radio nucleotides linked to a somatostatin analogue, tumour cells can be selectively targeted, sparing healthy tissue and thereby limiting the number of side effects. The most effective peptide receptor radiotherapy currently available for treatment of metastatic gastrointestinal NETs is ^{177}Lutetium bound to the somatostatin analogue, DOTA-Tyr^{3}octreotate. ^{177}Lu-DOTA-Tyr^{3}octreotate treatment leads to tumour responses in 35% and tumour stabilisation in 80–90% of NETs.(14) . The overall 5-year survival was 64.1% in 4548

patients with small intestinal NETs, whereas the survival rate was approximately 40% in patients with hepatic metastasis.(1)

1.5 Cannabinoids in cancer treatment

1.5.1 Overview

Cannabinoids are the active compound of *Cannabis sativa*. Extracts of this plant have been used for centuries for medical and recreational purposes because of their psychoactive and analgesic effects. The three major classes of active biomolecules in *Cannabis sativa* are flavonoids, terpenoids and more than 40 different cannabinoids.(15)

Cannabinoids exert many of their effects via activation of the cannabinoid receptors 1 and 2 (CB1 and CB2), which are Gαi protein-coupled receptors. These receptors have been well characterised in mammalian tissue. The main difference between the two receptors is their expression pattern throughout the body.(16) CB1 receptors are expressed ubiquitously in mammals, with a high presence in the central nervous system (basal ganglia, hippocampus, cerebellum and cortex), mediating the psychoactive effects of cannabinoids.(17) CB1 receptors are also expressed in tissues other than the central nervous system, such as in peripheral nerve terminals, testes, uterus, eye, spleen, ileum, adipocytes and vascular endothelium.(17) In contrast, the CB2 receptor is expressed in very few tissues, mainly in the immune system.(18) Other cannabinoid receptors also exist, such as TPRV1 (vanilloid receptor 1), GPR55 and PPARα.(19)

1.5.2 Classification

There are three subgroups of cannabinoids (Figure 5):

1.5.2.1 Phytocannabinoids

The most active compound of *Cannabis sativa* is Δ^9-tetrahydrocannabinol (Δ^9-THC), discovered between the 1940s and 1960s.(20) Together with cannabinol (CBN), it is the most prevalent cannabinoid in nature. Other phytocannabinoids are cannabidiol (CBD), cannabigerol (CBG), cannabichromene (CBC), cannabicyclol (CBL), cannabivarin (CBV), tetrahydrocannabivarin (THCV), cannabidivarin

(CBDV), cannabichromevarin (CBCV), cannabigerovarin (CBGV) and cannabigerol monoethyl ether (CBGM).(21)

1.5.2.2 Endocannabinoids

Endogenous cannabinoids are lipid molecules containing long-chain polyunsaturated fatty acids, amides, esters and ethers with a high affinity to CB1, CB2 and other cannabinoid receptors.(22) Endocannabinoids act as neuromodulators or retrograde messengers, affecting the release of various neurotransmitters in the peripheral and neural tissues.(23) They also influence inflammation, insulin sensitivity, and fat and energy metabolism.(21) The two well-known endocannabinoids are N-arachidonoylethanolamine (AEA/anandamide) and 2-arachidonoylglycerol (2-AG). Endocannabinoids affect mood, appetite, pain sensation, inflammation response, and memory.(24,25) Several other endogenous substances that activate cannabinoid receptors have been discovered and characterised, including palmitoyl-ethanolamide, N-(2-Hydroxyethyl) hexadecamide and homo-γ-linoenylethanolamide.(21)

1.5.2.3 Synthetic cannabinoids

Several synthetic cannabinoids have been developed to provide insights into the effects and possible clinical use of cannabinoids.

- **Classical cannabinoids:** isolated plant extracts of *Cannabis sativa* and its analogues:
- **Non-classical cannabinoids:** bi-/tricyclic cannabinoid analogues
- **Aminoalkylindoles:** a family of aminoalkylindoles, including WIN-55,212-2, which is the cannabinoid used in this study
- **Eicosanoids**: analogues of the endocannabinoids anandamide. Other compounds include arachidonyl-2-chloroethylamide (ACEA) and arachidonylcyclopropylamide (ACPA)
- **Others**(21)

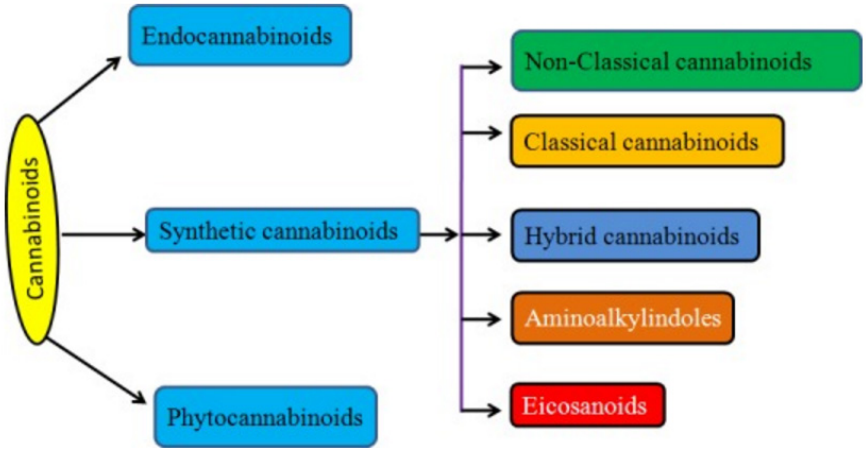

Figure 5: Classification of cannabinoids(21)

1.5.2.4 WIN-55,212-2

In this study, we used the unselective cannabinoid receptor agonist WIN-55,212-2, a synthetic aminoalkylindol with a high affinity to both CB1 and CB2 receptors, but a higher selectivity to CB2. A variety of studies have shown that WIN-55,212-2 has anti-proliferative and apoptosis-inducing effects on cancer cells and that it has similar effects to THC *in vivo*.(24) The concentration of WIN-55,212-2 used in those studies varies between 1–10 µM.(26,27)

1.5.3 Cannabinoid mediated cancer signalling pathways

Cannabinoids inhibit most of the major hallmarks of cancer, including tumour growth, invasion and metastasis, apoptosis evasion and angiogenesis. CB1 and CB2 receptor activation affects K^+ and Ca^{2+} channels. The most frequent downstream target is ERK1/2, activated by modulation of adenylylcyclases and cAMP (Figure 6). Activation of CB1 and CB2 receptors also regulates mitogen activated protein kinases (MAPKs) other than ERK1/2 as p38 and c-Jun N terminal kinase (JNK).(21)

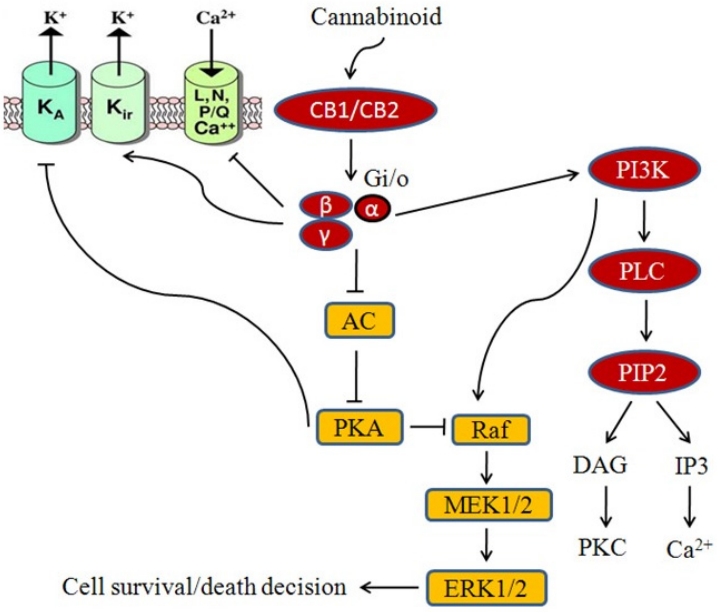

Figure 6: Cannabinoid signalling pathways in cancer(21)

The inhibition of proliferation and induction of apoptosis are among the most important features of anti-tumour drugs. Various studies have demonstrated that cannabinoids inhibit tumour growth and induce apoptosis in a variety of tumour entities. Endocannabinoids such as anandamide play an important role in regulating proliferation. Ranger *et al*.(28) showed that the inhibition of FAAH (fatty acid amide hydrolase), an enzyme that regulates the levels of anandamide, induces cell death by activation of the nuclear factor erythroid 2-related factor (Nrf2)/antioxidant responsive element (ARE) pathway and by the induction of heme oxidase-1 (HO-1). Additionally, anandamide inhibits basal and nerve growth factor (NGF) induced proliferation of MCF-7 and EFM-19 cell (both human breast cancer cell lines) *in vitro* through CB1 receptor activation, and Δ^9-THC inhibits 17-beta-estradiol-induced proliferation of MCF7 and MCF7-AR1 cells.(29–31) These effects are caused by the induction of cell cycle arrest after treatment with anandamide or Δ^9-THC respectively.(29) Further, anandamide inhibits adenylyl cyclase (AC) and thus activates the Raf-1/ERK/MAP pathway in ER^+/PR^+ (oestrogen receptor positive/progesterone receptor positive) breast cancer cells, and Δ^9-THC activates the transcription factor JunD, inducing apoptosis in ER^-/PR^+ breast cancer cells (Figure 7).(29,30,32)

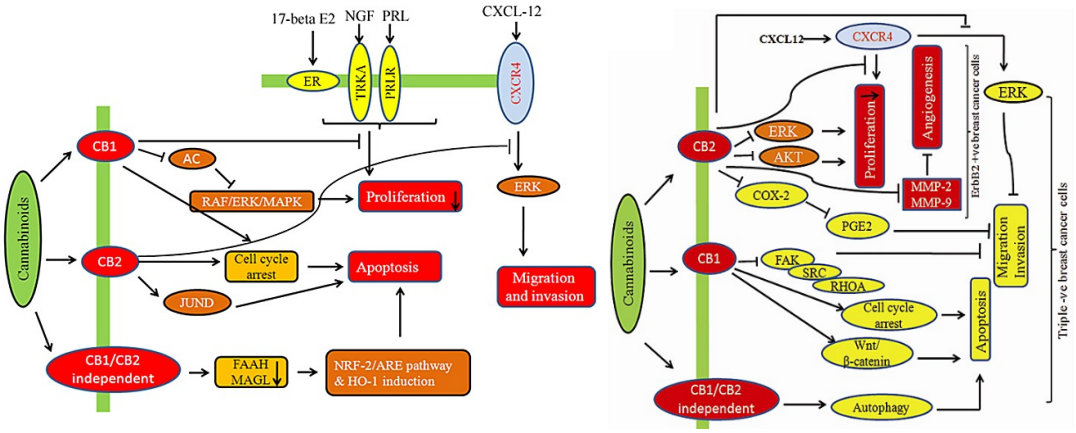

Figure 7: Cannabinoid signalling pathways in hormone receptor positive breast cancer cells(21)

Quamiri *et al.*(33) showed that WIN 55,212-2 inhibits proliferation through the COX-2/PGE2 signalling pathway in a xenograft-based model of triple-negative breast cancer. WIN 55,212-2 also inhibits the proliferation of MDA-MB-231 (human breast cancer) by blocking the G1 to S phase transition and inducing apoptosis.

Additionally, the same study(33) showed that cannabidiol inhibits AKT and mTOR signalling and decreases levels of phosphorylated mTOR and 4EBP1, and cyclin D1.(21) Cannabidiol also enhances the interaction between beclin1 and Vps34 and inhibits the binding of beclin1 and Bcl-2.

1.5.4 Cannabinoids in cancer

1.5.4.1 Cannabinoid receptor expression

CB1 and CB2 receptors are highly expressed in prostate cancer tissues and several cell lines.(21) Various studies have shown that Δ^9 –THC, WIN-55,212-2, R (+)-methanandamide, cannabidiol (CBD), anandamide, JWH-015, HU120, 2-AG and noladin (listed in appendix – 6.2) have anti-proliferative, apoptotic and anti-invasive effects in different prostate cancer cells both *in vitro* and *in vivo*.(30,34–40) Further, Δ^9 –THC induces apoptosis in PC-3 cells (human prostate cancer) via the PI3K/Akt pathway with sequential involvement of Raf-1/ERK1/2 and the induction of nerve growth factor.(34) Treatment with WIN-55,212-2 leads to sustained activation of ERK1/2 and inhibition of AKT, which is associated with the induction of phosphatases.(37,41)

Cannabinoids have similar effects as in breast and prostate cancer in a variety of cancer types, such as lung, skin, pancreatic and bone cancer, and gliomas, among others.(21)

1.5.4.2 Angiogenesis

The novel synthetic cannabinoids LYR-7 and LYR-8 reduce tumour growth by inhibiting VEGF-mediated angiogenesis signalling in MCF-7 and tamoxifen-resistant MCF-7 resistant cells (human breast cancer).(42) In skin cancer, treatment of WIN-55,212-2 or JWH-133 causes a reduced tumour vascularisation and decreases the expression of proangiogenic factors such as VEGF, placental growth factor and angiopoietin-2.(43)

In glioblastoma cells, Massi P. *et al*.(44) showed that CBD also inhibits angiogenesis by modulating the MMP-2 pathway and Id-1 gene expression.

1.5.4.3 Migration and invasion

Hall *et al.*(45) showed that the synthetic cannabinoid JWH-015 reduces CXCL12-induced cell migration and invasion of a highly metastatic MDA-MB-231-derived cell line (human breast cancer) by inhibiting ERK, cytoskeletal focal adhesion and stress fibre formation.(46) Additionally, cannabidiolic acid (CBDA) inhibits migration of MDA-MB-231 cells (human breast cancer cell line) *via* inhibition of the cAMP-dependent protein kinase A, coupled with an activation of the small GTPase, RhoA. Cannabidiol also inhibits the invasion of A549 cells (human lung cancer cell line) both *in vitro* and *in vivo*, accompanied by upregulation of the tissue inhibitor of matrix metalloproteinase-1 (TIMP-1) and decreased expression of plasminogen activator inhibitor-1 (PAI-1).(47,48) Additionally, P38 and ERK1/2 were identified as upstream targets for upregulation of TIMP-1.(48)

Cannabidiol inhibits cell proliferation and invasion of 4T1 cells (mammary metastatic cell line) and reduces the primary tumour volume as well as lung metastasis in 4T1-xenografted orthotopic model of nude mice.(49,50) This anti-metastatic effect is mediated by downregulation of Id-1 (a basic helix-loop-helix transcription factor inhibitor), ERK and also by inhibiting the ROS pathway.(21)

1.5.4.4 Cancer stem cells

Studies have shown that cannabinoid receptors modulate the differentiation of neural progenitors from ectoderm and hematopoietic progenitors from mesoderm.(21) Additionally, the synthetic cannabinoids HU210, WIN55,212-2 and AEA induced concentration-dependent cytotoxicity in P19 embryonal carcinoma (EC) cells.(51)

For further details on signalling pathways and the effects of various cannabinoids, see appendix – 6.2

1.6 Id-1 – a helix-loop-helix transcription factor inhibitor

1.6.1 Basic helix-loop-helix transcription factors and Id

Basic helix-loop-helix (bHLH) transcription factors are a group of proteins that share a common region consisting of several basic amino acids.(52) This highly conserved region is responsible for the binding to so-called “E-box” DNA sequences. These sequences regulate the transcription of genes responsible for terminal cell differentiation.(53,54) bHLH bind to the “E-box” by forming mono- or heterodimers with so-called E-proteins, activating the transcription.

A subgroup of helix-loop-helix proteins lacks the basic DNA binding region, but maintains its capability to form dimers with other bHLH and E-proteins. These heterodimers are unable to activate the “E-box”, therefore inhibiting the transcription of genes regulated by the “E-box”.(55) As most of these genes are responsible for terminal cell differentiation, this subgroup of bHLH-inhibiting helix-loop-helix proteins was named inhibitor of differentiation proteins (Id).

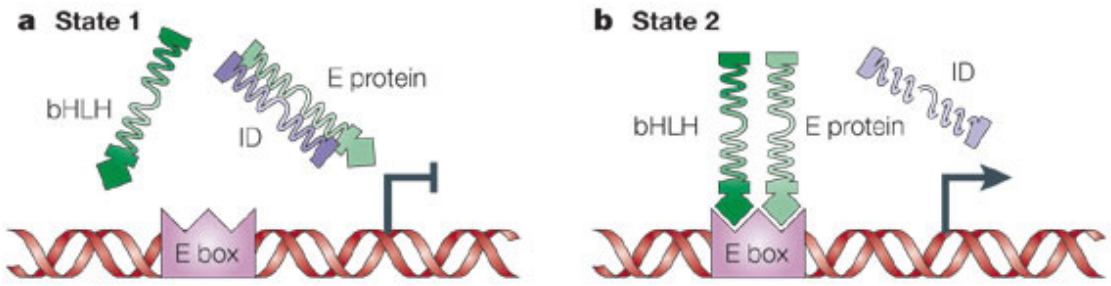

Figure 8: Interaction between Id proteins and bHLH/E-proteins. a) Id proteins form heterodimers with bHLH and E-proteins, attenuating their ability to bind to the “E-box”. b) Normal binding pattern of bHLH/E-protein dimers(56)

Four Id proteins (id1-id4) have been identified in mammals. These proteins have a highly conserved HLH region and they are all of a similar size (between 13–20 kDa). The sequence of the various Id proteins differs greatly, however.(57) For each Id protein, there are two subtypes, due to alternative splicing.(58)

1.6.2 Regulation of Id protein expression

The regulation of Id expression depends on the type of tissues. In epithelial cells, the Id-1 expression is mainly regulated by members of the TGF-β family and the bone morphogenic protein (BMP). The bone morphogenic protein (BMP) upregulates the expression of Id via phosphorylation of its downstream targets Smad1/Smad5. Phosphorylated Smad1/Smad5 then bind to the Smad-binding elements (SBEs) in the Id promoter region and activate transcription.(59–62) The transforming growth factor β (TGF-β), however, downregulates Id expression via phosphorylation of Smad2/Smad3 in epithelial cells. TGF-β phosphorylates Smad2/Smad3, which then bind to the SBE in the Id promoter region and downregulate the Id expression.

Therefore, upregulation and downregulation are both caused by the binding of Smads to SBEs of the Id promoter. The discrimination between the two signalling pathways is possible, due to the presence of activating transcription factor 3 (ATF3) in the downregulation signal. The synthesis of ATF3 is induced by TGF-β and ATF3 is, therefore, only present in the downregulating signalling pathway with TGF-β. The interaction of Smad3 with ATF3 then allows the distinction between TGF-β and BMP mediated signals.

In endothelial cells, the biological effect of TGF-β is concentration-dependent. Low TGF-β concentrations upregulate the Id expression in a similar way to BMP in epithelial cells, whereas high levels of TGF-β suppress the Id expression via Smad2/Smad3.(63)

This is a result of the balance between the activation of the TGF-β receptors Alk1 and Alk5. In the presence of high TGF-β levels, Alk5 is activated to a greater extent than Alk1 and vice versa.(63) Activation of Alk5 leads to the expression of the plasminogen activator inhibitor (PAI) via Smad2/Smad3. PAI then represses migration and proliferation by suppressing Id-1(64).

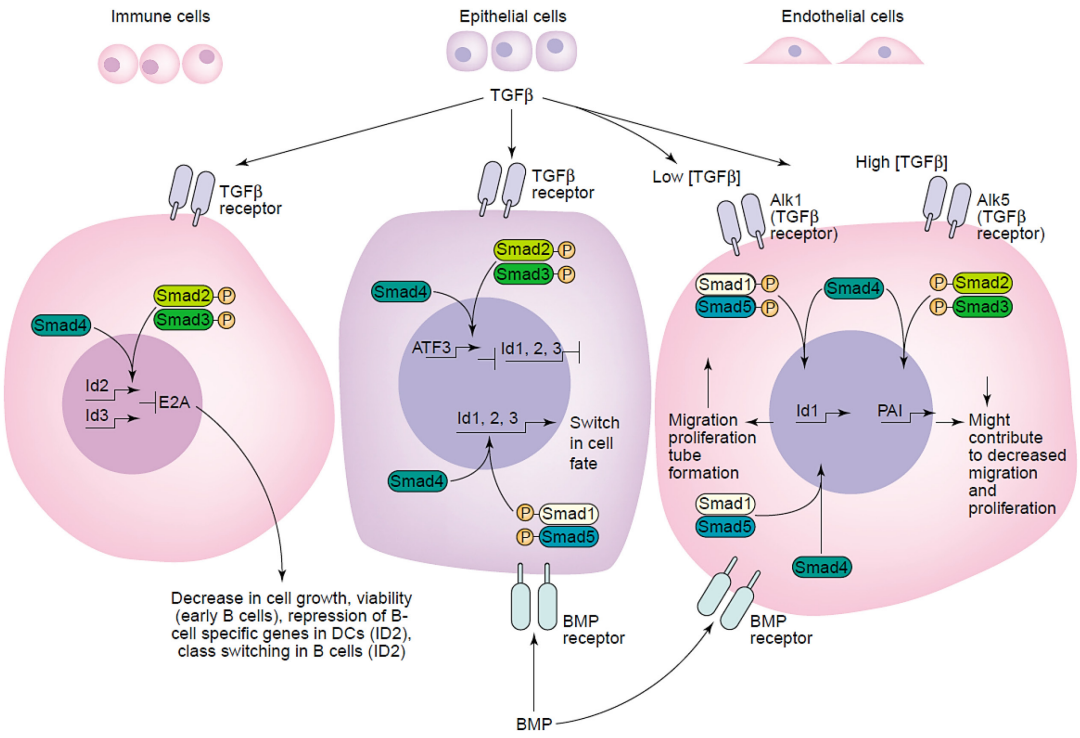

Figure 9: The expression of Id is regulated by TGF-β. In epithelial cells, BMP upregulates expression, whereas TGF-β downregulates it. In endothelial cells, Id regulation is either upregulated or downregulated by TGF-β, depending on the concentration.(65)

1.6.3 Id proteins in cancer

Id proteins are upregulated in several cancer types, such as prostate, breast, colon, rectum, pancreas, liver and medullary thyroid cancer, and leukaemia.(66) According to Wong Y-C *et al.*,(52) Id-1 is involved in a variety of tumorigenic processes, such as regulation of cellular senescence, tumour growth and invasion.

1.6.3.1 Id-1 in cellular senescence

It has been suggested that escaping cellular senescence is one of the mechanisms leading to malignant transformation.(67)

Telomere shortening, and the p53 and Rb tumour suppressor pathways are responsible for inducing and maintaining replicative senescence in normal human cells.(52) The activities of Rb proteins are regulated by phosphorylation trough cyclin-dependent kinases (CDK). The inhibitors of CDKs such as p16INK4a, p21WAF1 and p27Kip1 have therefore been indicated as key regulators in replicative senescence.(68,69)

Tang *et al.* and Nickoloff *et al.*(70,71) showed that p53 and Rb pathways are inactivated in Id-1 transfected cells (for possible pathways, see Figure 10). For instance, ectopic Id-1 expression in human keratinocytes leads to decreased levels of p16INK4a and p21WAF1 and, therefore, increased phosphorylation of the Rb protein.(70,71)

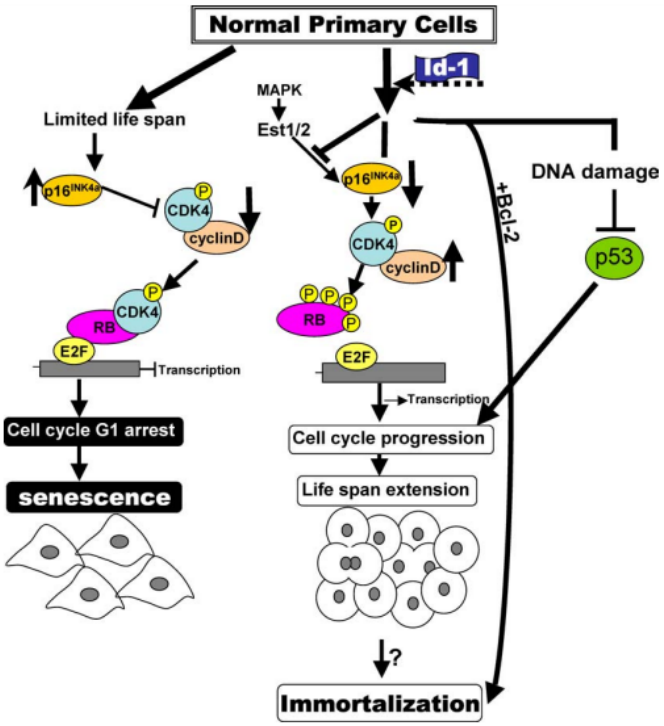

Figure 10: Id-1 signalling pathways regulating cellular senescence. Inactivation of the p16INK4a/RB and p53 tumour suppressor pathways results in a lifespan extension.(52)

1.6.3.2 Tumour growth

Upregulation of Id-1 in normal cells leads to the initiation of DNA synthesis and progression of G1 to S phase of the cell cycle, thus promoting normal cell proliferation (for possible signalling pathways, see Figure 11).(70,71)

In prostate cancer, Id-1 induced cell proliferation is associated with downregulation of p16INK4a expression, which is accompanied by increased phosphorylation of Rb.(72)

Another pathway through which Id-1 induces cell proliferation in cancer is the MAPK signalling pathway. Several regulators of the MAPK pathway, such as Raf and MEK1/2, are expressed in LNCaP prostate cancer cells ectopically expressing the Id-1 protein. Additionally, higher levels of Id-1 expression lead to higher levels of the

downstream target of the MAPK pathway, EGR-1.(73) Since the activation of the MAPK pathway increases the expression of its downstream targets, the increased levels of EGR-1 indicate that Id-1 activates this pathway. Furthermore, the inhibition of the phosphorylation of the MEK1/2 kinase, which is involved in the MAPK pathway, leads to decreased EGR-1 expression.(73)

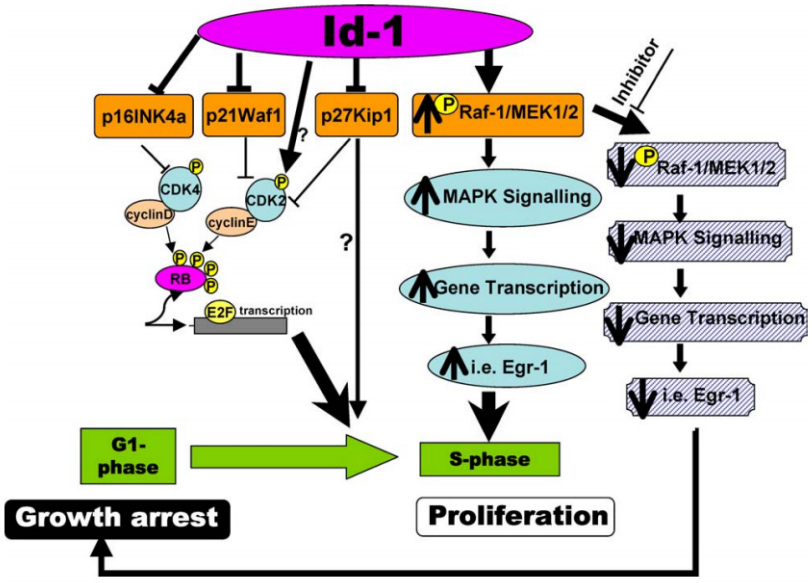

Figure 11: Id-1 interacts with Rb and MAPK pathways in cancer cells, leading to increased cell proliferation. Interaction between Id-1 and p16INK4a/Rb and MAPK pathways leads to increased cancer cell growth.(52)

1.6.3.3 Id-1 and apoptosis

There are many studies with contradictory results regarding the role of Id-1 in apoptosis. Kim D. *et al*., for example, found that Id-1 overexpression induces massive apoptosis in T-cell deficient Id-1 transgenic mice.(74) However, Id-1 induces proliferation in mammary epithelial cells at sub-confluent conditions, but induces apoptosis when cultured at high density.(75) Furthermore, Id-1 inhibits apoptosis in prostate cancer cells: LNCaP cells with undetectable levels of Id-1 showed a much higher apoptosis rate than Id-1 positive cells upon treatment with the apoptosis inducer TNF-α. In addition, the fragmentation of Bax and PPAR is increased in Id-1 negative cells. Moreover, Id-1 exerts this protective role against apoptosis in prostate cancer through the activation of NfκB, which activates downstream targets such as ICAM-1 and Bcl-xl (Figure 12).(76)

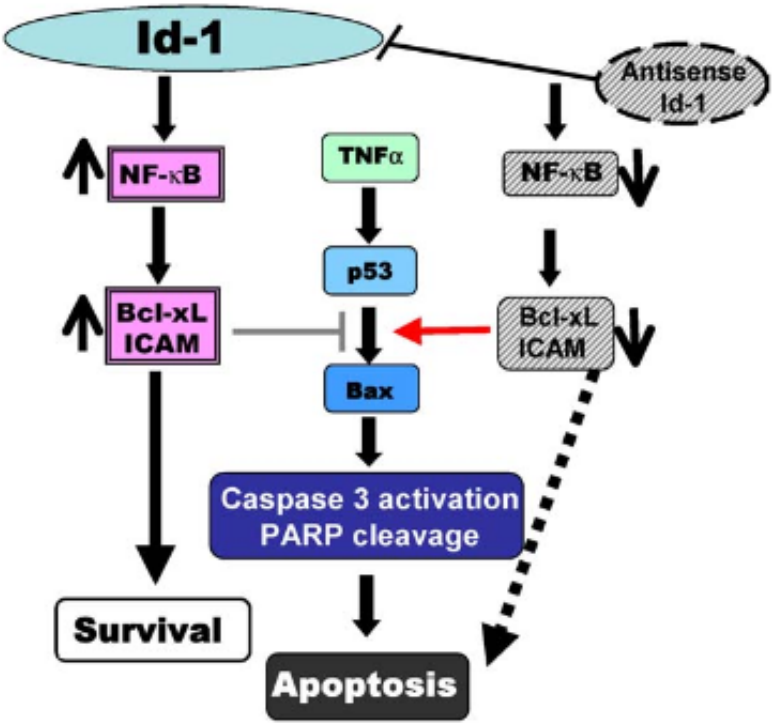

Figure 12: Id-1 signalling pathways regulating apoptosis(52)

1.6.3.4 Id-1 – invasiveness and angiogenesis

There is evidence that Id-1 plays a role in tumour invasiveness and angiogenesis. Desprez PY. *et al*.(77) showed that constitutive expression of Id-1 in mouse mammary epithelial cells leads to an increase of invasiveness and cell migration, mediated via a matrix metalloproteinase. Additionally, Id-1−/−Id-3+/− knockout mice do not support the growth of xenografts due to poor vascularisation and necrosis of the tumours.(78) The reason for this reduced angiogenesis is a reduced VEGF-dependent recruitment of endothelial precursor cells from the bone marrow for newly developing tumour vessels.(79) Additionally, the endogenous neoangiogenesis inhibitor thrombospordin-1 (TSP-1) has been identified as a downstream target of Id-1, which leads to the consequential inhibition of bFGF and VEGF-induced angiogenesis.(80) Also, the loss of Id-1 function in endothelial tumour cells results in the downregulation of a variety of pro-angiogenetic geneses, such as intergrin α6 and β4, matrix metalloprotease-2 and fibroblast growth factor receptor-1.(81)

1.7 Aims of this study

In this study, we investigated the effects of the unselective synthetic cannabinoid receptor agonist WIN-55,212-2 on the small intestine neuroendocrine cell line P-STS and Id-1 as a possible signalling pathway of these effects. As parameters for anti-tumorigenic effects, we measured cell count and viability, apoptosis, Ki67 expression, DNA fragmentation, tumour morphology, invasiveness, angiogenesis and Id-1 expression of the small intestine neuroendocrine cancer cell line P-STS after treatment with WIN-55,212-2. Furthermore, we measured Id-1 levels to observe whether WIN-55,212-2 treatment leads to the downregulation of Id-1 and we also investigated the mediating role of Id-1 regarding the WIN-55,212-2 effects on P-STS cells.

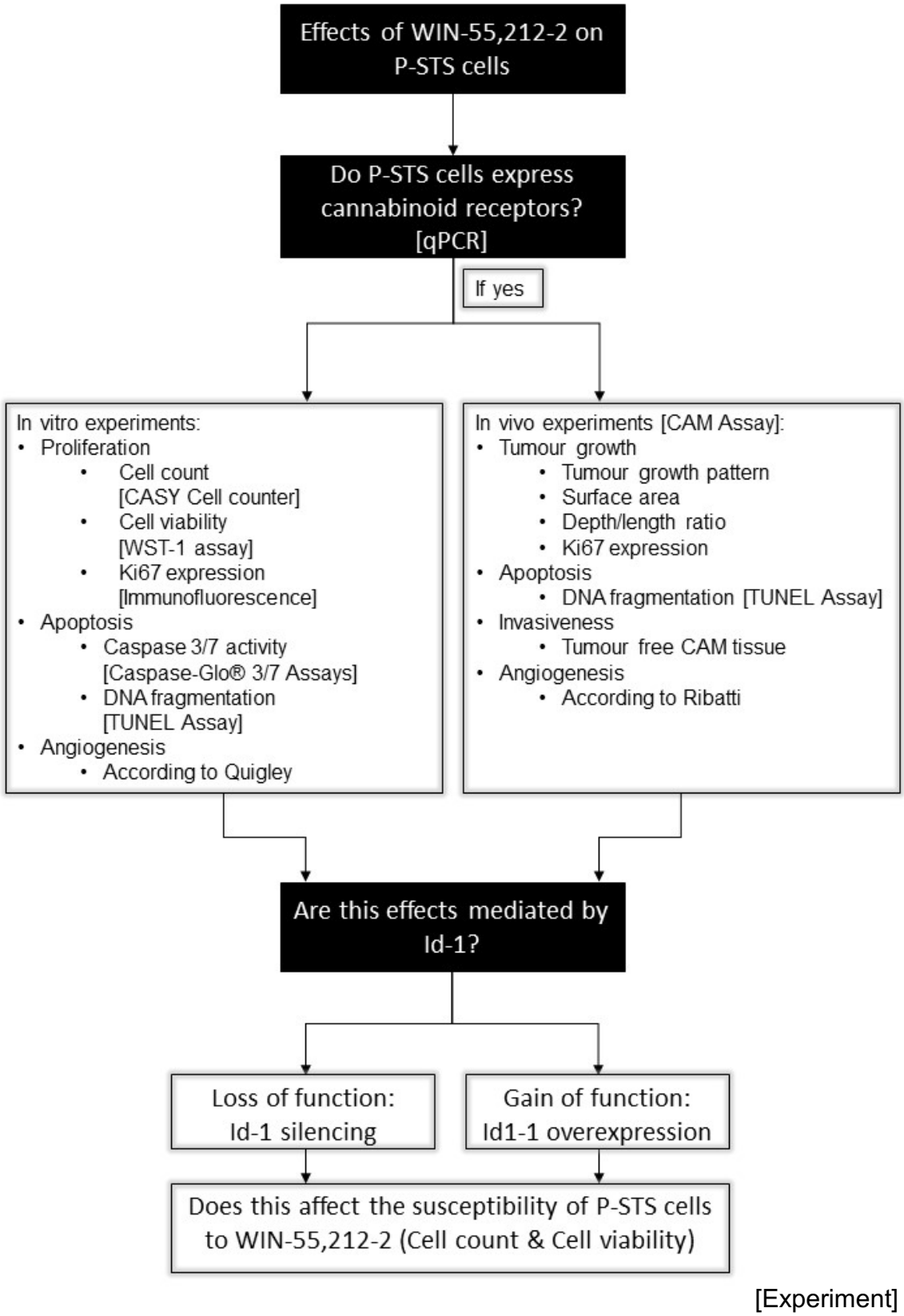

Figure 13: Schematic diagram of the study

2 Materials and methods

2.1 Cell culture

2.1.1 P-STS cell line

All the experiments in this study were carried out with the small intestine neuroendocrine tumour cell line P-STS. This cell line was established from the primary tumour of a small intestine neuroendocrine metastatic cancer, localised in the terminal ileum of a 42-year-old male patient. Clinically, the patient displayed a carcinoid syndrome with flush and respiratory distress. The tumour was diagnosed at stage pT4pNpos(9/15)nM1 and corresponded histologically to a poorly differentiated neuroendocrine carcinoma. The patient underwent surgery and received therapy with octreotide. Unfortunately, he died after the surgery. The P-STS cell line established from the primary tumour of this patient has two cell fractions with distinct growth patterns. Initially, P-STS cells form loosely attached monolayers. After reaching confluence, regions with multi-layered aggregates develop, and cells detach from these regions and form a second fraction with suspension cells. The approximate population doubling time of P-STS cells is 4 days. P-STS cells appear round-shaped, with an irregular and often single, prominent nucleus. The ultrastructure is characteristic for neuroendocrine cells, with numerous cytoplasmic granules, with typical features of membrane-bound, dense-core neurosecretory granules. Another striking feature is a hyperplastic Golgi apparatus, which, together with the neurosecretory granules, suggests the secretory activity of the cells.(82)

P-STS cells express a variety of NET markers, including serotonin, synaptophysin and gastrin-releasing factor. Genetically, they feature an aclonal tetraploidy and a chromosomal aberration in q18, although none of the most frequent menin gene mutations. Therefore, the tumour was most probably caused by a sporadic mutation, rather than as a result of MEN syndrome.(82)

2.1.2 Cell passaging

The P-STS cells were maintained in Ham's F12:M199 (1:2) medium with 10% superior fetal bovine serum (FBS) (Biochrom, Berlin), 100 IU penicillin/ml and 100

µg streptomycin/ml (P/S) (Sigma Aldrich, St. Luis, USA) at 37 °C and 5% CO_2. Cells were seeded at a concentration of $2x10^5$ cells/ml and a volume of 3 ml in a T25 cell culture flask and fed with an additional 4 ml cell culture medium on day 4. On day 7, cells were passaged. For this purpose, cells were detached mechanically from the surface using a cell scraper, and the cell suspension was transferred into a falcon and centrifuged for 5 minutes at 1200 rpm. After centrifugation, the supernatant was discarded and the cell pellet resuspended in 1 ml cell culture medium. Then a further 2 ml cell culture medium was added and the cell count was determined with the CASY® Cell Counter. Cells were subsequently seeded at a concentration of $2x10^5$ cells/ml in new cell culture flasks.

2.1.3 Cell starving

To avoid unspecific binding and interactions with components of the FBS in the cell culture medium and cannabinoid receptors, the cells were starved in Ham's medium containing 1% FBS for 24 hours prior to the experiments. For this purpose, cells were harvested as described in 2.1.2 and resuspended in Ham's medium containing 1% FBS after the first centrifugation step. The cells were then seeded in 24-well plates at a concentration of $2x10^5$ cells/ml and a volume of 1 ml per well. After a starving period of 12 hours, treatment with respective concentrations of WIN-55,212-2 was started.

2.1.4 Cell harvesting

Because P-STS cells grow semi-adherently as described in 2.1.1, it was necessary to detach them from the surface prior to the measurements. To achieve this, the cells were washed off by repeatedly resuspending the cell culture medium and successful detachment was verified microscopically.

2.2 WIN-55,212-2 – a synthetic CB1 and CB2 receptor agonist

WIN-55,212-2 was purchased from Tocris Bioscience, Bristol (UK). It is a synthetic unselective CB1 and CB2 receptor agonist, which has similar effects to tetrahydrocannabinol (THC).(24) All experiments in this study were carried out using WIN-55,212-2 as a cannabinoid agonist. Stock solutions were diluted in DMSO at a concentration of 10 mM and stored at -80 °C. For further dilution, sterile ddH_2O (Fresenius, Bad Homburg) was used. After the starving period (see 2.1.3), P-STS cells were treated with WIN-55,212-2 at concentrations of 1 µM, 2 µM, 5 µM and 10 µM every 24 hours over a period of 3 days.

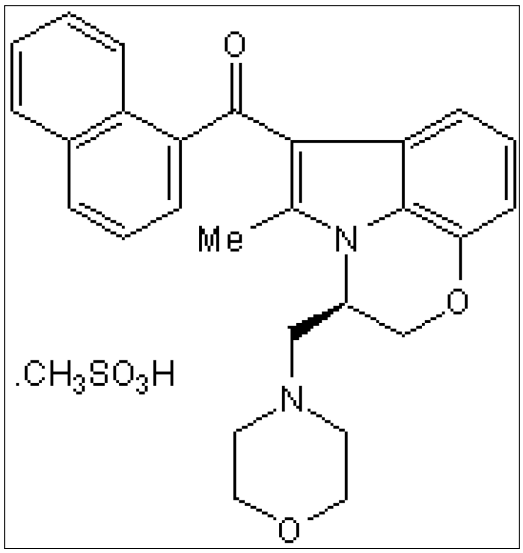

Figure 14: WIN-55,212-2 (Tocris, Bristol): Unselective CB1 and CB2 receptor agonist (Ki values = 6.23 nM and 3.3 nM)(83)

2.3 RNA isolation, cDNA synthesis and qPCR

2.3.1 RNA isolation

The RNA isolation was performed using TriReagentRT (Molecular Research Center, Cincinnati).

P-STS cells were seeded and then starved for 24 hours prior to the experiment (see 2.1.3). Subsequently, the cells were treated with WIN-55,212-2 in the respective concentrations (see 2.2) every 24 hours over 3 days. Cells were harvested by detaching adherent cells mechanically with a cell scraper (see 2.1.4)

The P-STS cells were then transferred into a falcon and centrifuged for 5 minutes at 1200 rpm. Then the supernatant was discharged and the remaining cell pellet was frozen at -20 °C for storage. The cell pellet was warmed up at room temperature (RT), and then lysed and homogenised by adding 500 µL TriReagent and repeated pipetting. Then 50 µL 4-bromoanisole (BAN) was added to ensure the complete dissociation of nucleoprotein complexes. The solution was incubated for 5 min and subsequently centrifuged at 12,000 g for 15 min at 4 °C. This centrifugation step separates the sample into 3 phases: a red organic phase (containing protein), an interphase (containing DNA), and a colourless upper aqueous phase (containing RNA).(84)

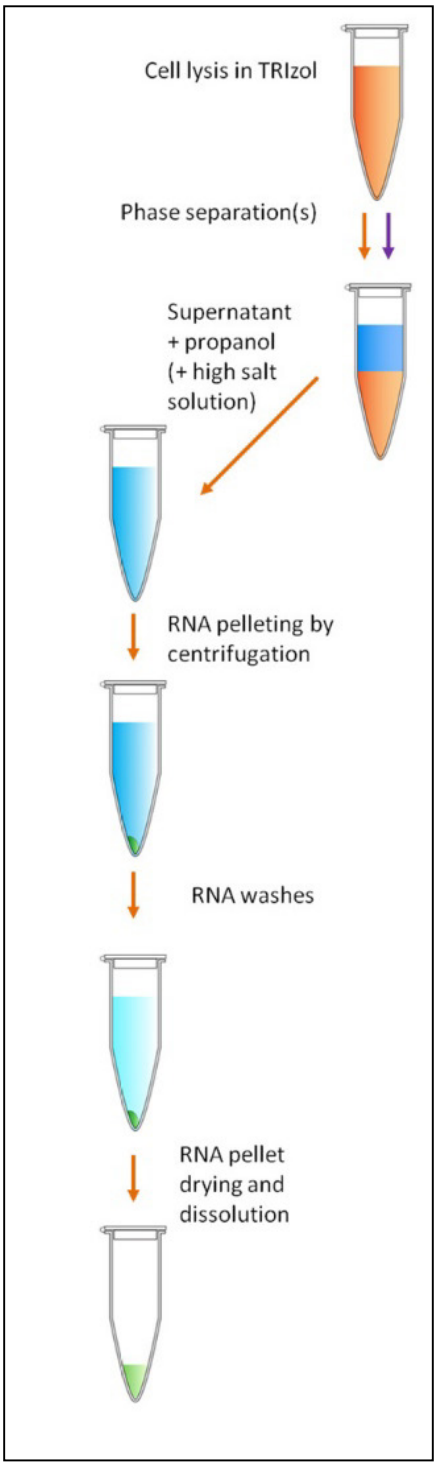

Figure 15: RNA isolation (85)

The aqueous phase was transferred into a fresh tube, and 500 µL of isopropanol was added. The sample was then incubated at RT for 10 min. Afterwards, the sample was centrifuged again at 12,000 g for 8 min at 4 °C. The centrifugation causes the RNA precipitate to form a pellet at the bottom of the tube. The supernatant was discharged and the pellet washed with 1 ml 70% ethanol. Again, the supernatant was discharged carefully and the remaining RNA pellet was then air dried for 5 min at room temperature. Finally, the pellet was dissolved in RNAse-free water for 10 min at 55 °C and 300 rpm on a heat block. The RNA concentration and quality was evaluated with the NanoDrop©ND-1000 Spectrophotometer (Thermo scientific, USA).

The final purity was estimated with optical density measurements. All samples had an A260/A280 ratio >1.9, ensuring protein- and DNA-free RNA samples.

2.3.2 cDNA synthesis

To analyse the expression levels of various mRNAs, cDNA had to be synthesised from the isolated RNA samples. This was achieved by incubating the isolated RNA samples with the RT-qPCR reaction mix (Applied Biosystems High Capacity RNA to cDNA Kit) containing the enzyme reverse transcriptase.

Substance	**Volume [µL]**
H_2O	4.2
10x RT buffer	2
10x Random primer	2
RT enzyme	1
25x dNTP mix (100 mM)	0.8
Total	**10**

Table 1: RT PCR reaction mix.

The RNA was diluted to 2,000 pg in 10 µL. Then 10 µL each of RNA and reaction mix were transferred into a tube and incubated in the thermocycler (BioRaq C1000 thermocycler). Every cDNA synthesis included a control without reverse transcriptase. 39 cycles were performed by the thermocycler. Table 2 shows the temperature program used.

Time	**Temperature**
0 min	25 °C
120 min	37 °C
5 sec	85 °C
Standby	4 °C

Table 2: Temperature program run by the thermocycler

2.3.3 Real-time quantitative PCR

To quantify the mRNA expression levels, we performed real-time qPCRs with SYBR© Green (Bio-Rad). Each plate contained controls consisting of a reverse transcriptase control and a no template control. To begin with, the cDNA was diluted

to 5 ng/µL. Then the general reaction mix (see table 4) was transferred into the respective wells of a 96-well qPCR plate.

Time	Temperature
3 min	95 °C
10 sec	95 °C
40 sec	60 °C
10 sec	55 °C

Table 3: Temperature program (qPCR)

After all the samples had been transferred into the 96-well qPCR plate, a run of 40 cycles was performed with the Real-Time CFX96 System of Bio-Rad. See table 3 for the temperature program used.

Substance	Volume [µL]
IQ™ SYBR© Green Supermix	7.50
cDNA (5 ng/µL)	4.00
H_2O	2.90
Primer fwd. (0.3 µM)	0.30
Primer rev. (0.3 µM)	0.30
Total	**15.00**

Table 4: General reaction mix for the qPCR

Melting curves were established for a better interpretation of the respective amplificates. To establish the melting curves, the temperature was increased from 55 °C to 95 °C in 0.5 °C steps, while measuring the relative fluorescence unit (RFU) every 10 sec. The level of mRNA expression was calculated with the ΔΔCq method. The C_q value (quantification cycle) is the cycle at which the fluorescence exceeds the background fluorescence.

$$\Delta C_q = C_{q(S)} - C_{q(REF)}$$

$$\Delta C_q \text{Expression} = 2^{-\Delta C_q}$$

$$\Delta\Delta C_q = \frac{\Delta C_{q(S)}}{\Delta C_{q(Ctrl)}}$$

Equation 1: Calculation of the ΔΔCq value (relative mRNA expression relative to control). S=Cq value of the sample, REF=reference gene, Ctrl=control

2.3.4 Real-time qPCR – Cannabinoid receptors

The level of cannabinoid receptor expression was determined by qPCR. The PCR was performed with cDNA of P-STS cell RNA extracts. The primers for CB1, CB2 and GPR55 receptors were purchased from Bio-Rad (Vienna, Austria). To quantify the mRNA expression, HPRT-1 was used as a reference gene. The level of mRNA expression for the respective receptors was quantified with the $\Delta\Delta$Cq method (see Equation 1).

2.3.5 qPCR – Id-1 mRNA expression

Changes in the mRNA expression of Id-1 upon treatment with WIN-55,212-2 were compared by performing qPCRs on cDNA gained from P-STS cells treated with the respective concentrations of WIN-55,212-2 for 16 hours. We used the Id-1 primers (Invitrogen, Karlsbad) suggested by Locklin *et al.*(86) to amplify the cDNA. To quantify the mRNA expression, we used L30 (Biomol, Hamburg) as a reference gene. The level of Id-1 expression was calculated with the $\Delta\Delta$Cq method.

Gene	RefSeq no.	Primer location	Sequence	Product length
Id-1	NM_002165.3	5´-113	5´-TGGTCGCTGTCTGTCTGAG-3´	300
	NM_181353.2	3´-403	5´-GCCGTTGAGGGTGCTGAG-3´	

Table 5: PCR Primers for Id-1 and L30

2.4 Spheroid formation

The synthesised cDNA retrieved from 3D spheroids was provided by Marlies Christina Hölzl.(87)

To compare the cannabinoid receptor expression between cells growing in 2D (conventional cell culture conditions) and cells growing in 3D spheroids, P-STS cell spheroids were generated. For this purpose, single cell suspensions were seeded in ultra-low-adhesion round-bottomed 96-well plates (Costar® cell culture plates) containing 7500 cells/well and cultured in Ham's F12/M199 (1:2) medium supplemented with 10% FBS. The spheroids were harvested after 10 days and the RNA was isolated (see 2.3.1).(87)

2.5 CASY® Cell Counter

The CASY® Cell Counter & Analyzer TTC (Schärfe Systems, Reutlingen) was used to determine various cell counts. In principle, it measures the electrical impedance of cells passing through an electrical field to determine the cell count.

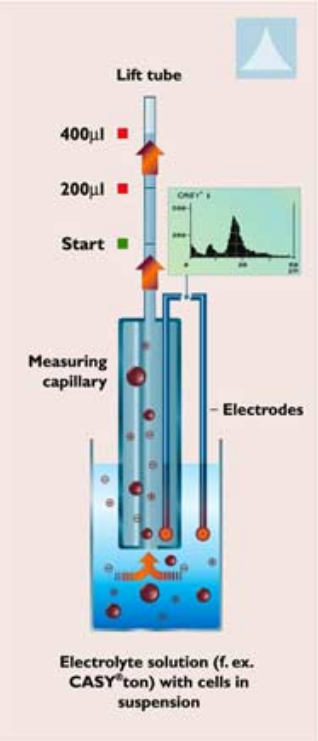

Figure 16: CASY® Cell Counter – measurement principle(88)

Firstly, 50 µl of the cell suspension is suspended in 10 ml of an electrolyte buffer (CASYton®, Schärfe Systems, Reutlingen). The cell suspension is then aspirated through a high-precision capillary and flows through an electrical field between two platinum electrodes. The phospholipid layer of the cell membranes acts as an isolator and increases the resistance in the electrical field, i.e. the passage of each cell causes an electrical impedance signal which can be detected. The number of signals generated indicates the number of cells passing through the electrical field. As the resistance correlates with different parameters of the cell membrane (integrity, volume, etc.), a clear-cut differentiation between cell debris, dead cells and viable cells can be made.

2.6 WST-1 Assay

The WST-1 Assay allows the quantification of cell viability. In principle, it detects the mitochondrial metabolisation of a tetrazolium salt into a formazan salt to quantify the viability of cells.

The tetrazolium salt is reduced to formazan through electron transfer by the succinate-tetrazolium-reductase (EC). This reductase is part of the mitochondrial respiration chain and therefore only active in living organisms. Consequently, the amount of reduced tetrazolium salt correlates to the viability and the amount of living cells. Since formazan is a dark red dye and has a different absorption from WST-1 (light red), the amount of formazan formed can be measured photometrically.

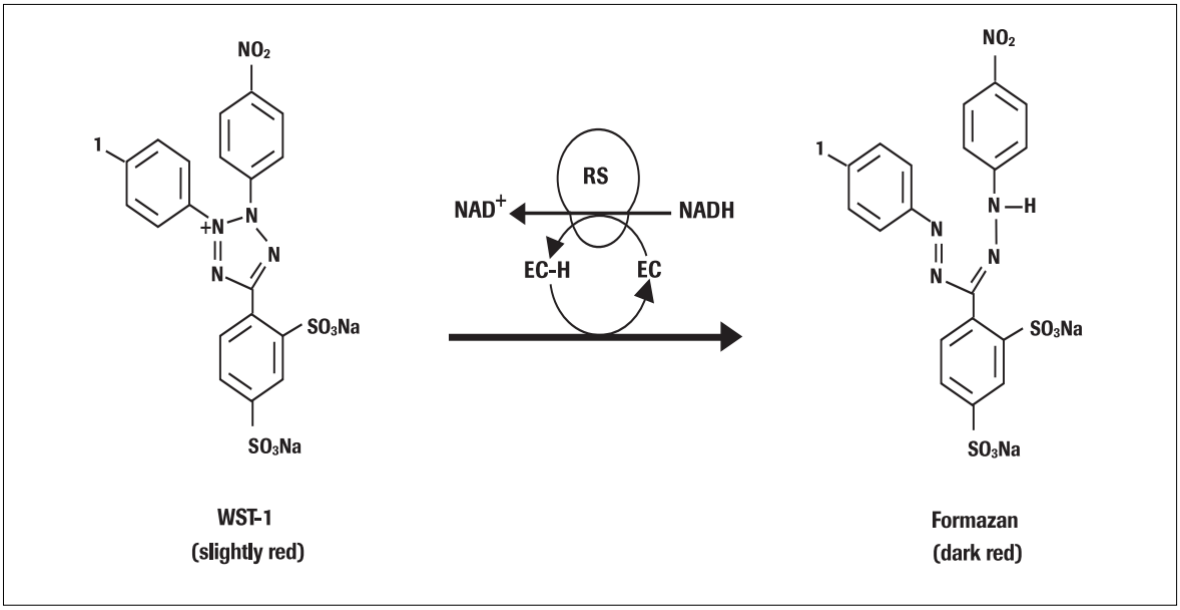

Figure 17: The WST-1 Assay is based on the mitochondrial oxidation of WST-1, transforming it into formazan. This change can be quantified photometrically.(89)

To perform the WST-1 Assay, we treated cells with WIN-55,212-2 as described in 2.1. WST-1 Assays were performed every 24 hours over the course of 3 days. Cells were harvested as described in 2.1.4 and 100 µl of the cell suspension was transferred into a flat-bottom 96-well plate. Then 10 µl of the WST-1 reagent was added and the plate was incubated for 1 hour at 37 °C and 5% CO_2. After the incubation period, the absorption was measured photometrically and normalised to the control.

2.7 Caspase-Glo® 3/7 Assay

The Caspase-Glo® 3/7 Assay Kit was purchased from the Promega Cooperation (Madison, USA).

By adding the Caspase-Glo® 3/7 reagent to the cell suspension, the cell membranes are lysed, releasing intracellular, already activated caspases. Once freed, the caspases cleave the reagent and this generates a luminescent signal induced by a luciferase. This signal can then be detected, and the caspase activity can therefore be measured.

To perform the caspase assay, we seeded, starved and treated P-STS cells with WIN-55,212-2 as described in 2.1. Caspase assays were performed every 24 hours over the course of 3 days. Cells were harvested as described in 2.1.4 and 50 µl of the cell suspension was transferred into a white microwell plate. Then 50 µl of the Caspase-Glo® 3/7 reagent was added and the microwell plate was placed on a shaker for 30 seconds. After an incubation period of 1 hour at room temperature, the plate was measured (GlowMax©, Promega) and analysed statistically.

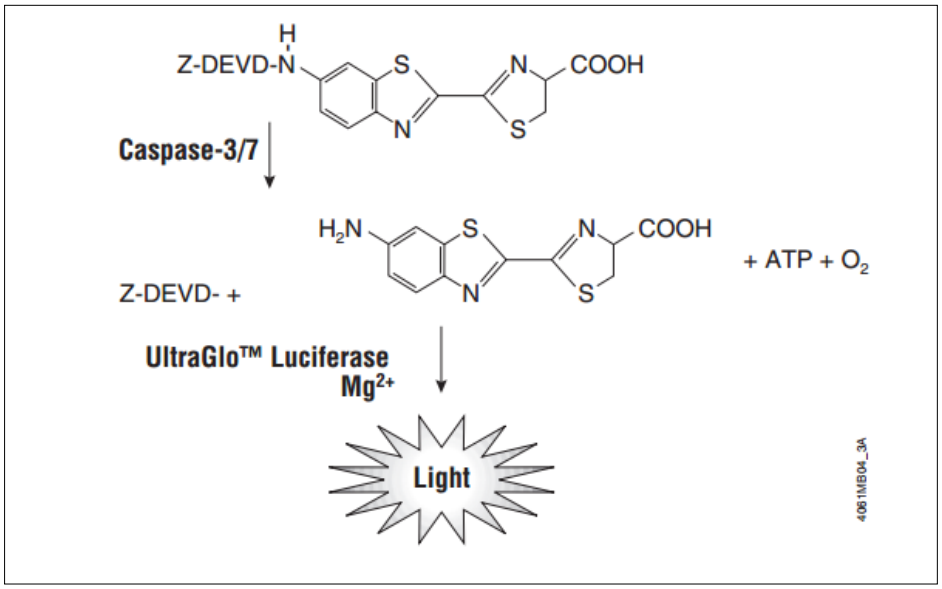

Figure 18: Principle of the Caspase-Glo® 3/7 Assay: Caspases released from lysed cells cleave the Caspase-Glo® 3/7 reagent, resulting in a light signal generated by a luciferase.(90)

2.8 Immunofluorescence staining

2.8.1 Ki67 staining

The Ki67 mouse anti-human antibody was purchased from Dako (Glostrup, Denmark. Ki67 is a protein that is expressed in proliferating cells, but not in stationary cells in the G0 phase.(91) It is therefore an ideal marker for proliferation. To detect the Ki67 of P-STS cells, indirect immunofluorescence was used. This technique uses a primary unconjugated antibody to label a specific antigen, in this case Ki67, and a secondary antibody, labelled with a fluorescent dye targeting the primary antibody. The use of the secondary antibody enhances the signal.

Firstly, P-STS cells were treated for 24 hours with 5 µM WIN-55,212-2. The cell suspension was then transferred into chamber slides and cytospins were performed to concentrate the cells on the slides. The supernatant was discharged and the slides were dried at room temperature for 30 minutes. The cells were then fixated using 4% paraformaldehyde for 5 minutes and then washed with T-BST buffer. Subsequently, the primary antibody was added and the slides were incubated overnight at 4 ºC. After 12 hours, the slides were washed repeatedly with T-BST buffer and then incubated with the secondary antibody for 1 hour at room temperature. Finally, the slides were washed again with T-BST buffer and counterstained with 4′,6-Diamidin-2-phenylindol (DAPI), which stains cell nuclei. Then photographs were taken with the with the Olympus BX53 fluorescence microscope and the Ki67 labelling index (number of Ki67 positive cells/total number of cells) was calculated.

Figure 19: Principle of indirect immunofluorescence staining (antigen=Ki67)(92)

2.8.2 *In situ* TUNEL assay

The TUNEL assay kit was purchased from abcam (Cambridge, United Kingdom). This assay utilises Br-dUTP (bromolated deoxyuridine triphosphate nucleotides), which are incorporated into fragmented DNA strands, occurring during apoptosis, by a deoxynucleotidyl transferase (TdT). A higher incorporation gives rise to a brighter signal when the Br-dUTP sites are identified by a red fluorescence labelled anti-BrdU monoclonal antibody.(93)

Firstly, the cells were fixated on slides as described in 2.8.1. The following solutions were then added consecutively with intercalated washing steps with PBS: proteinase K (table 6) solution, wash buffer, DNA labelling solution (table 7), anti-Br-dUTP antibody, DAPI. Finally, photographs were taken with the Olympus BX53 fluorescence microscope and the ratio between the number of Br-dUTP positive cells and the total number of cells was calculated.

Substance	**Volume [µL]**
Proteinase K 10 mg/ml	2
100 mM TrisHCl pH 8.0 + 50 mM EDTA	998
Total	**1000**

Table 6: Proteinase K solution

Substance	**Volume [µL]**
Reaction buffer	10
TdT enzyme	0.75
Br-dUTP	8
ddH_2O	32.25
Total	**51**

Table 7: DNA labelling solution

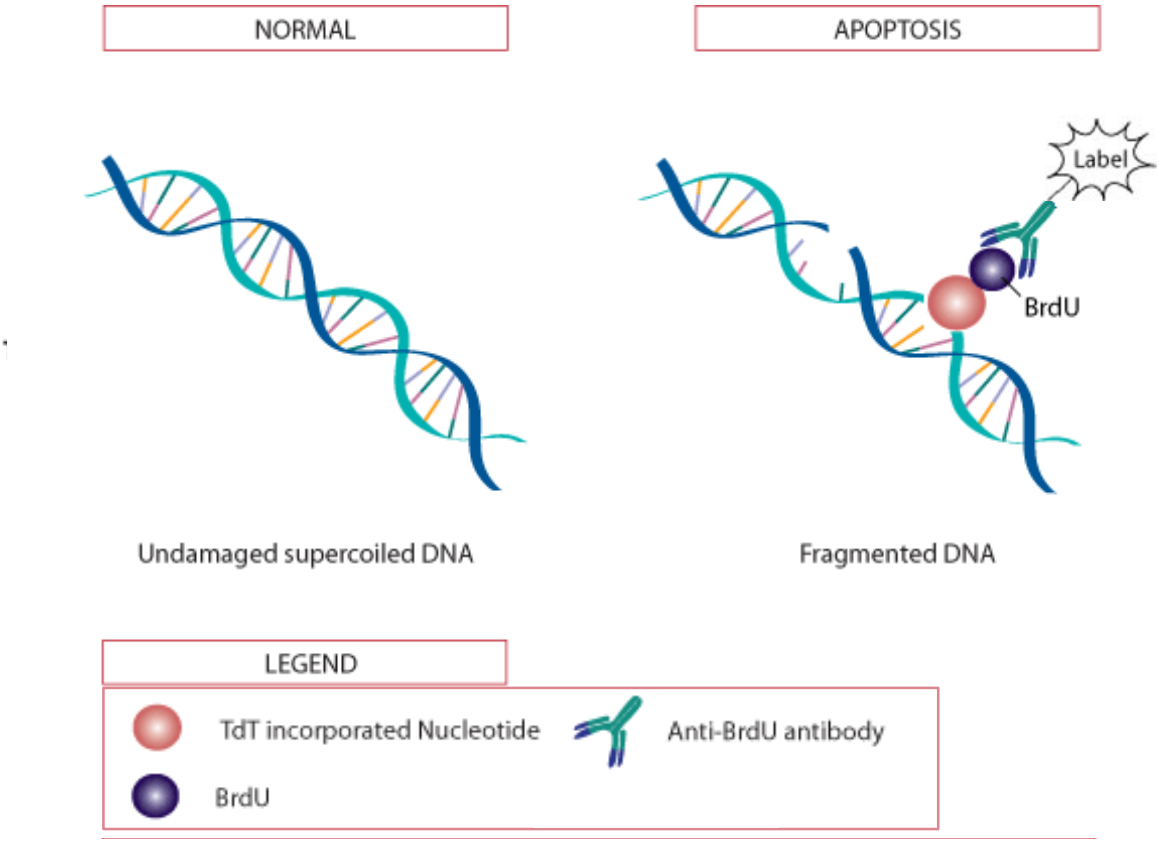

Figure 20: Principle of TUNEL assay(94)

2.9 Id-1 silencing and overexpression

The Id-1 silenced and Id-1 overexpressing P-STS cells were transfected and established by Florian Kleinegger.(63)

The plasmid utilised constructs were purchased from abm (Canada, Richmond).
In principle, P-STS cells were transfected with lentiviral vectors carrying 3 different constructs, which all expressed GFP, kanamycin and the Pac (puromycin N-acetyltransferase) gene as a general feature for further selection. The 3 constructs were(63):

- **Id-1:** Id-1 overexpressing construct
- **SiA:** Id-1 silencing siRNA (variant 1)
- **SiB:** Id-1 silencing siRNA (variant)

The efficiency of the transfection was verified with westernblots.(63)

2.10 Workflow – *in vitro* experiments

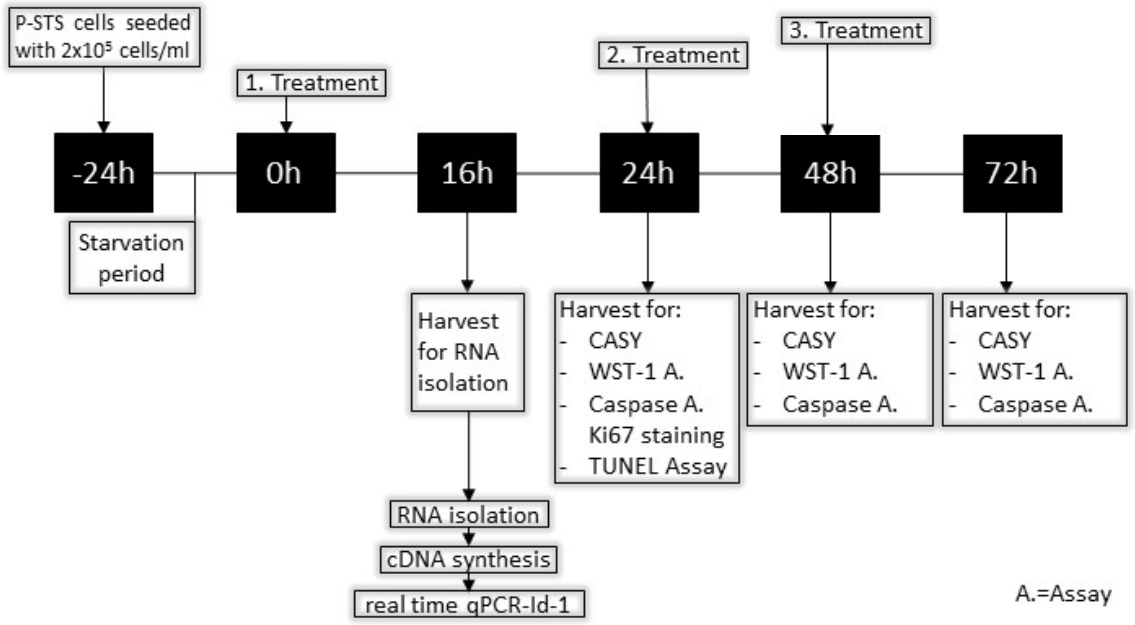

Figure 21: Workflow *in vitro* experiments

2.11 Chorioallantoic membrane assay

The chorioallantoic membrane (CAM), located beneath the eggshell, is an extra-embryonic tissue layer, responsible for oxygenation and waste storage in eggs of birds and reptiles. It develops from the chorion and the allantois, two mesenchymal membranes, fusing together on day 7 to form the chorioallantoic membrane – resembling the placenta in mammals. The chorioallantoic membrane is fully developed on day 10 after incubation, consisting of three distinct layers: the primary stratum, the capillary plexus and a thin stratum composed of specialised chorionic epithelial cells.(95)

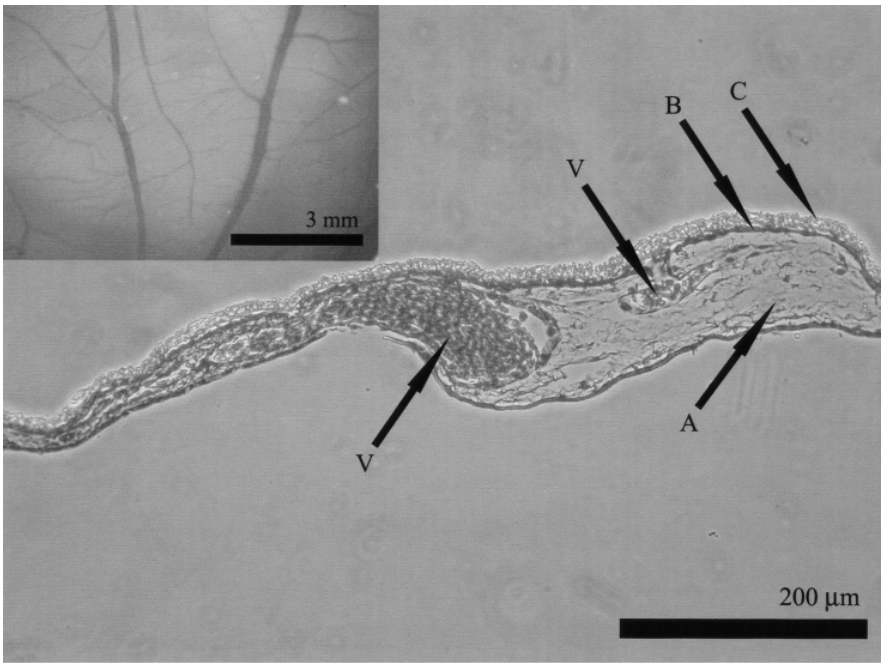

Figure 22: Cross-section of CAM. Primary stratum (A), thin stratum (B), inner shell membrane (C), blood vessels (V)(95)

The good vascularisation through the capillary plexus, the immunodeficiency of the chick embryo and nutrient-rich environment make the chorioallantoic an ideal model for implanting tumour cell xenografts onto the surface and analysing tumour growth, invasion and angiogenesis.

There are two different approaches to CAM assays: the *ex ovo* and the *in ovo* method. For the *in ovo* method, a small window is cut into the eggshell to access the CAM, whereas for the *ex ovo* method, the egg shell is broken and the egg is then further cultivated in a sterile container. In this study, the *ex ovo* method was used, because of the better visibility and accessibility of the graft site.

Fertilised white leghorn eggs (Schropper, Gloggnitz) were washed with 5% H_2O_2. The eggs were then incubated for 3 days at 37.6 °C, 5% CO_2 and 70–75% humidity, while being turned mechanically. On day 3, the eggs were cracked and transferred into a sterile container (weigh boats covered with a plastic petri dish lid) and incubated under the same conditions as previously for 7 further days. After 10 days, 500 µM high silicone rings (Ø 5 mm) were placed onto the CAM. A solution of $1x10^6$ P-STS cells, suspended in 15 µL of a 1:3 mixture of Matrigel in CMF-PBS, was transferred into these rings. The tumour cells were incubated for 24 hours and 15 µl WIN-55,212-2 was added in the respective concentrations every 24h over a course

of 3 days. As control, part of the xenografts was treated with a solution containing DMSO solved in distilled water, without WIN-55,212-2.

2.11.1 CAM assay – macroscopic analysis of the xenografts

2.11.1.1 Morphology

To investigate the effect of WIN-55,212-2 on *in vivo* tumour morphology, P-STS xenografts were photographed and the tumour growth pattern was assessed. Tumours were divided into two groups, according to their growth patterns: solid growth or diffuse growth pattern. The division into the two groups was based on the criteria we established (see table 8 for details). For each criterion, 0–1 points were awarded. Tumours with <2 points formed the diffuse growth pattern group and tumours with >2 points formed the solid growth pattern group.

Criteria	Points
Solid appearance	1 pt
Defined borders	1 pt
CAM-vascular network not visible throughout tumour	1 pt
Distinct colour difference from surrounding tissue	1 pt
Total	**4 pt**

Table 8: Criteria for evaluating solid tumour growth

2.11.1.2 Surface area

The tumour surface area was calculated by measuring the surface area of the tumour surface with the CellSensDimension software. Using the ratio between tumour surface area and the known surface area of the silicone ring (78.54 mm^2), the effective tumour surface area could be calculated.(96)

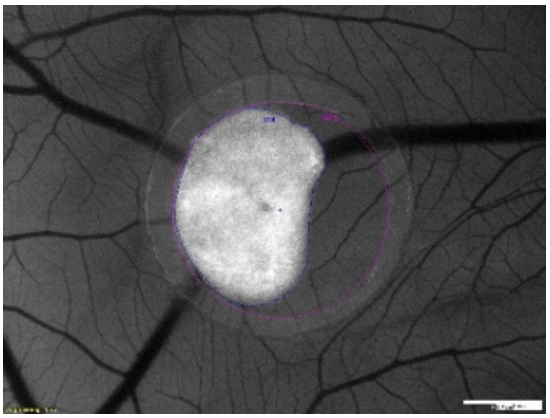

Figure 23: Measurement of the tumour surface area with the CellSensDimension software

2.11.1.3 CAM angiogenesis assay according to Quigley *et al.*(97)

This angiogenesis assay is based on the detection of newly formed blood vessels. In principle, the supernatant of tumour cell suspensions is retrieved after centrifugation and mixed with collagen. This mixture is then transferred onto a nylon mesh with 180-µm grid size, and the polymerised construct is then placed onto the chorioallantoic membrane. The neoangiogenesis is assessed after 72 hours, by calculating the ratio between the number of vascularised squares and the total number of squares of the mesh under the microscope.

Firstly, the Nitex nylon mesh is cut into 2x2 mm and 3x3 mm squares and UV radiated for 20 minutes. The squares are then placed on top of each other with the 3x3 mm squares underneath (see Figure 24).

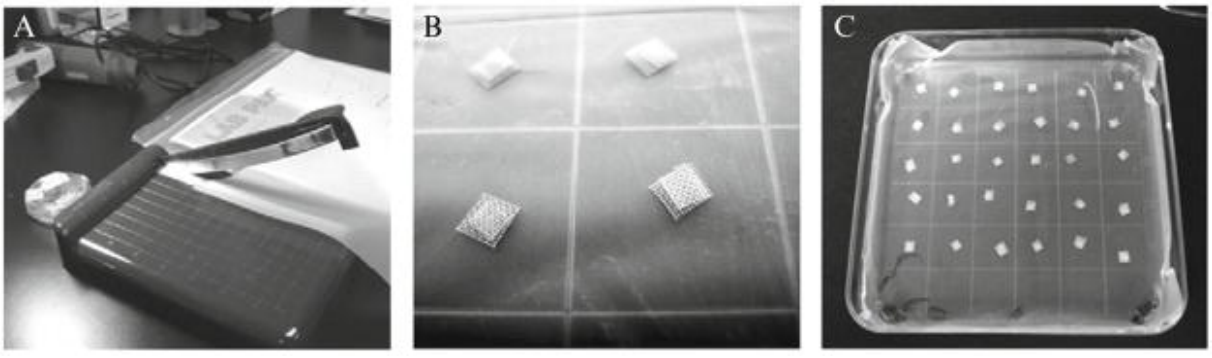

Figure 24: Preparation of the collagen meshes. A) cut 2x2 mm and 3x3 mm squares. B-C) Place squares on top of each other with the 3x3 mm square underneath.(97)

Subsequently, 50 µL of the Mastermix (see table 9) is transferred onto the grid and incubated at 37 °C for >30 min, to let the collagen polymerise. The construct is then transferred onto the CAM and incubated for further 72 hours (see Figure 25).

Substance	Volume [µL] (25 meshes)
MEM	75
Collagen 2 mg/ml	390.60
Hepes 1mM	7.5
NaOH 1M	30.0
P-STS cell supernatant	247.5
Total	**750.0**

Table 9: Mastermix for collagen meshes

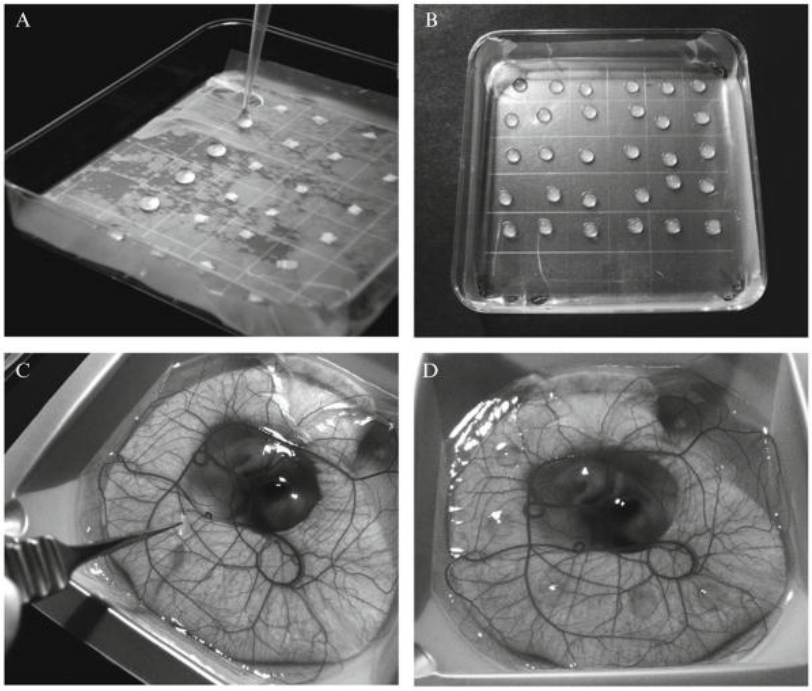

Figure 25: A-B) Meshes with Mastermix after >30 min incubation at 37 °C. C-D) Placement of collagen meshes onto the CAM(97)

The neoangiogenesis is measured under the stereomicroscope (Olympus SZX16) by calculating the ratio of the number of vascularised squares (see Figure 26) to the total number of squares of the upper mesh.

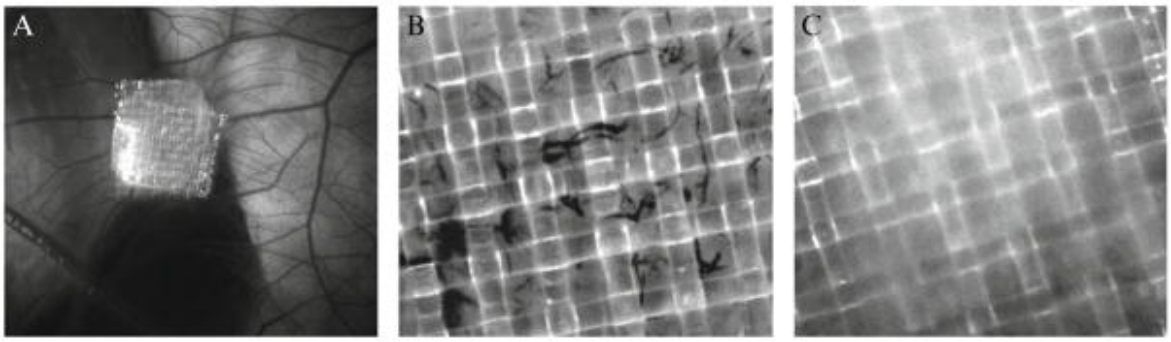

Figure 26: Analysis of collagen onplant results. A) Collagen mesh on CAM. B) vascularised cells. C) Unvascularised cells.(97)

2.11.1.4 Angiogenesis according to Ribatti *et al.*(98)

To examine the *in vivo* tumour angiogenesis upon treatment with WIN-55,212-2, we used 3 different macroscopic semiquantitative angiogenetic response scoring systems suggested by Ribatti *et al.*(98)

1.) Absolute number of converging blood vessels: The number of blood vessels converging towards the xenograft was counted every 24 hours after implantation and compared with the control.(98)

2.) Density of blood vessels close to the graft site: To score the density of blood vessels in the proximity of the graft site, arbitrary values from 0–5 were assigned to different levels of density. 0 describes an unchanged vascular network, 1 a slight increment in the density of the vascular network and the values 2–5 correspond to a gradual increase in density.(98) (see figure 27 for the macroscopical morphology of the respective values)

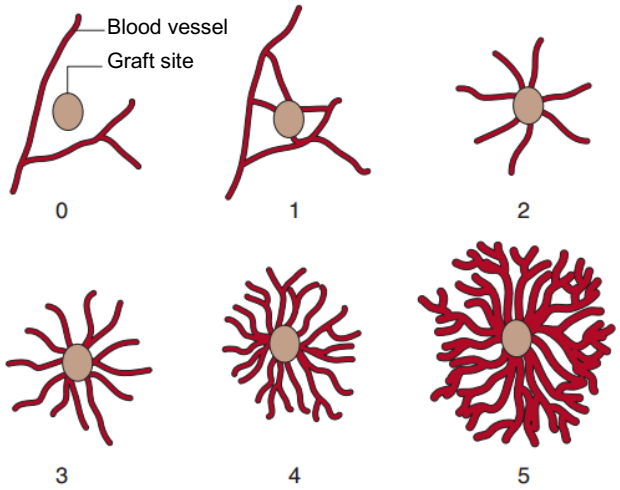

Figure 27: Angiogenetic response – vessel density macroscopic scoring system. Each value from 0–5 corresponds to a vascular network density.(98)

3.) Blood vessel branching: The blood vessels that were converging towards the graft and contained in a 1 mm diameter ring superimposed on the graft were scored from 0–2 according to their branching pattern. 2 points are assigned to vessels branching outside of the 1 mm Ø ring, 1 point was assigned to vessels without branches and which formed an angle of less than 45° with the edge of the implant, and 0 points were assigned to vessels without branches and which formed an angle of less than 45° with the edge of the implant.(98)

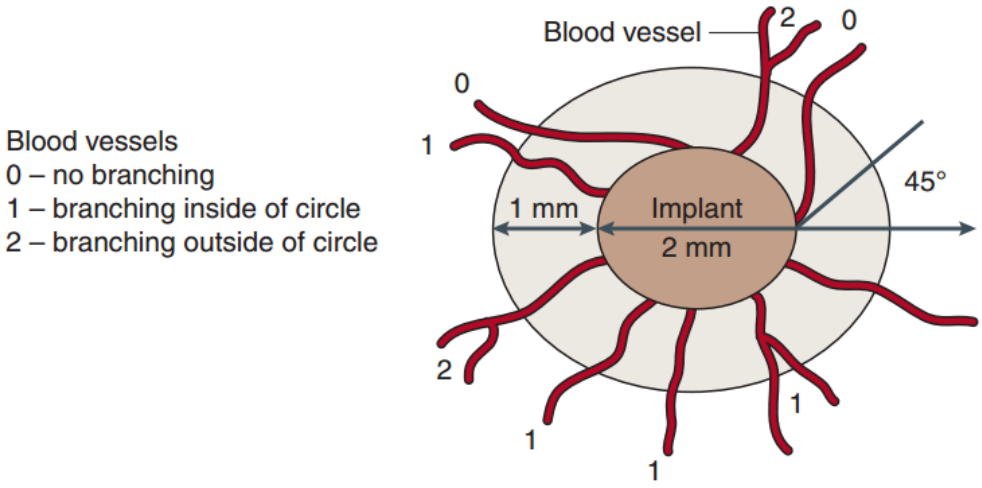

Figure 28: Angiogenetic response – vessel branching macroscopic scoring system. Blood vessels were assigned points from 0–2 according to their branching pattern.(98)

2.11.2 CAM assay – microscopical analysis of the xenografts

2.11.2.1 Tissue processing – harvesting, fixation, embedding and cutting

Tissue harvesting:

After 72 hours, the tumours and the surrounding tissue was excised using sterile surgical equipment.

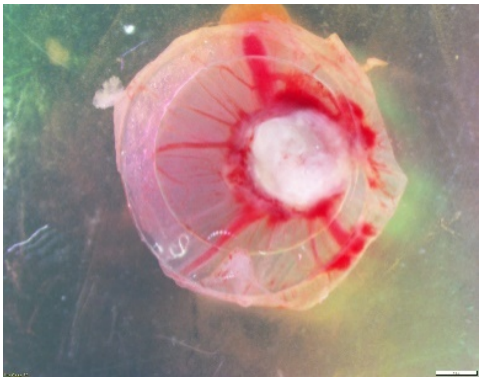

Figure 29: Harvested xenograft with the P-STS cell tumour and the surrounding tissue.

Reagent	Duration
70% Ethanol	30
95% Ethanol	30
95% Ethanol	15
100% Ethanol	30
100% Ethanol	15
Toluene	30
Toluene	15
Parafine #6	30
Parafine #9	30

Table 10: Dehydration and paraffination protocol

Fixation and dehydration:

The harvested tissue was then washed in 3 ml PBS and transferred into a solution with 3 ml PFA for 16 hours to fixate the tissue. After the incubation in PFA, the tissue was then passed through an ascending alcohol series and toluene to dehydrate the tissue, followed by incubation steps in #6 Paraffin and #9 Paraffin. (for the detailed dehydration and paraffination, see table 10)

Embedding and cutting:

The tissue was then embedded in Paraffine #9 using tissue moulds. Paraffin sections were cut with the Microtome MICROM HM335E and transferred onto slides.

2.11.2.2 Tumour dimensions and invasion

To quantify the dimensions and the invasiveness of the P-STS cell tumours upon treatment with WIN-55,212-2, the tissue sections through the largest portion of the tumours were selected and stained with a fluorescence labelled lens culinaris agglutinin (LCA), purchased from Vector Laboratories (Burlingame, United States). LCA binds to α-linked mannose and therefore stains the chorioallantoic membrane. The staining protocol consists of 1 hour incubation with the LCA antibody and 20 min incubation with DAPI. (for the detailed protocol, see table 11)

Reagent	Time
LCA	60 min
PBS	3x2 min
DAPI	20 min
PBS	3x2 min

Table 11: LCA fluorescence staining protocol

The result was viewed with the Olympus BX53 fluorescence microscope. The tumour and CAM dimensions were then measured with the CellSensDimensions software purchased from SFL (Stallhofen, Austria).

2.11.2.3 Immunofluorescence – Ki67 staining and TUNEL assay

To show the effects of WIN-55,212-2 on the *in vitro* mitosis and apoptosis rate, Ki67 stainings and TUNEL assays were performed on CAM tissue sections.

P-STS tumour cells were xenografted onto the chorioallantoic membrane and treated as described in 2.11.1. After 3 days, the tissue was then harvested, fixated, embedded and cut into sections (see 2.11.2.1). The parafined tissue sections were then deparafined by passing them through a descending alcohol series. (For detailed steps see Table 12)

Reagent	**Duration**
Xylol	10
Xylol	10
100% Ethanol	5
100% Ethanol	5
95% Ethanol	5
95% Ethanol	5
70% Ethanol	5

Table 12: Deparafination protocol

After the deparafination, immunofluorescence staining for Ki67 and TUNEL assays were performed as described in 2.8. The result was viewed with the Olympus BX53 fluorescence microscope and statistical analyses were performed with the GraphPad Prism.

2.12 Workflow – *in vivo* experiments

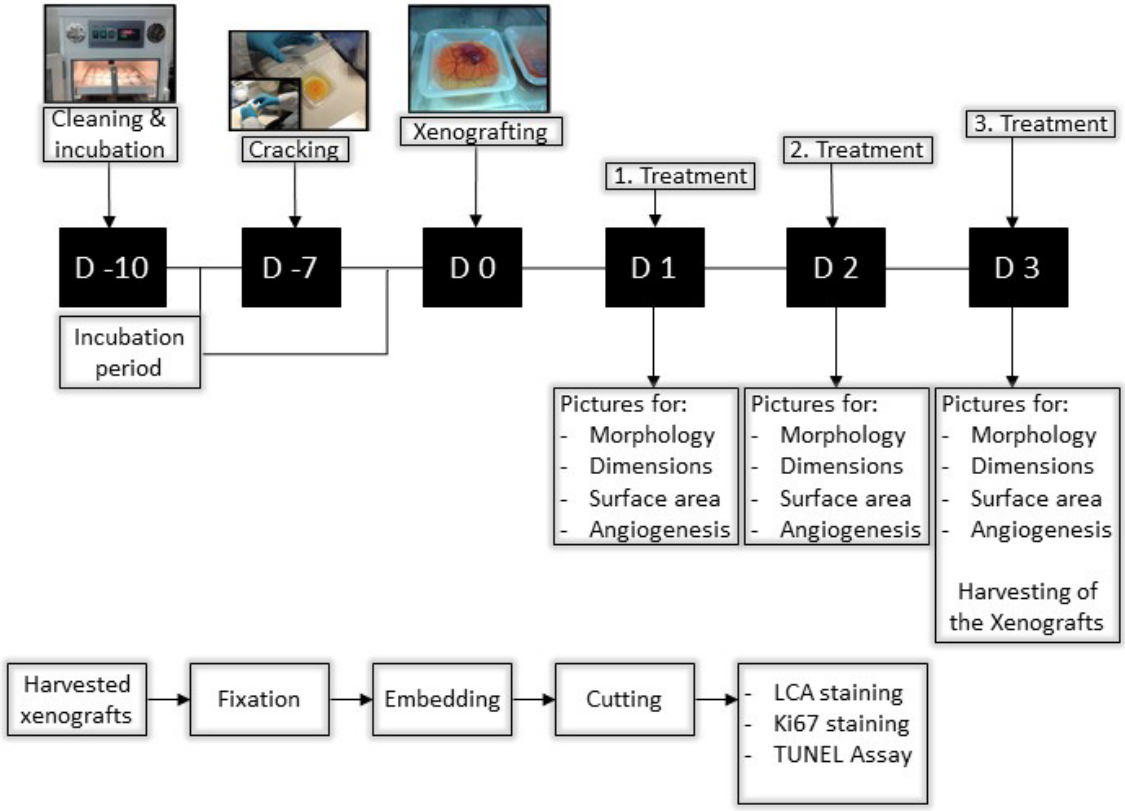

Figure 30: Workflow – *in vivo* experiments

3 Results

3.1 *In vitro* experiments

3.1.1 Starving conditions with Ham's medium and 1% FBS do not affect the proliferation of P-STS cells

To determine the optimum FBS concentration for cell starving, we assessed the cell proliferation in Ham's medium with decreasing FBS concentrations and in Opti-MEM® (minimal essential medium) (Thermo Fisher Scientific, Massachusetts). The P-STS cells were harvested as described in 2.1.2 and resuspended in the various cell culture media. Ham's medium with FBS concentrations of 10%, 1%, 0.5% and 0.1% and Opti-MEM® were used as cell culture media. Subsequently, the cells were seeded in 24-well plates at a concentration of $2x10^5$ cells per well. To assess changes in cell proliferation, the cell count was measured after 24h, 48h and 72h using the CASY® Cell Counter as described in 2.5. As control we used standard Ham's medium with 10% FBS.

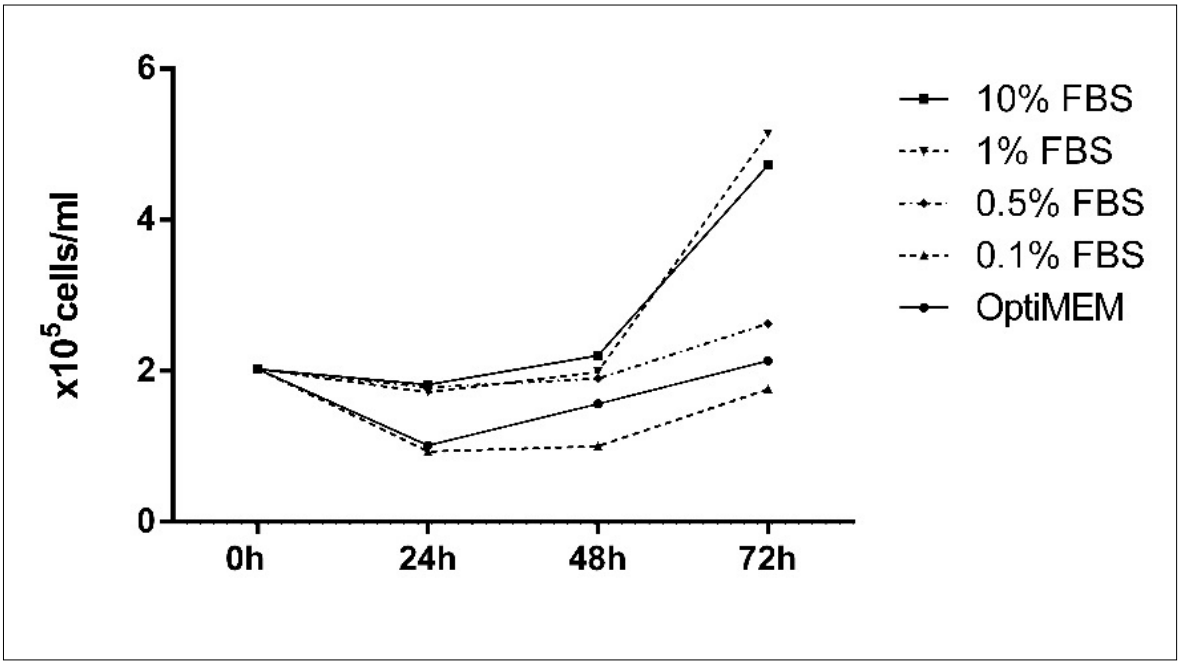

Figure 31: The cell count of P-STS cells incubated under starvation conditions in Ham's medium with 1% FBS was not significantly reduced compared to the control (Ham's medium with 10% FBS). The cell count was, however, significantly reduced with FBS concentrations under 1% and Ham's.

The growth curves of cells grown in Ham's medium with 10% and 1% FBS were nearly identical, whereas the growth curves of cells grown in Ham's medium with

under 1% FBS and cells grown in Opti-MEM®, were much flatter than the growth curve of the control.

During the incubation period of 3 days, lower FBS concentrations and Opti-MEM® lead to a reduced cell count. To represent the results more clearly, we normalised the cell counts at the respective time points to the control.

After 24 hours the cell count of P-STS cells incubated in Ham's medium with 0.1% and in Opti-MEM® was significantly reduced (p=0.05), whereas the cell count of cells incubated in Ham's medium with over 0.1% FBS did not differ significantly from the control. (Ham's medium with 1% FBS: 0.943 fold; 0.5% FBS: 0.979 fold; 0.1% FBS: 0.514 fold; Opti-MEM®: 0.557 fold – compared to the control)

The cell count of cells incubated in Ham's medium with 0.1% and in Opti-MEM® was again significantly reduced (p=0.05) after 48 hours, whereas the cell count of cells incubated in Ham's medium with over 0.1% FBS was not affected by the starving conditions. (Ham's medium with 1% FBS: 0.902 fold; 0.5% FBS: 0.862 fold; 0.1% FBS: 0.455 fold; Opti-MEM®: 0.708 fold – compared to the control)

After 72 hours the cell count of cells incubated in Ham's medium with under 0.5% FBS, and in Opti-MEM® was significantly reduced (p=0.05), whereas the cell count in Ham's medium with 1% FBS was not affected by the starving conditions. (Ham's medium with 1% FBS: 1.088 fold; 0.5% FBS: 0.556 fold; 0.1% FBS: 0.372 fold; Opti-MEM®: 0.451 fold – compared to the control) We therefore chose to use cell culture medium containing 1% FBS for our experiments.

3.1.2 CB1 and CB2 receptors are expressed by P-STS cells

3.1.2.1 Cannabinoid receptor expression

To establish whether cannabinoid receptors are expressed by the cell line P-STS, we measured the relative mRNA expression of CB1, CB2 and GPR55 receptors with qPCRs. The mRNA was isolated from P-STS cells (see 2.3.1) and cDNA templates were synthesised (see 2.3.2). Then real-time qPCRs were performed as described in 2.3.5.

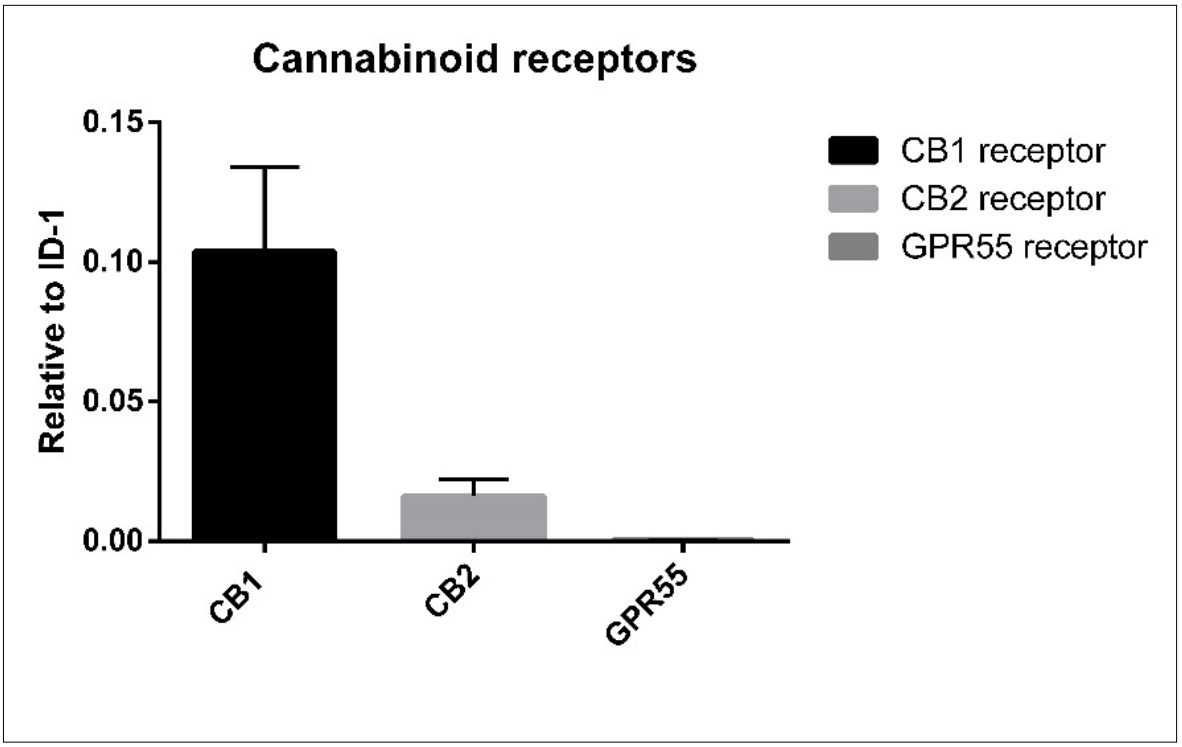

Figure 32: Cannabinoid receptor expression in P-STS: CB1 and CB2 receptors are expressed by P-STS, whereas no GPR55 expression could be detected.

Relative to Id-1, a highly expressed protein in P-STS,(87) both CB1 and CB2 receptors were expressed by P-STS cells, whereas GPR55 receptors were not expressed significantly.

3.1.2.2 Id-1 and cannabinoid receptors are upregulated in 3D P-STS cell spheroids

To examine whether the expression of cannabinoid receptors varies between 2D and 3D cultivation, RNA was isolated from P-STS cells grown in 2D and from P-STS cells grown in 3D spheroids. (see 2.4) Then cDNA was generated from the isolated RNA and further analysed by RT-qPCR (see 2.3.1-2.3.3).

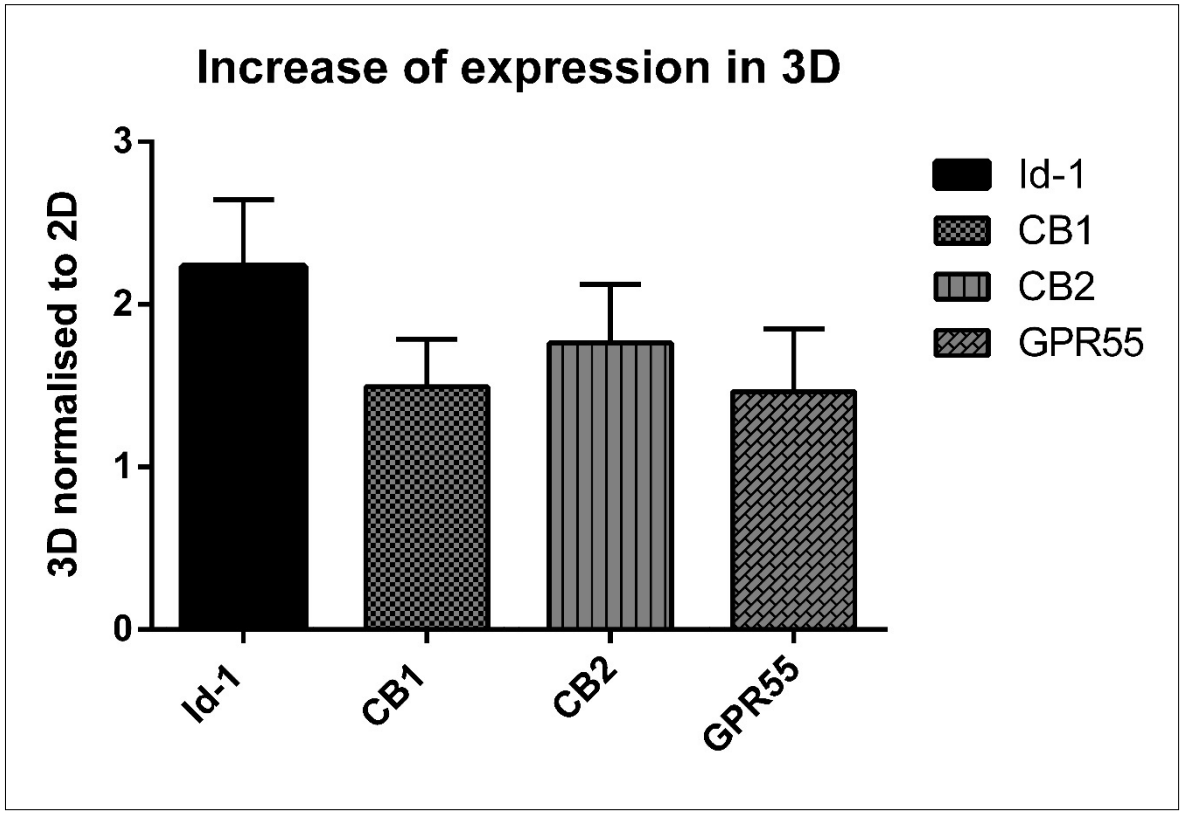

Figure 33: 3D receptor expression normalised to 2D expression. The Id-1 expression was increased significantly in 3D spheroids compared to cells grown in 2D, whereas the expression of cannabinoid receptors was not increased significantly (right).

The expression Id-1 was increased significantly (p=0.01) in 3D spheroids compared to conventional 2D cultivation. In contrast, CB1, CB2 and GPR55 receptors were not upregulated significantly in 3D spheroids, although a slightly increased expression could be observed. (Id-1: 2.23 fold; CB1 receptors: 1.49 fold; CB2 receptors: 1.76 fold; GPR55 receptors: 1.46 fold – increase from 2D to 3D)

3.1.3 Treatment with WIN-55,212-2 leads to a concentration dependent reduced proliferation of P-STS cells.

3.1.3.1 WIN-55,212-2 reduces the cell growth of P-STS cells.

To examine whether WIN-55,212-2 leads to a reduced cell count in the small intestine neuroendocrine tumour cells, PSTS-cells were seeded, starved (see 2.1.3) and treated with the respective concentrations of WIN-55,212-2 (see 2.2). The cells were then harvested (see 2.1.4) and the cell count was measured after 24h, 48h and 72h with the CASY® Cell Counter & Analyzer TTC (see 2.5).

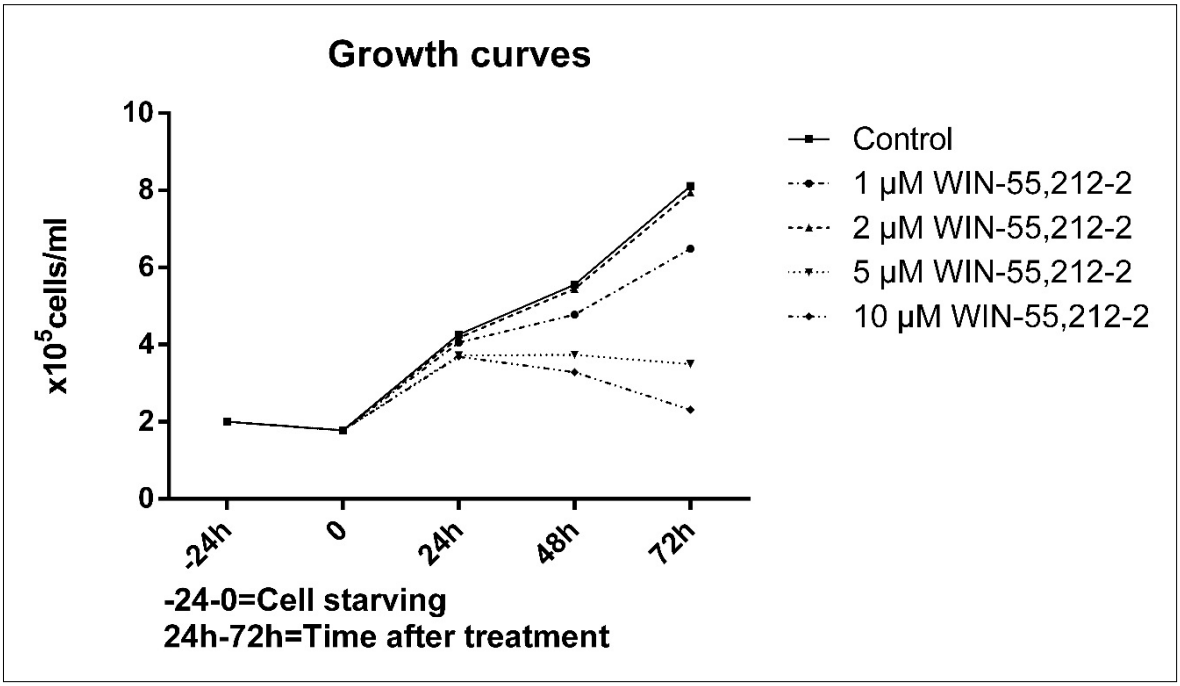

Figure 34: After treatment with WIN-55,212-2 P-STS cells showed a concentration-dependent reduced proliferation. No significant effect occurred at a concentration of 2 µM.

Over the incubation period of 3 days, the cell count was significantly reduced (p=0.0001) in P-STS cells treated with WIN-55,212-2 at concentrations between 1–10 µM. In P-STS cells treated with 2 µM WIN-55,212-2, the cell count remained unchanged compared to untreated cells. To present the results in detail and more clearly we normalised the various cell counts to the control.

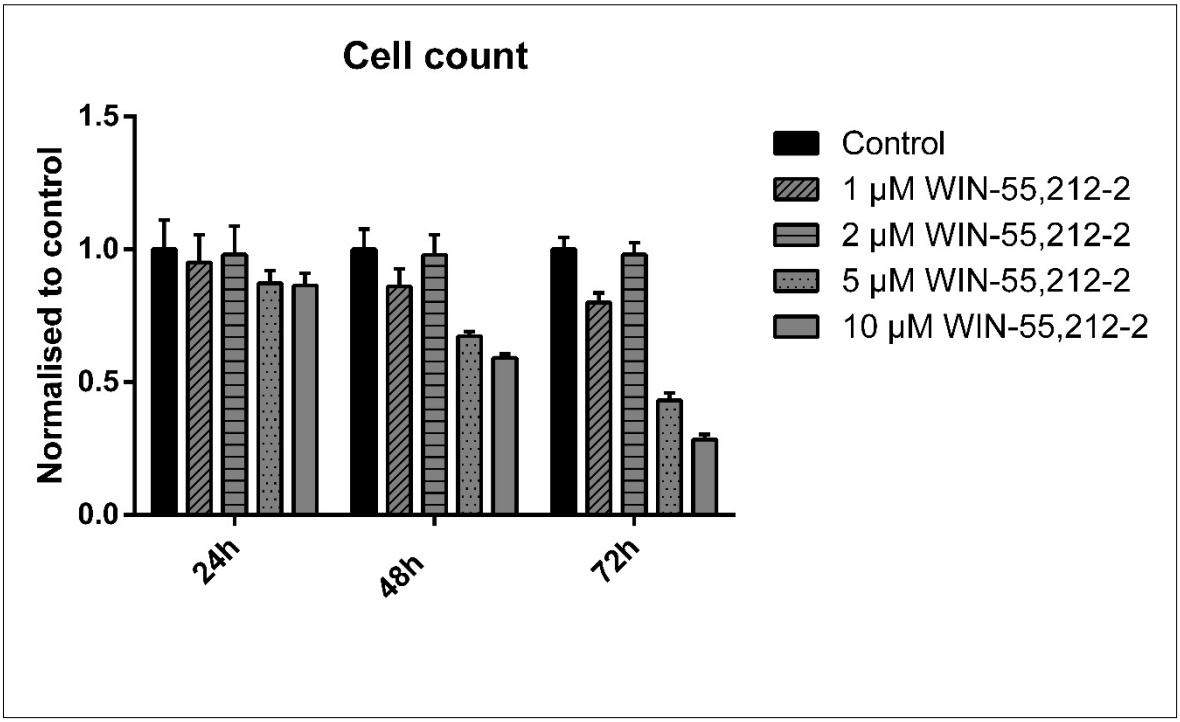

Figure 35: Cell count normalised to the respective control

After 24 hours, treatment with WIN-55,212-2 led to a significantly reduced cell count at 5–10 µM WIN-55,212-2. (p=0.05 respectively). In contrast, no effect occurred at 1–2 µM. (Control: $4.342x10^5$ cells/ml; 1 µM: $4.053x10^5$ cells/ml; 2 µM: $4.181x10^5$ cells/ml; 5 µM: $3.724x10^5$ cells/ml; 10 µM: 3.868 cells/ml)

The cell count was significantly reduced at 1 µM (p=0.01), 5 µM and 10 µM WIN-55,212-2 (p=0.0001, respectively) after 48 hours. No effect occurred in the population treated with 2 µM WIN-55,212-2. (Control: $5.554x10^5$ cells/ml; 1 µM: $4.777x10^5$ cells/ml; 2 µM: $5.443x10^5$ cells/ml; 5 µM: $3.737 x10^5$ cell/ml; 10 µM: 3.289 $x10^5$ cell/ml)

After 72 hours, treatment with WIN-55,212-2 led to a significantly reduced cell count at 1–10 µM WIN-55,212-2 (p=0.0001, respectively), except for 2 µM at which no effect occurred. (Control: $8.110x10^5$ cells/ml; 1 µM: $6.488x10^5$ cells/ml; 2 µM: $7.947x10^5$ cells/ml; 5 µM: $3.498x10^5$ cell/ml; 10 µM: $2.309x10^5$ cell/ml)

3.1.3.2 Treatment with WIN-55,212-2 leads to a reduced cell viability in P-STS cells

To investigate the effects of WIN-55,212-2 on cell viability, we performed WST-1 Assays (see chap. 2.6) on cells treated with WIN-55,212-2 after 24h, 48h and 72h. Prior to the experiments, P-STS cells were seeded, starved and treated as described in 2.1.3 and 2.2.

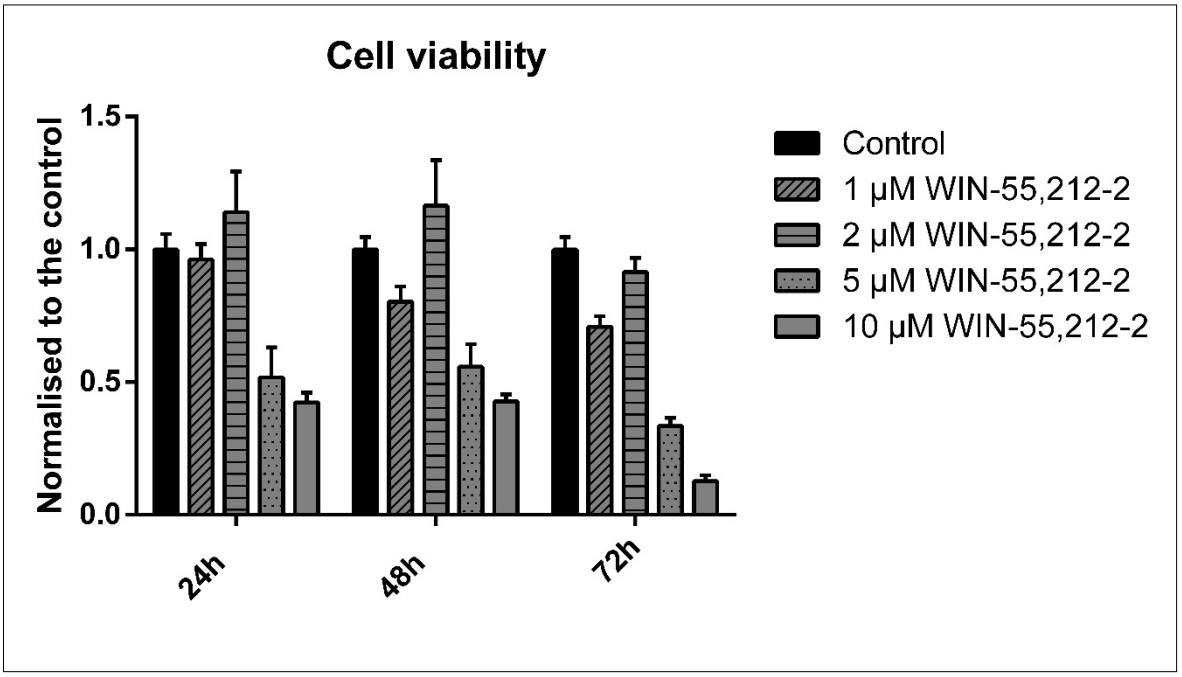

Figure 36: WST-1 Assay – cell viability (normalised to untreated cells)

After 24 hours, treatment with 5–10 µM WIN-55,212-2 reduced the cell viability significantly (p=0.0001, respectively). In contrast, the cell viability was significantly increased (p=0.05) upon treatment with 2 µM WIN-55,212-2, whereas no effect occurred at 1 µM. (1 µM: 0.962 fold; 2 µM: 1.141 fold; 5 µM: 0.518 fold; 10 µM: 0.424 fold – change of cell viability compared to the control)

The cell viability was significantly reduced at WIN-55,212-2 concentrations of 1–10 µM (p=0.001 at 1 µM; p=0.0001 at 5 and 10 µM respectively) after 48 hours, except for 2 µM. In contrast, the cell viability was significantly increased (p=0.01) upon treatment with 2 µM WIN-55,212-2. (1 µM: 0.804 fold; 2 µM: 1.164 fold; 5 µM: 0.558 fold; 10 µM: 0.427 fold – change of cell viability compared to the control)

After 72 hours, treatment with 1–10 µM WIN-55,212-2 reduced the cell viability significantly (p=0.0001, respectively), except for 2 µM, at which no effect occurred. (1 µM: 0.708 fold; 2 µM: 0.914 fold; 5 µM: 0.334 fold; 10 µM: 0.127 fold – change of cell viability compared to the control)

3.1.3.3 Treatment with WIN-55,212-2 leads to a decreased Ki67 labelling index

The Ki67 labelling index is frequently used to determine proliferation rates of tumour cells. To verify the effect of WIN-55,212-2 treatment on proliferation on a subcellular level, we performed Ki67 immunofluorescence staining on P-STS cells and calculated the Ki67 labelling index (Ki67 positive cells/total cell count) (see 2.8.1). Pictures for further analysis were taken with the Olympus BX53 fluorescence microscope and analysed statistically with GraphPad Prism. Figure 37 shows the positive and negative control of the Ki67 staining. There is a clear intranuclear signal in the positive control, whereas there is no signal in the negative control.

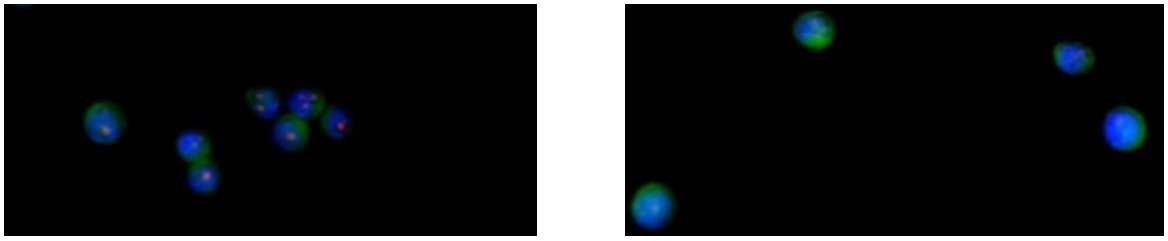

Figure 37: Ki67 staining positive control (left), negative control (right)

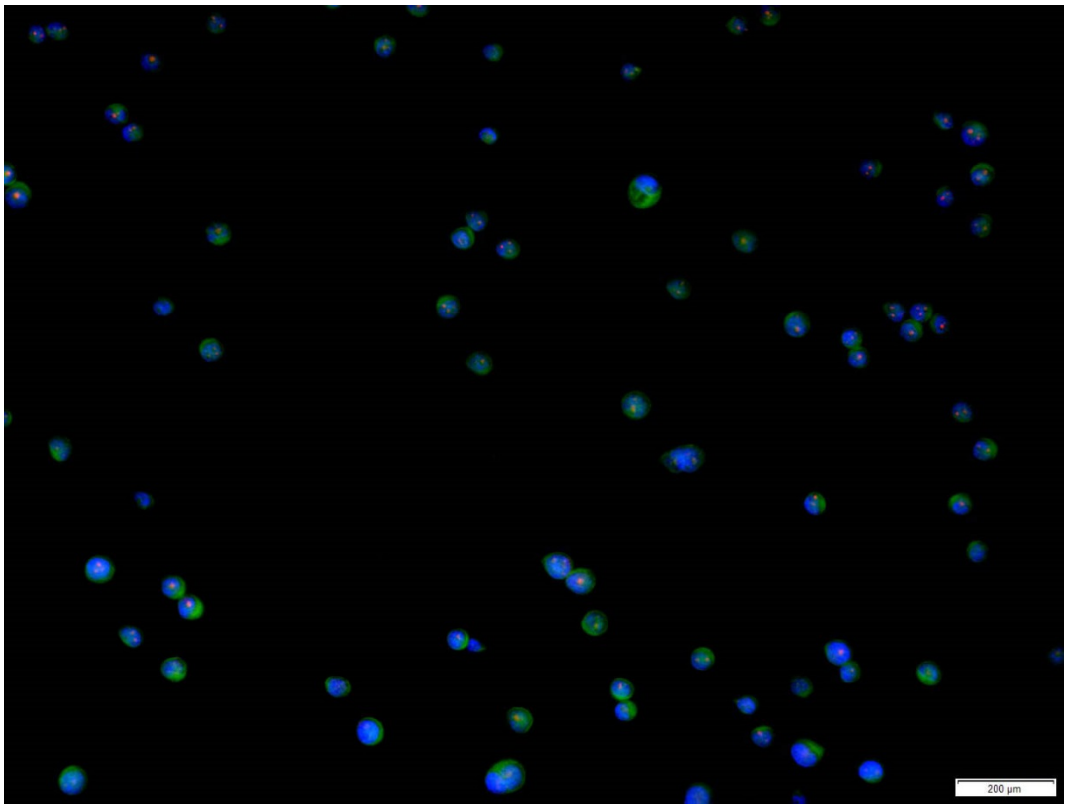

Figure 38: Ki67 immunofluorescence staining of untreated P-STS cells. More frequent Ki67 positive cells compared to the Ki67 staining of treated cells. Untreated P-STS cells have a homogenous morphology and there are two morphologically distinct cell fractions.

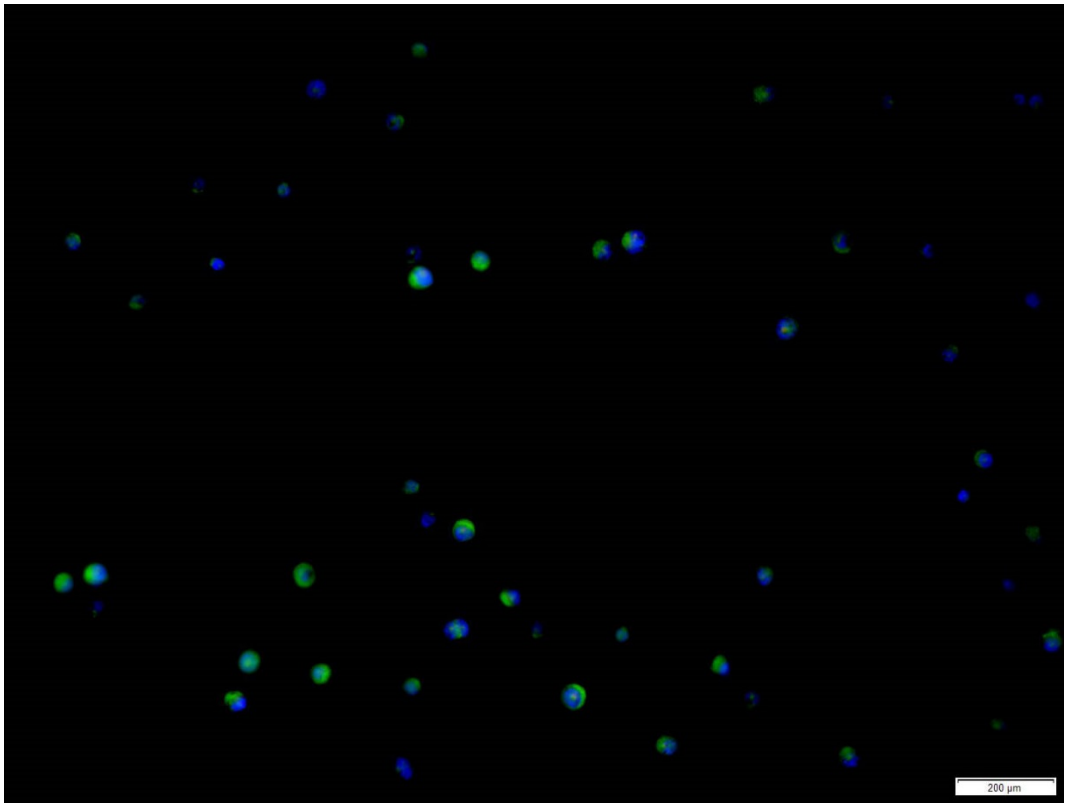

Figure 39: Ki67 immunofluorescence staining of P-STS cells treated with 5 µM WIN-55,212-2. Less frequent Ki67 positive cells compared to untreated cells. Treated P-STS cells have an irregular and heterogeneous morphology.

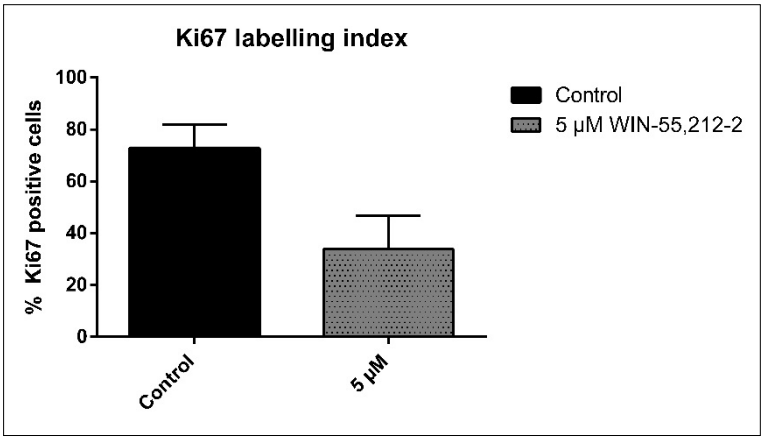

Figure 40: Statistical analysis – immunofluorescence staining. The Ki67 labelling index was significantly decreased in treated cells (p=0.0001).

From a morphological point of view, cells treated with WIN-55,212-2 for 24 hours were far more polymorph and had noticeably smaller nuclei compared to untreated cells. The Ki67 labelling index for untreated cells was 72.74% compared to 33.91% upon treatment with 5 µM WIN-55,212-2 (p=0.0001).

3.1.4 WIN-55,212-2 induces apoptosis in P-STS cells

3.1.4.1 Treatment with WIN-55,212-2 increases caspase 3/7 activity in the small intestine cancer cell line P-STS

To investigate whether WIN-55,212-2 induces apoptosis in the small intestine cancer cell line P-STS, we performed Caspase-Glo® 3/7 Assays (see 2.745) on P-STS cells. In principle, the caspase assay measures the induction of apoptosis by detecting the levels of activated caspases, a family of proteinases that play an essential role during apoptosis.

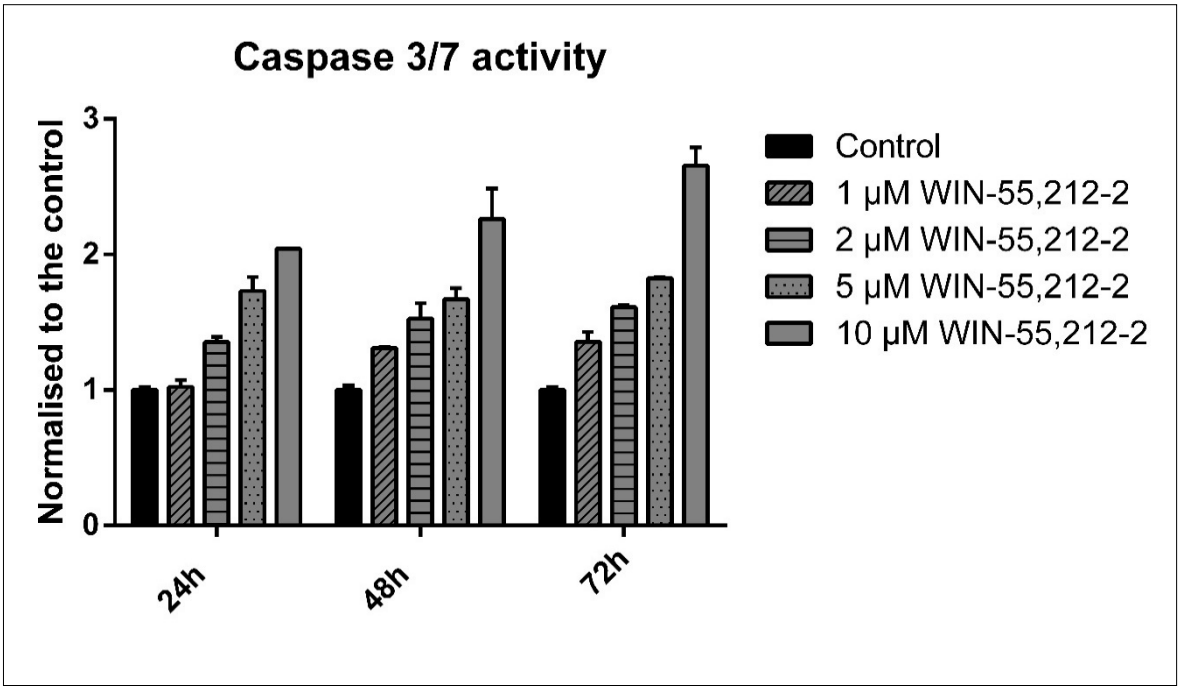

Figure 41: Caspase 3/7 activity normalised to the control. Treatment with WIN-55,212-2 increased the caspase 3/7 activity significantly.

After 24 hours, treatment with WIN-55,212-2 increased the caspase 3/7 activity significantly at concentrations of 2–10 µM (p=0.0001, for the respective concentrations). No effect occurred at 1 µM. (1 µM: 1.025 fold; 2 µM: 1.354 fold; 5 µM: 1.732 fold; 10 µM: 2.044 fold – increase of caspase activity compared to the control)

The caspase 3/7 activity was significantly increased (p=0.001 for 1 µM; P=0.0001 for 2, 5 and 10 µM respectively) at all concentrations of WIN-55,212-2 used after 48 hours. (1 µM: 1.310 fold; 2 µM: 1.527 fold; 5 µM: 1.671 fold; 10 µM: 2.262 fold – increase of caspase activity compared to the control)

After 72 hours, treatment with WIN-55,212-2 increased the caspase 3/7 activity significantly at all concentrations used (p=0.0001 respectively). (1 µM: 1.356 fold; 2 µM: 1.611 fold; 5 µM: 1.823 fold; 10 µM: 2.656 fold – increase of caspase activity compared to the control)

3.1.4.2 WIN-55,212-2 increases DNA fragmentation in P-STS cells

To investigate whether WIN-55,212-2 induces apoptosis in the small intestine cancer cell line P-STS, we performed *in situ* hybridisation TUNEL assays on P-STS cells (see 2.8.2 for details). The ratio between TUNEL positive cells and the total number of cells was then calculated.

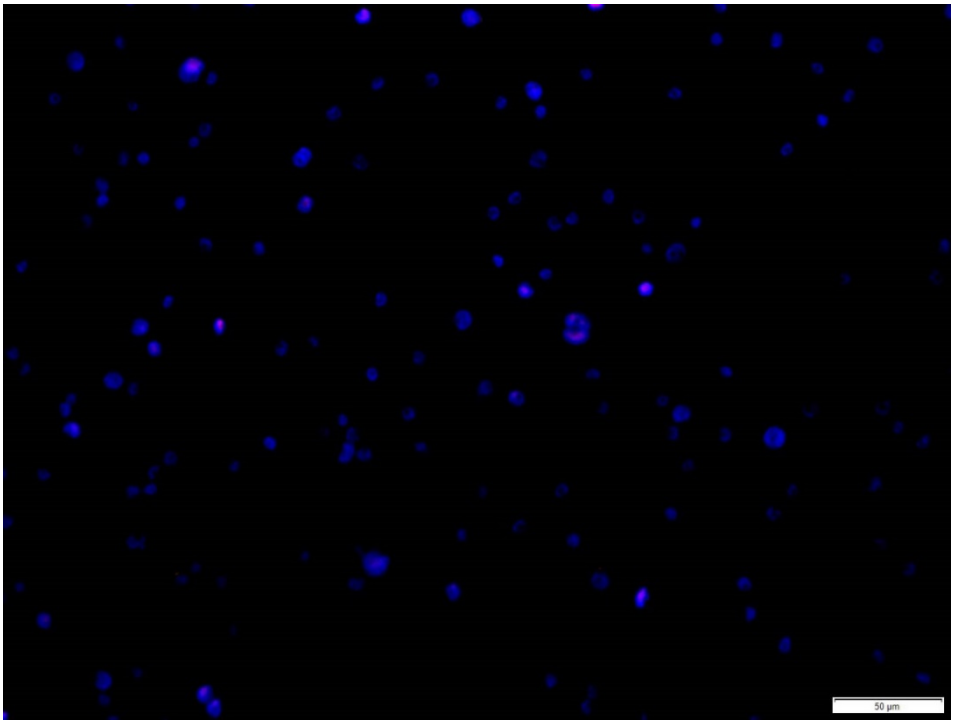

Figure 42: *In situ* hybridisation TUNEL assay of untreated P-STS cells

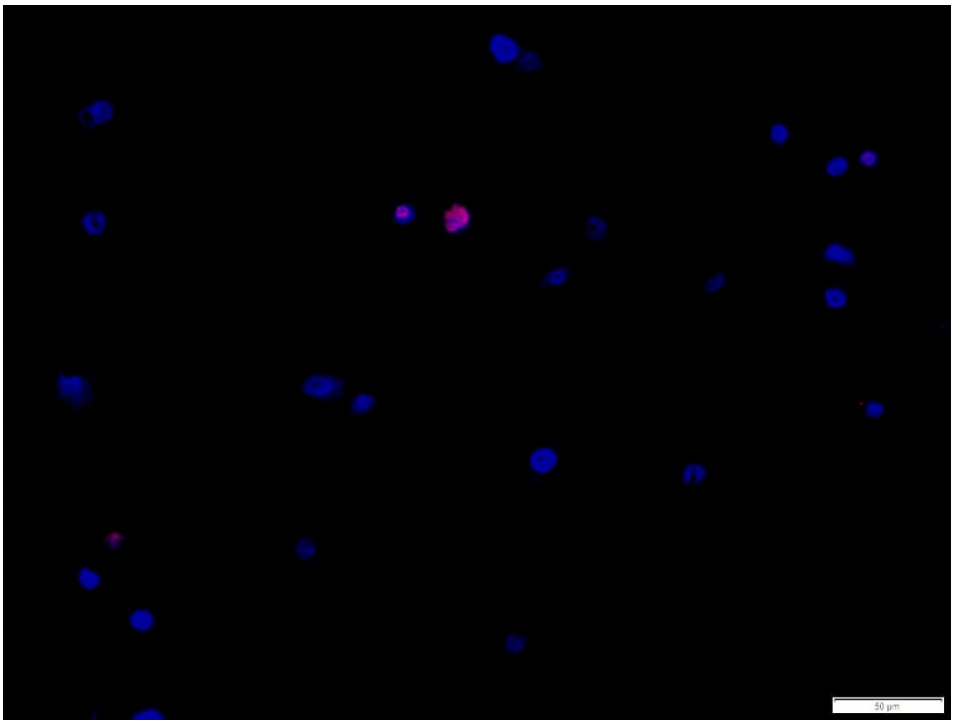

Figure 43: *In situ* hybridisation TUNEL assay of P-STS cells treated with 5 µM WIN-55,212-2

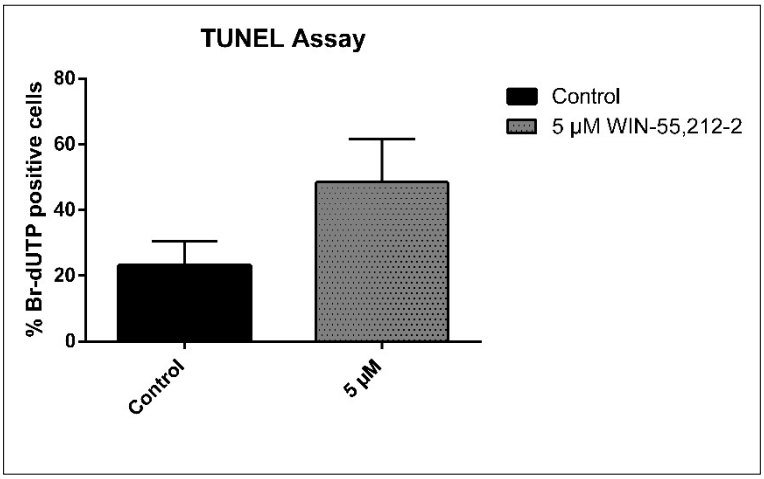

Figure 44: Statistical analysis of *in situ* hybridisation TUNEL assays

Macroscopically, more cells were Br-dUTP positive in the population treated with 5 µM WIN-55,212-2. From a morphological point of view, cells treated with WIN-55,212-2 were far more polymorph and had noticeably smaller nuclei compared to untreated cells. The percentage of Br-dUTP positive cells was 23.01% in untreated cells, compared to 48.52% in cells treated with 5 µM WIN-55,212-2. The Br-dUTP uptake was therefore significantly increased (p=0.0001) in treated cells.

3.1.5 WIN-55,212-2 increases neoangiogenesis *in vitro*

3.1.5.1 WIN-55,212-2 treatment increases pro-angiogenetic factors secreted by P-STS cells

To investigate whether WIN-55,212-2 inhibits proangiogenetic factors in P-STS cells, we assessed neoangiogenesis induced by tumour factors, retrieved *in vitro*, according to Quigley *et al.*(97) (see 2.11.1.3 for further details).

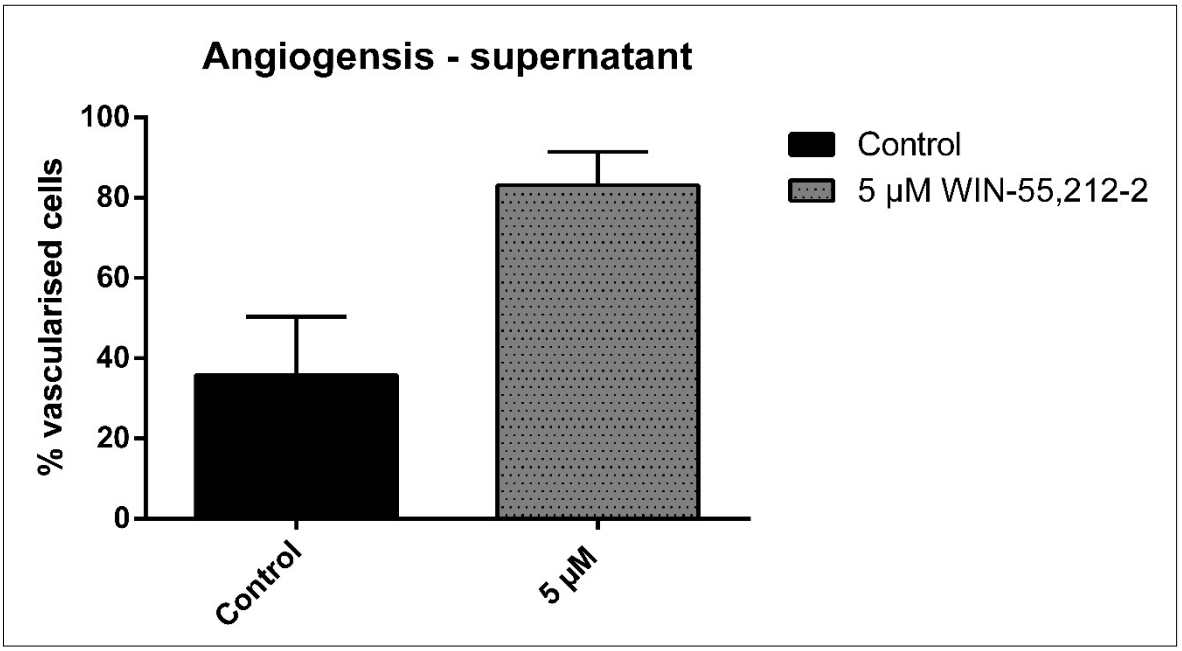

Figure 45: Neoangiogenesis was significantly increased (p=0.0001) with supernatant retrieved from treated cells.

Neoangiogenesis was significantly increased (p=0.0001) in grids with the supernatant of P-STS cells treated with 5 µM WIN-55,212-2. Treatment with WIN-55,212-2 led to a vascularisation of 83.15% of the cells, whereas only 35.77% of the cells in the control were vascularised.

3.2 *In vivo* experiments

3.2.1 WIN-55,212-2 treatment affects tumour growth and morphology of P-STS cell xenografts

3.2.1.1 WIN-55,212-2 induces a more diffuse tumour growth pattern

To observe whether treatment with WIN-55,212-2 changes the growth pattern of tumours, P-STS cell xenografts were treated with WIN-55,212-2, and the tumours formed after a 3-day incubation period were graded according to the criteria listed

in figure 46 and 47 (for detailed score, see table 8, chapter 2.11.1.1). Subsequently, the tumours were divided into two groups: solid growth pattern and diffuse growth pattern, according to their score.

Solid growth pattern	Morphology
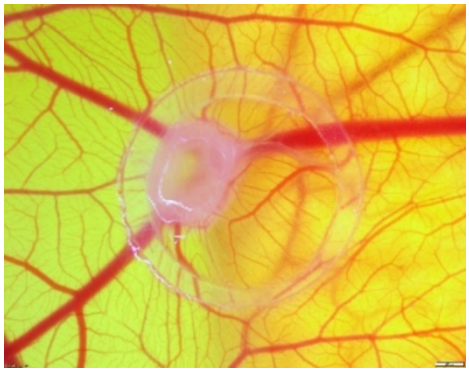	Solid appearance Regular borders CAM-vascular network not visible through the tumour Dense colour

Figure 46: Morphological criteria of solid tumour growth pattern

Diffuse growth pattern	Morphology
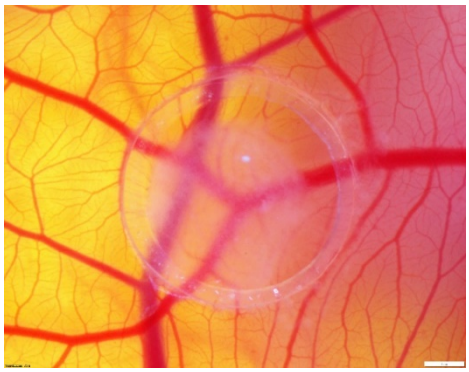	Diffuse appearance Irregular borders CAM-vascular network visible through the tumour Opaque colour

Figure 47: Morphological criteria of diffuse tumour growth pattern

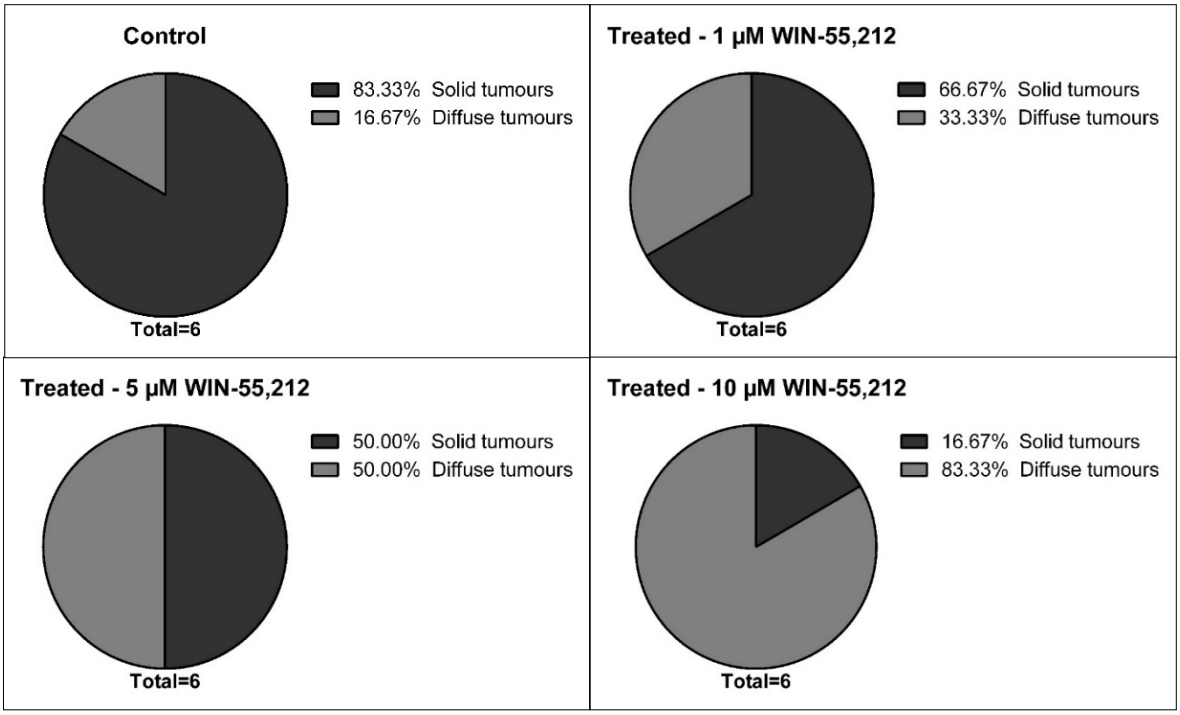

Figure 48: Comparison of solid tumour growth to diffuse tumour growth pattern of P-STS cell tumours treated with different concentrations of WIN-55,212-2

The percentage of P-STS cell tumours with solid tumour growth patterns decreased proportionately to the WIN-55,212-2 concentration applied.

After 3 days, untreated P-STS cell tumours formed solid tumours in 83.33% of the cases, whereas only 66.67% of the tumours treated with 1 µM WIN-55,212-2 were solid tumours. Additionally, treatment with 5 µM WIN-55,212-2 led to a solid tumour growth pattern in 50%, whereas the tumours treated with 10 µM WIN-55,212-2 formed solid tumours in only 16.67% of the cases.

3.2.1.2 Xenografts treated with WIN-55,212-2 have a larger surface area

Changes of the tumour surface area could indicate an *in vivo* effect of WIN-55,212 on P-STS cell tumours. We therefore determined the surface area of tumours formed on the CAM after 24h, 48h and 72h (see 2.11).

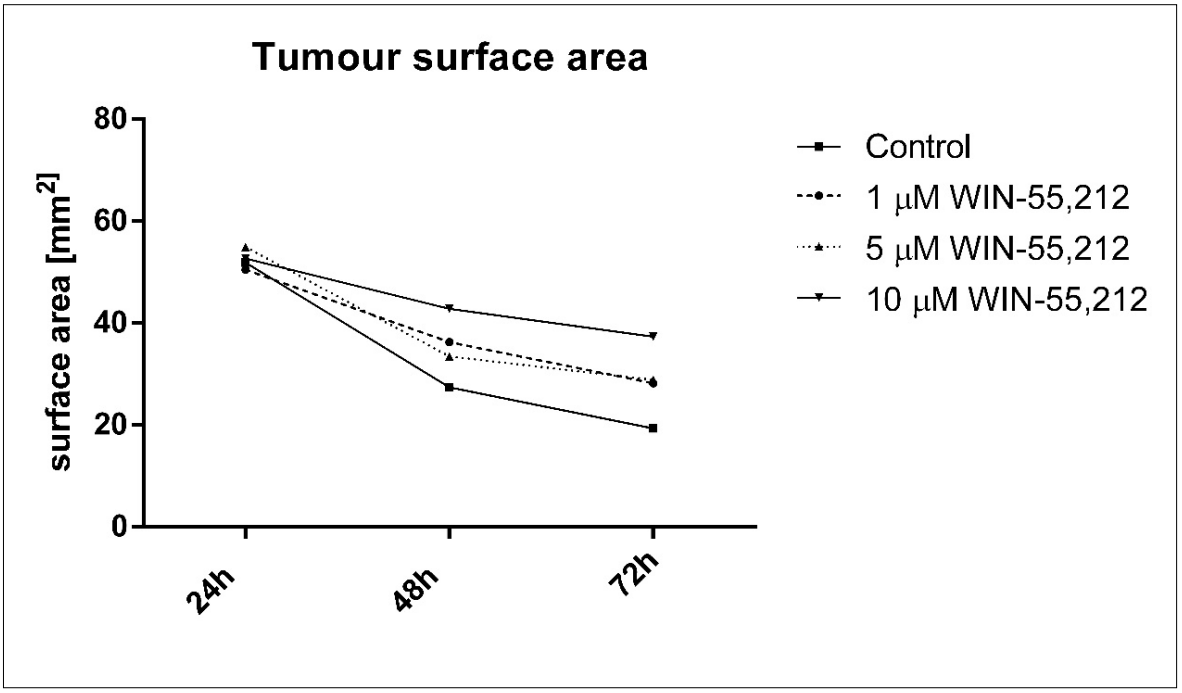

Figure 49: Tumour surface area upon WIN-55,212 treatment

P-STS cell tumours treated with WIN-55,212 generally displayed a slower reduction of their surface area than untreated tumours (Figure 49).

After the 24-hour incubation period, no significant difference of surface area could be observed between the different tumours.

The surface area of tumours treated with 1 µM WIN-55,212 was significantly larger, by 8.82 mm^2 after 48 hours and, although not statistically significant, by 8.92 mm^2 after 72 hours, compared to the control.

The P-STS cell tumours treated with 5 µM WIN-55,212 had a significantly larger surface area than untreated tumours. The mean difference was 6.03 mm^2 after 48 hours and 9.55 mm^2 after 72 hours, compared to the control. Treatment with 10 µM WIN-55,212 also led to a significantly larger surface area. The mean difference was 9.53 mm^2 after 48 hours and 13.54 mm^2 after 72 hours.

3.2.1.3 WIN-55,212-2 inhibits the rate of tumour surface area reduction

The mean change of surface area per day was calculated from the data in the previous chapter (3.2.1.2) and compared to the change of surface area in untreated tumours.

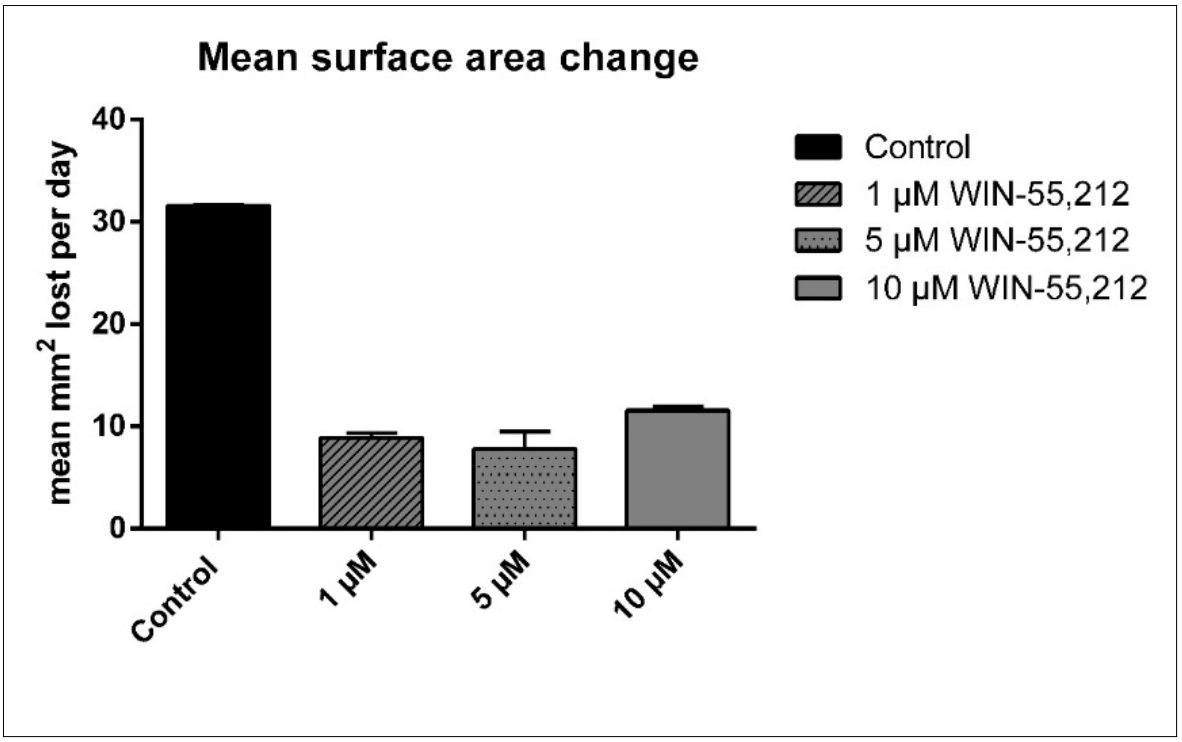

Figure 50: Mean change of surface area per day [mm^2]

Untreated tumours showed a significantly increased rate of surface area reduction compared to tumours treated with WIN-55,212.

P-STS cell tumours without WIN-55,212 treatment lost 31.58 mm^2 on average per day. In comparison, tumours treated with 1 µM WIN-55,212 lost 8.87 mm^2 on average per day, which is significantly less, compared to the surface area lost by untreated tumours (p=0.0001). Tumours treated with 5 µM WIN-55,212 showed a significantly reduced rate of surface area reduction compared to the control, with an average loss of surface area of 7.79 mm^2 per day. Furthermore, the mean surface area reduction per day was significantly reduced in tumours treated with 10 µM WIN-55,212, with an average loss of 11.53 mm^2 per day.

3.2.1.4 Tumours treated with WIN-55,212-2 have a lower depth/length ratio

To measure the dimensions of P-STS cell xenografts, the tumour section with the largest tumour surface was chosen and stained with LCA. The stained sections were viewed with the Olympus BX53 microscope, and the tumour dimensions were measured with the CellSensDimension software.

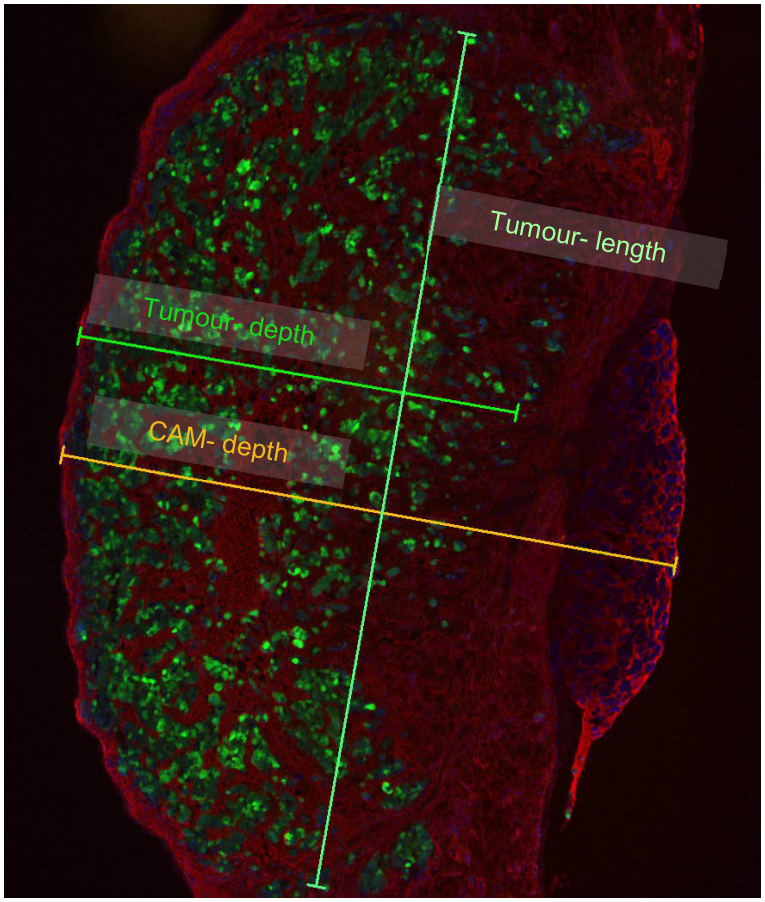

Figure 51: Measurement of CAM xenograft dimensions with the CellSensDimension software.

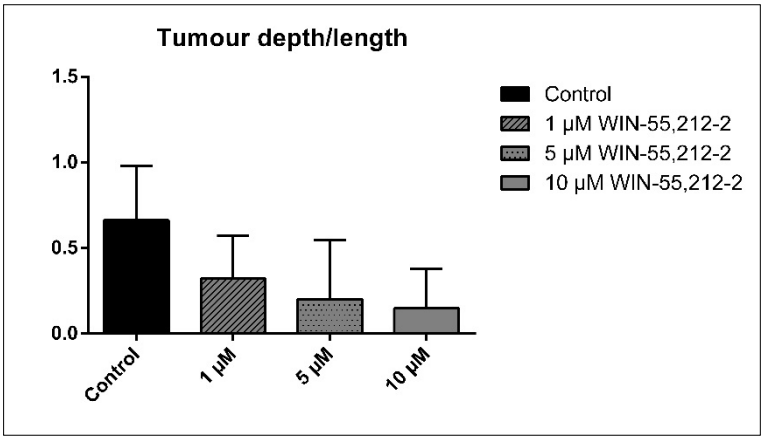

Figure 52: Ratio tumour depth/length of P-STS cell xenografts on CAM assays

The mean ratio of tumour depth to tumour length of untreated P-STS cell tumours was 0.66. However, the same ratio was <0.35 (1 µM WIN-55,212-2: 0.32; 5 µM WIN-55,212-2: 0.20; 10 µM WIN-55,212-2: 0.15) in all treated tumours.

3.2.1.5 WIN-55,212-2 reduces the Ki67 expression in treated xenografts

To examine the effect of treatment with WIN-55,212-2 on tumour proliferation *in vivo*, we performed Ki67 staining on sections of P-STS cell xenografts from CAM assays.

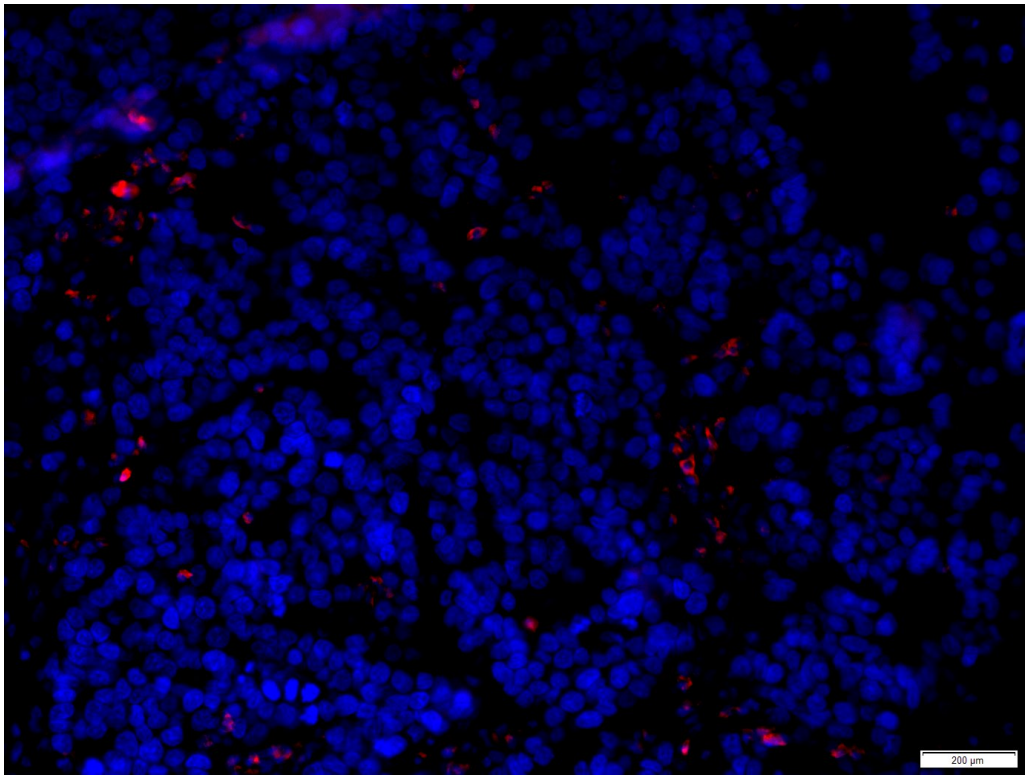

Figure 53: Ki67 staining of xenograft tissue after 72 hours of untreated P-STS cell grafts

The tissue of untreated P-STS cell xenografts showed a moderate level of Ki67 expression. Tumour cell nuclei appeared regular and of homogenous morphology.

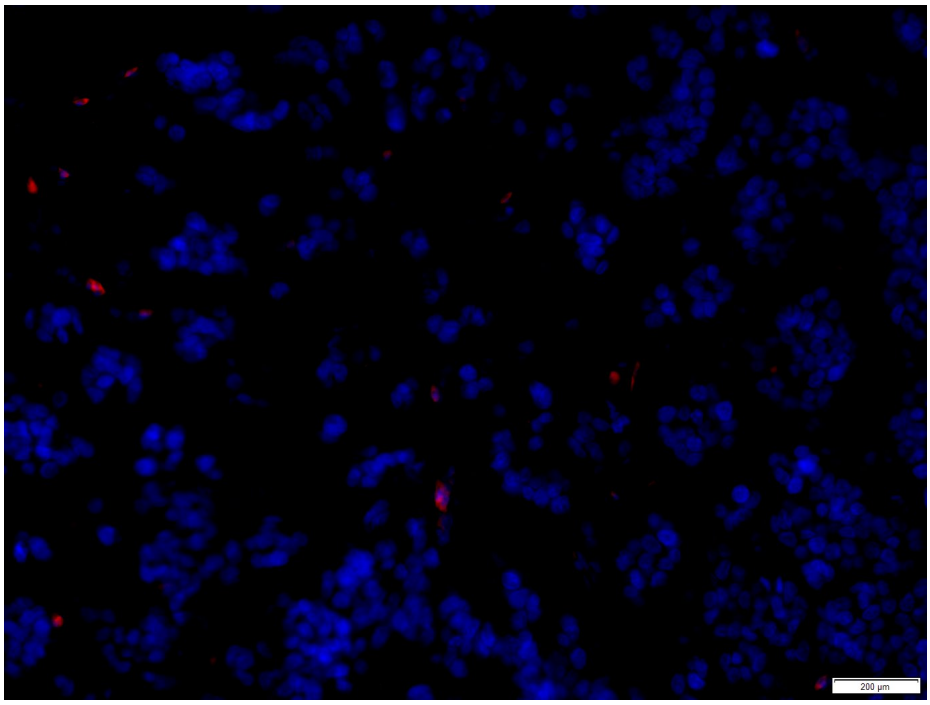

Figure 54: Ki67 staining of xenograft tissue after 72 hours of P-STS cell grafts treated with 5 µM WIN-55,212-2

Tissue section of xenografts treated with 5 µM WIN-55,212-2 showed a low level of Ki67 expression. The nuclei show a more heterogeneous morphology. Tumour growth appears to be less dense compared to untreated xenografts, and the tumour cells are organised in clusters with many unpopulated spaces in-between.

3.2.2 WIN-55,212-2 does not induce apoptosis in treated xenografts

To examine the effect of treatment with WIN-55,212-2 apoptosis *in vivo*, we performed *in situ* hybridisation TUNEL assay on sections of P-STS cell xenografts from CAM assays.

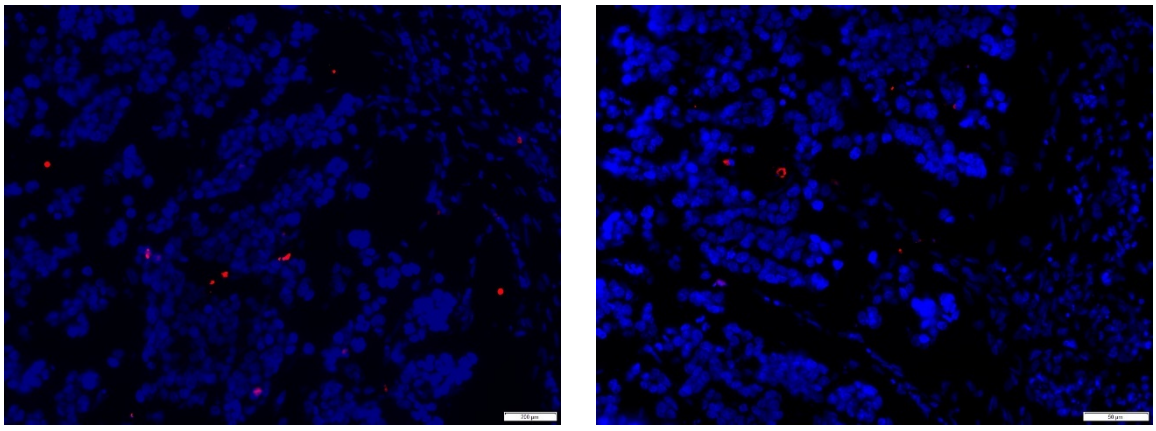

Figure 55: *In situ* hybridisation TUNEL assay of untreated xenografts (left) and cells treated with 5 µM WIN-55,212-2 (right). No difference in Br-dUTP uptake can be seen macroscopically.

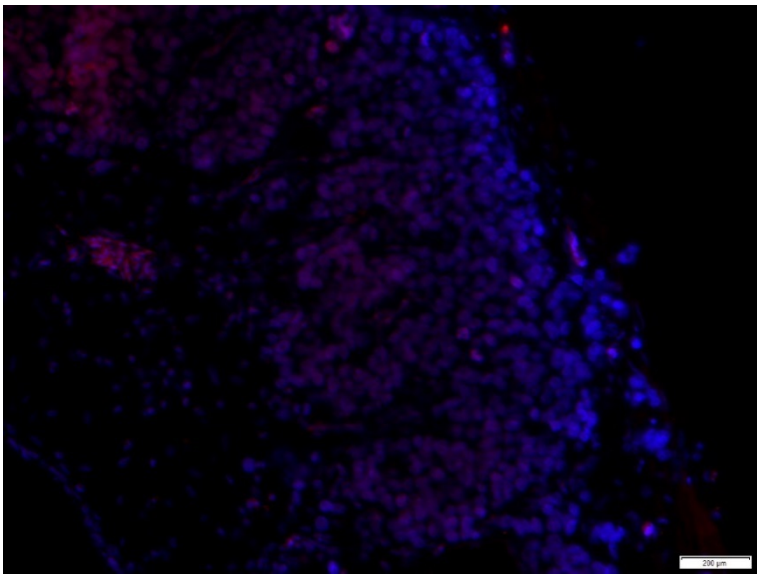

Figure 56: *In situ* hybridisation TUNEL assay of cells treated with 10 µM WIN-55,212-2

There was no difference in Br-dUTP uptake between untreated xenografts and xenografts treated with 5 µM WIN-55,212-2. The Br-dUTP was increased, however, in the xenografts treated with 10 µM WIN-55,212-2.

3.2.3 Treated tumours are less invasive

To assess the invasiveness of the tumours, we measured the depth of the tumour-free section of the chorioallantoic membrane and compared the depth of untreated tumours with tumours treated with WIN-55,212-2 at the respective concentrations as described in 3.2.1.2.

$$Tumour\ free\ depth = CAM\ depth - tumour\ depth$$

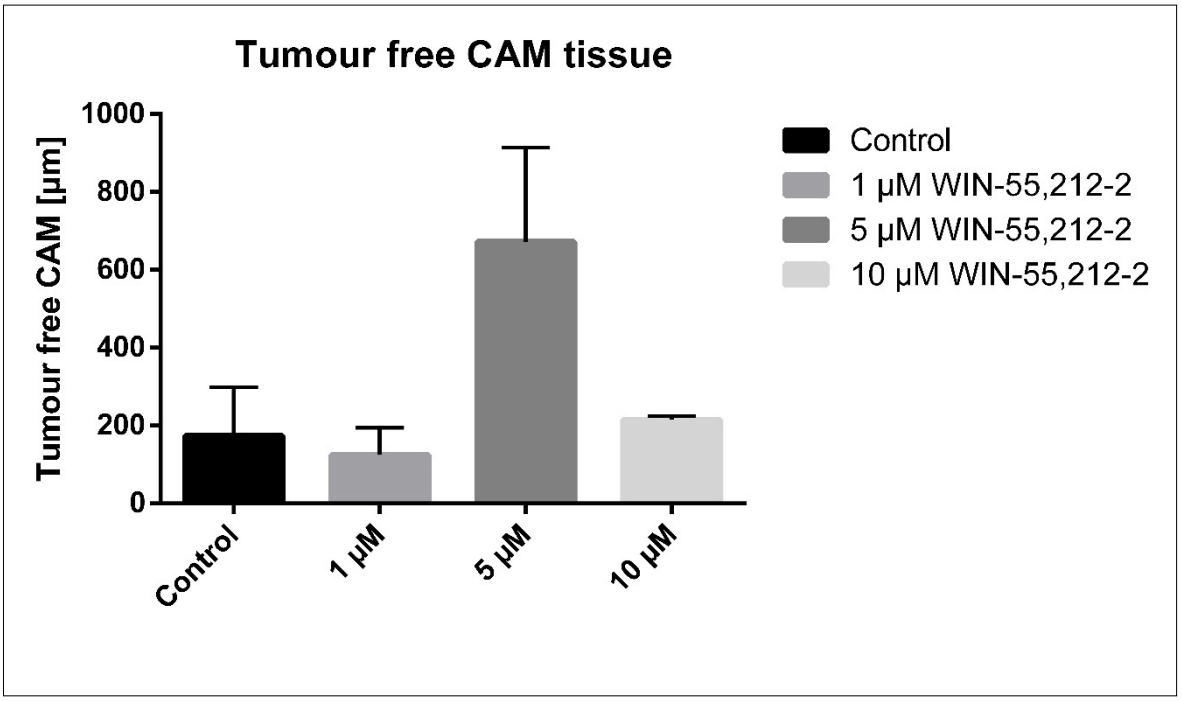

Figure 57: Comparison of the tumour free CAM tissue

The mean tumour-free depth was 173.36 µm with untreated tumours and was unchanged compared to the control at WIN-55,212-2 concentrations of 1 and 10 µM (1 µM: 124.86 µm; 10 µM: 214.71 µm). Treatment with 5 µM WIN-55,212-2, however, led to a significantly increased tumour-free depth, with a mean tumour-free depth of 672.20 µm (p=0.05).

3.2.4 WIN-55,212-2 inhibits neoangiogenesis

3.2.4.1 WIN-55,212-2 decreases the number of blood vessels converging to the graft site

To assess tumour neoangiogenesis upon WIN-55,212-2 treatment, P-STS cells were xenografted onto a chorioallantoic membrane and treated every 24 hours for three days. Neoangiogenesis was measured by counting the number of vessels converging to the tumour after 24h, 48h and 72h.

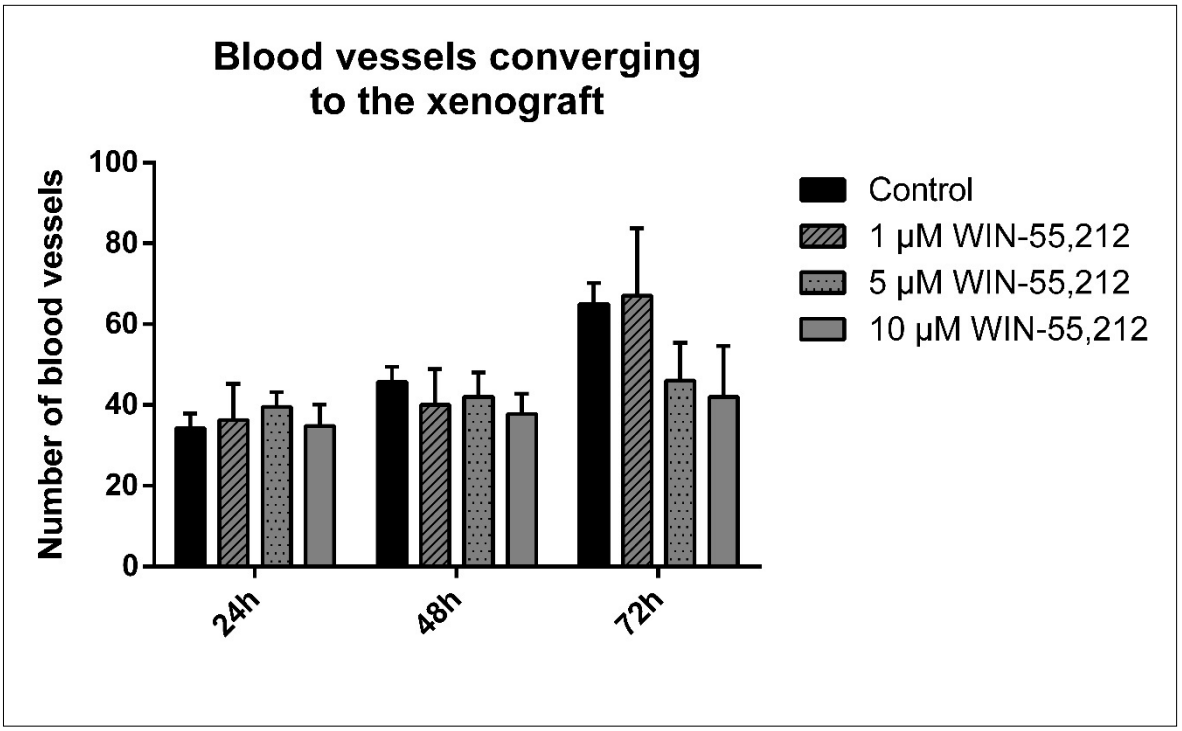

Figure 58: Number of blood vessels converging to the xenograft. After 72 hours of incubation, the number of vessels was significantly increased (p=0.001) upon treatment with 5 and 10 µM WIN-55,212-2.

On day 1, the mean number of blood vessels converging to the xenograft did not differ significantly from the control upon WIN-55,212-2 treatment. (Control: 34.3; 1 µM: 36.25; 5 µM: 39.5; 10 µM: 34.75) There was also no significant effect on day 2 compared to the control. (Control: 45.66; 1 µM: 40.00; 5 µM: 42.00; 10 µM: 37.75) On day 3, the number of blood vessels was significantly decreased (p=0.001 respectively) upon treatment with 5 µM and 10 µM WIN-55,212-2, whereas no effect occurred with 1 µM. (Control: 65.00; 1 µM: 67.00; 5 µM: 46.00; 10 µM: 42.00)

3.2.4.2 WIN-55,212-2 decreases the density of vascularisation around the xenograft

To assess tumour neoangiogenesis, we scored the vascular density around the xenografts according to Ribatti *et al.*(98).

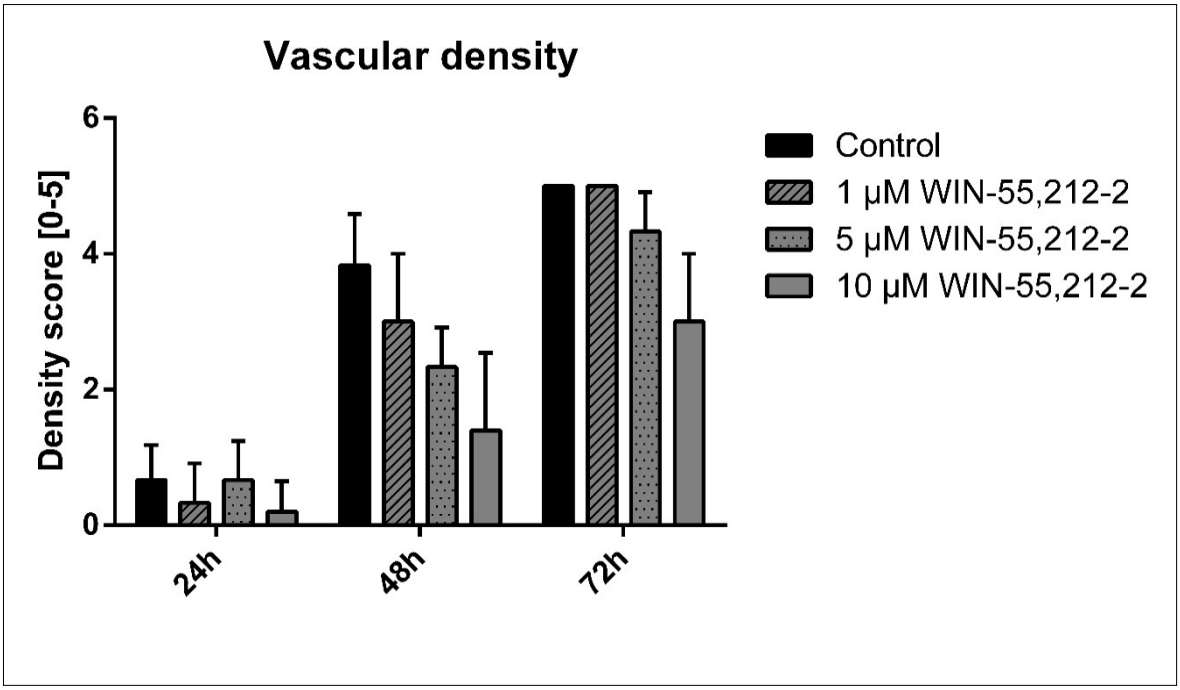

Figure 59: Vascular density scores after treatment with WIN-55,212-2. The density is significantly reduced upon 5 and 10 µM WIN-55,212-2 treatment after 48h and 72h.

After 24 hours, vascular density did not differ from the control upon treatment with WIN-55,212-2. (Control: 0.67; 1 µM: 0.33; 5 µM: 0.67; 10 µM: 0.2) After 48 hours, the vascular density was unchanged upon treatment with 1 µM WIN-55,212-2, but was significantly decreased ($p=0.001$) at concentrations higher than 5 µM. (Control: 3.83; 1 µM: 3.00; 5 µM: 2.33; 10 µM: 1.40) The vascular density was also significantly reduced for concentrations higher than 5 µM ($p=0.001$) after 72 hours, whereas no effect occurred at 1 µM. (Control: 5.00; 1 µM: 5.00; 5 µM: 4.30; 10 µM: 3.00)

3.2.4.3 WIN-55,212-2 decreases vascular branching in the proximity of the graft site

In addition to the previous experiments regarding tumour neoangiogenesis, we scored vessels according to their branching behaviour in the proximity of the graft site. The scoring was performed according to Ribatti *et al.*(98).

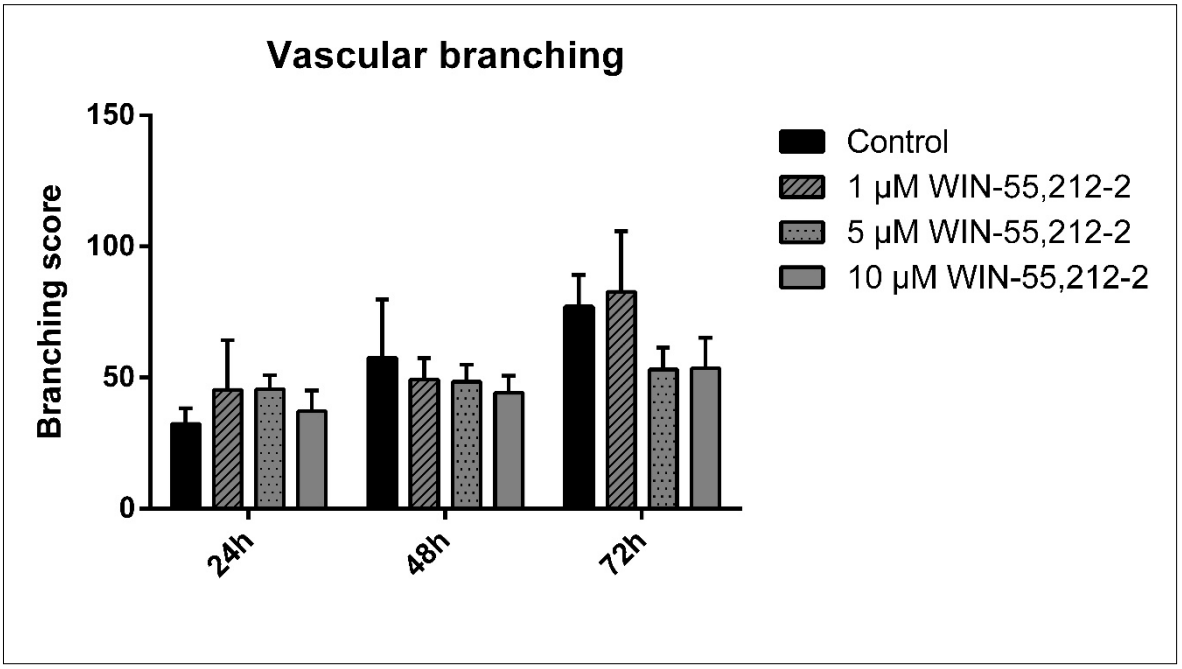

Figure 60: Vascular branching scores. The scores were significantly decreased (p=0.0001) upon treatment with concentrations higher than 5 µM WIN-55,212-2.

The vascular branching score was not significantly decreased after 24 hours at all concentrations of WIN-55,212-2 used. (Control: 32.33; 1 µM: 45.33; 5 µM: 45.60; 10 µM: 37.20) Similarly, after 48 hours no effect on vascular branching could be observed. (Control: 57.50; 1 µM: 49.33; 5 µM: 48.40; 10 µM: 44.20) After 72 hours however, the branching score was decreased significantly (p=0.0001) at WIN-55,212-2 concentrations above 5 µM WIN-55,212-2, but no effect occurred at 1 µM. (Control: 77.00; 1 µM: 82.67; 5 µM: 53.00; 10 µM: 53.60)

3.3 WIN-55,212-2 and Id-1 in P-STS cells

3.3.1 Id-1 is downregulated upon treatment with WIN-55,212-2

To compare the expression level of Id-1 upon treatment with WIN-55,212-2, qPCRs were performed (see 2.3.1–2.3.3).

Cells were starved and treated with the respective concentrations of WIN-55,212-2. After an incubation period of 16 hours, the cells were harvested and the RNA was isolated (see 2.1.4 and 2.3.1). After the isolation, cDNA was generated from the isolated RNA and analysed by real-time qPCR (see 2.3.2 and 2.3.3).

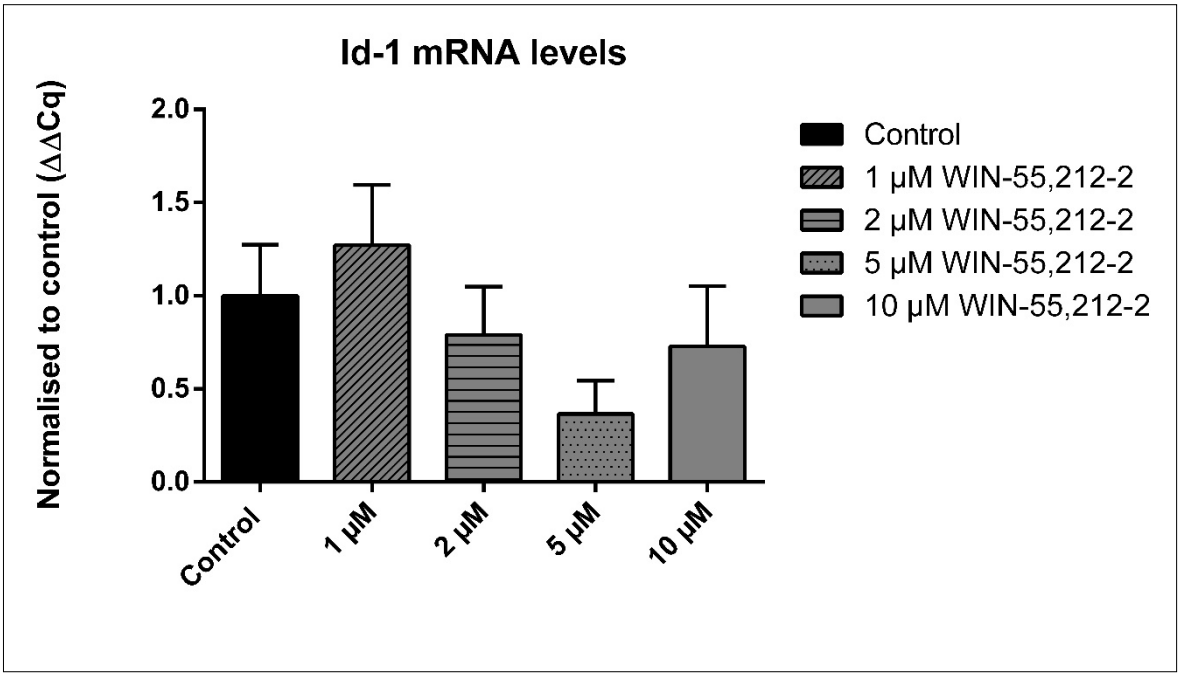

Figure 61: mRNA expression normalised to the control: Treatment with 1 µM WIN-55,212-2 led to a significantly increased Id-1 expression, whereas treatment at concentrations from 2–10 µM WIN-55,212-2 decreased the Id-1 expression significantly.

Treatment with 1 µM WIN-55,212-2 significantly increased the Id-1 expression by a factor of 1.27 compared to the control. By contrast, treatment with 2 µM WIN-55,212-2 decreased the Id-1 expression by a factor of 0.79 and treatment with 5 µM WIN-55,212-2 decreased it by a factor of 0.366. Id-1 expression was decreased by a factor of 0.728 upon treatment with 10 µM WIN-55,212-2.

3.3.2 Id-1 plays a protective role against the cell growth inhibition of WIN-55,212-2 in P-STS cells

To investigate whether the effects of WIN-55,212-2 on P-STS cells in terms of cell growth (see 3.1.3.1) are mediated by Id-1, we compared cell growth of normal P-STS cells and Id-1 silencing or overexpressing P-STS cells (see 2.9) after treatment with WIN-55,212-2.

The following P-STS cell variants were seeded, starved and treated with 5 µM WIN-55,212-2:

- **Control:** wild-type P-STS
- **Id-1 silencing P-STS:** siA and siB, scr as control
- **Id-1 overexpressing P-STS**: Id-1, BB as control

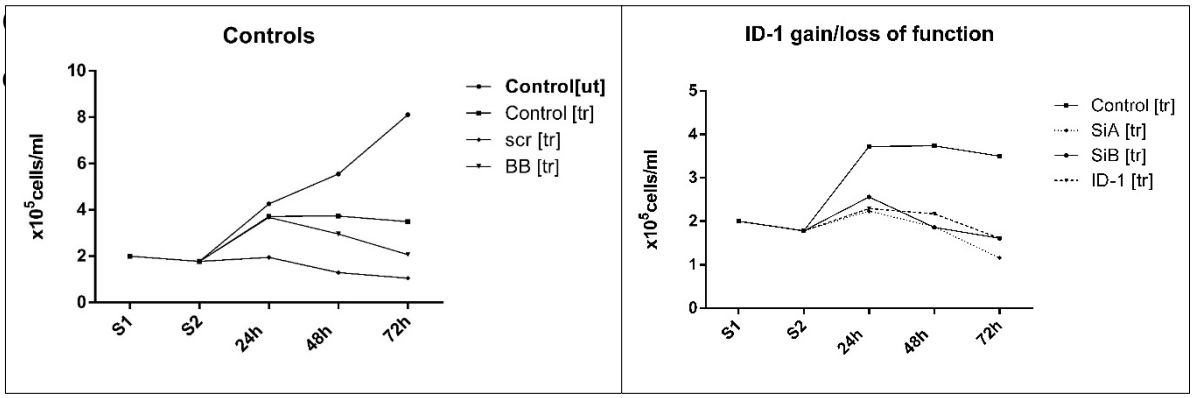

Figure 62: Id-1 gain/loss of function: Growth curves of controls ([ut]=untreated, [tr]=treated). (left) Growth curves f Id-1 silencing and overexpressing P-STS cells treated with 5 µM WIN-55,212-2. (right)

The growth curves of treated and untreated P-STS cells correspond to the results in 3.3. Cells treated with 5 µM WIN-55,212-2 entered a stationary phase 24 hours post-treatment. The growth curves of the treated controls for silencing and overexpression vary greatly from the control [tr]. Cells of the scrambled variant entered a death phase 24 hours upon treatment and cells of the backbone variant showed hardly any proliferation at all (see Figure 62 left).
The comparison between Id-1 silencing and overexpressing P-STS cells with the control shows that the variants siA, siB and Id-1 proliferate at a lower rate than the treated control. All variants entered a cell death phase after 24 hours of treatment.

After 24 hours, the cell count was significantly reduced compared to the control in all variants except for BB. (p=0.001 respectively) No significant differences of the cell count were observed between Id-1, siA and siB cells.

On day 2 of WIN-55,212-2 treatment, the cell count was significantly reduced for all Id-1 overexpressing and silencing variants and their respective controls compared to treated P-STS cells. (p=0.001 respectively) No difference of the cell count was observed between Id-1 overexpressing cells and Id-1 silenced cells.

After 72 hours of treatment with 5 µM WIN-55,212-2, the cell count was significantly reduced for all Id-1 overexpressing and silencing variants and their respective controls compared to treated P-STS cells. (p=0.001 respectively) A significantly reduced cell count was observed between Id-1 and siA (p=0.05) but not between Id-1 and SiB.

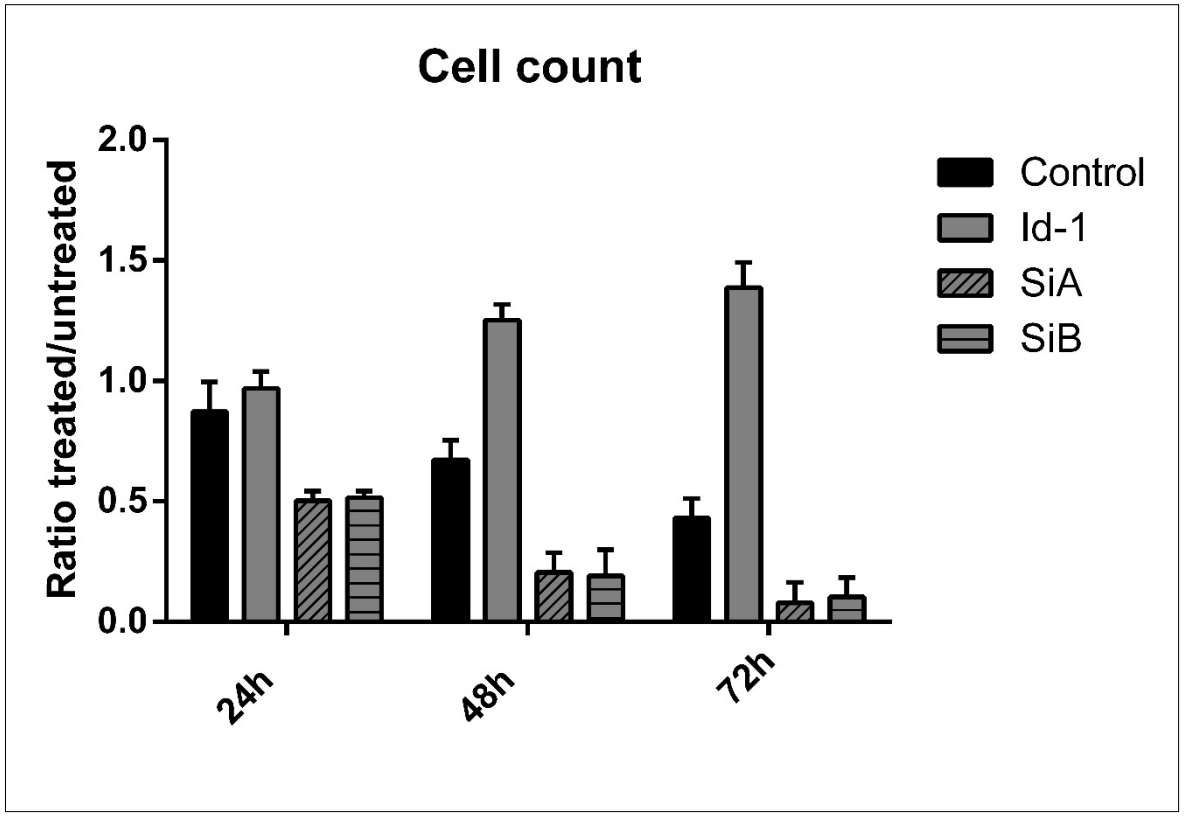

Figure 63: The cell count was normalised to the respective controls and the relative cell count of treated cells compared to untreated cells was calculated. The cell count was decreased in the Id-1 silenced cells, whereas it was increased in Id-1 overexpressing cells compared to the control (wild type).

We normalised the cell count to the respective controls and calculated the relative change of the cell count through treatment with WIN-55,212-2.

After 24 hours, the cell count of Id-1 overexpressing cells was unchanged upon treatment. WIN-55,212-2 treatment reduced the cell count significantly (p=0.0001) in treated Id-1 silenced cells and P-STS wild-type cells (control). (Control (wild type): 0.87; Id-1: 0.97; SiA: 0.50; SiB: 0.52)

The cell count after 48 hours was increased significantly (p=0.001) in treated Id-1 overexpressing cells compared to untreated cells. The cell count was decreased significantly (p=0.0001) in treated Id-1 silenced cells and the control. (Control (wild type): 0.67; Id-1: 1.25; SiA: 0.21; SiB: 0.19)

After 72 hours, the cell count was also increased significantly (p=0.0001) in treated Id-1 silenced cells, whereas it was decreased significantly (p=0.0001) in treated Id-1 silenced cells compared to untreated cells. (Control (wild type): 0.43; Id-1: 1.39; SiA: 0.08; SiB: 0.10)

3.3.3 Id-1 increases P-STS cell susceptibility to cannabinoid treatment

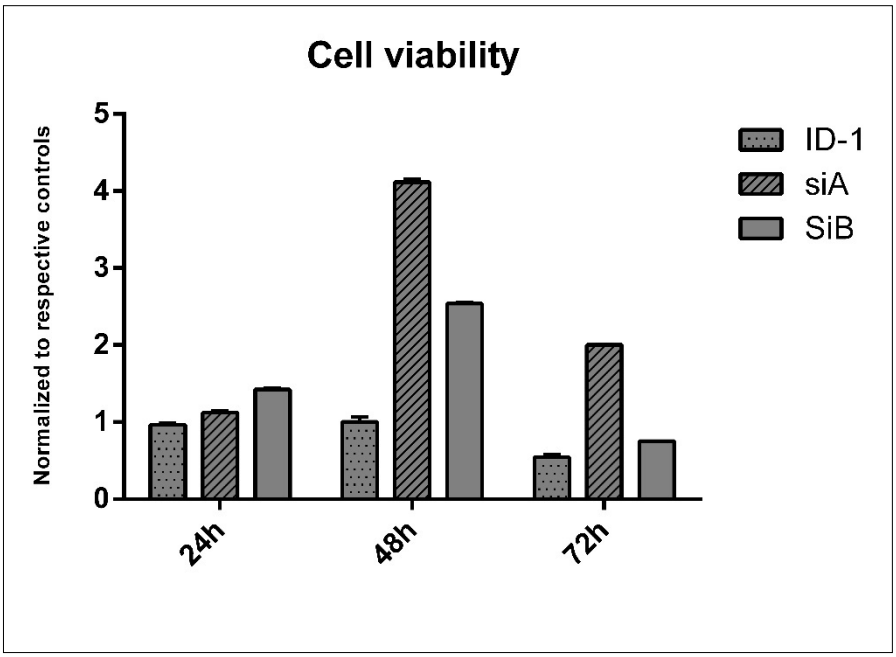

Figure 64: Cell viability of Id-1 silenced and Id-1 overexpressing cells normalised to their respective control.

On day 1, the cell viability of the Id-1 overexpressing cells was reduced by a factor of 0.96 compared to the control. By contrast, the cell viability of the Id-1 silenced variant A (SiA) was increased by 1.12 and the cell viability of variant SiB was also increased by 1.42. There was a significant difference between the cell viability of Id-1 overexpressing P-STS cells and Id-1 silenced P-STS cells ($p=0.001$).

On day 2, the cell viability of Id-1 overexpressing cells was unchanged compared to the control. The viability of the Id-1 silenced cells was increased by a factor of 4.12 for variant A and by a factor of 2.54 for variant B. The difference between the viability of silenced cells and overexpressing cells was significant ($p=0.001$).

On day 3, the cell viability of Id-1 overexpressing cells was decreased by a factor of 0.54 compared to the control. The viability of the Id-1 silenced cells was increased by a factor of 2.00 for variant A. Treated cells of the Id-1 silenced variant B were decreased by a factor of 0.75 for variant B. The difference between the viability of silenced cells and overexpressing cells was significant ($p=0.001$).

4 Discussion

Cannabinoids have been used for centuries for their psychoactive and analgesic effects. However, they are not very well known for their effects on cancer. Recent evidence suggests that cannabinoids have a variety of anti-tumorigenic effects, such as inhibition of tumour growth, metastasis and angiogenesis and induction of apoptosis.(21) These effects on proliferation and apoptosis have been shown in breast, prostate, lung, skin, pancreatic and bone cancer and in gliomas, among others.(21)

In this study, we investigated the effects on proliferation, apoptosis, tumour growth, invasiveness and neoangiogenesis of WIN-55,212-2, a synthetic CB1 and CB2 agonist on the small intestine neuroendocrine cell line P-STS. We performed *in vitro* as well as *in vivo* experiments to observe the effect of WIN-55,212-2 treatment on cell count and viability, apoptosis, Ki67 expression, DNA fragmentation, tumour morphology, invasiveness, angiogenesis and Id-1 expression.

The fetal bovine serum (FBS) used in standard cell culture medium can be the source of unspecific interactions and binding with various chemical agents. Additionally, activation of receptors by components of the FBS can lead to changes in the receptor expression patterns of cells cultivated with FBS. To avoid this when treating P-STS cells with WIN-55,212-2, we conducted preliminary experiments to find the optimal concentration of FBS. The lowest FBS concentration at which P-STS cells grow without a significant difference to cells in standard Ham's medium (10% FBS) was 1% FBS. We therefore starved the P-STS cells in Ham's F12:M199 (1:2) medium containing 1% FBS for 24 hours prior to our experiments.
After the starvation period, P-STS cells were seeded in 24-well plates for the *in vitro* experiments and grafted onto the chorioallantoic membrane for the *in vivo* experiments. The P-STS cells and xenografts were then treated with the respective concentrations of WIN-55,212-2 (1–10 µM) every 24 hours over the course of 3 days. During this time, experiments were carried out to assess the various parameters outlined in the experimental setup.

The distribution of cannabinoid receptors has been well characterised in mammalian tissue.(16) CB1 receptors are ubiquitously expressed, with a high presence in the

central nervous system, mediating the psychoactive effects of cannabinoids, while CB2 receptors are expressed in very few tissues, mostly in particular elements of the immune system.(17,18) Cannabinoid receptors are also highly expressed in different types of cancer (see appendix – 6.2).(21) We therefore hypothesised that this was also the case in the small intestine cancer cell line P-STS. We performed real-time qPCRs to verify the levels of CB1, CB2 and GPR55 receptor expression. The results in figure 32 show that CB1 and CB2 receptors are expressed in P-STS cells, whereas GPR55 is not expressed. This indicates that P-STS cells are susceptible to treatment with the selective CB1 and CB2 agonist WIN-55,212-2.

It has been suggested that the level of gene expression varies between cells grown in 2D (conventional cell culture flasks) and in 3D spheroids. A previous study by our group showed that the Id-1 expression does in fact differ from cell cultivated in 2D to cells cultivated in 3D.(87) The levels of the cannabinoid receptors were slightly increased (≈1.5 fold) in 3D spheroids, compared to 2D cell culture conditions. The increased receptor expression could be caused by intercellular signalling of cells growing in a cluster, rather than as single cells usually found in conventional cell culture.

4.1 WIN-55,212-2 and proliferation

Various studies have demonstrated that cannabinoids can reduce cell proliferation *in vitro*. The endocannabinoid anandamide, for example, inhibits basal and nerve growth factor (NGF) induced proliferation of MCF-7 and EFM-19 cells *in vitro* through CB1 receptor activation, and Δ^9-THC inhibits 17-beta-estradiol-induced proliferation of MCF7 and MCF7-AR1 cells.(29–31) It has also been demonstrated that WIN 55,212-2, the cannabinoid used in this study, leads to an inhibition of MDA-MB-231 proliferation by blocking the G1 to S phase transition.(33)
In this study, we assessed the effect of treatment with WIN-55,212-2 on the proliferation of P-STS cells. We measured cell count, viability and Ki67 expression as parameters for proliferation *in vitro* and we performed Ki67 immunofluorescence staining on treated xenografts to assess the proliferation *in vivo*.

The cell count was measured every 24 hours upon treatment with the CASY® Cell Counter and growth curves were established for each concentration (1–10 µM).

The growth curve of untreated P-STS cells exhibited the classic shape, with an initial lag phase during the starvation period of 24 hours and a subsequent growth acceleration, entering a phase of exponential growth (24–72h). This shape was maintained upon treatment with 1 µM and 2 µM WIN-55,212-2, although the final cell count was significantly reduced, and the curve was much flatter in the population treated with 1 µM WIN-55,212-2. However, the growth curve, as well as the final cell count of cells treated with 2 µM WIN-55,212-2, was unchanged compared to the control. Populations treated with 5 µM WIN-55,212-2 entered a stationary phase after 24 hours, and populations treated with 10 µM WIN-55,212-2 entered a death phase, also after 24 hours. The final cell count was reduced significantly upon treatment with concentrations higher than 5 µM. Therefore, the of WIN-55,212-2 on the cell growth of P-STS cells was concentration dependent.

A possible explanation for the lack of response to treatment with 2 µM WIN-55,212-2 is that the balance between CB1, CB2 and possibly other cannabinoid receptor activation at this concentration is different from at other concentrations, activating different pathways and reversing the inhibiting effect of WIN-55,212-2 on proliferation. The results at the other concentrations indicate that WIN-55,212-2 inhibits proliferation at concentrations from 1 to 5 µM. This effect might be caused by blocking the G1 to S phase transition, as suggested by *Melck et al*.(30,31) The effects measured at 10 µM are likely to be caused by cytotoxic effects in addition to the inhibiting effects at concentrations of 1–5 µM. This is also supported by the growth curve at 10 µM, with a very short growth phase, followed by a death phase and a very low final cell count.

Several studies have shown that Id-1, a helix-loop-helix transcription factor inhibiting protein, mediates cannabinoid signalling in breast cancer.(49,50) Additionally, Tang J *et al.* demonstrated that upregulation of Id-1 promotes normal proliferation by regulating the progression of the G1 to S phase of the cell cycle.(70,71)

We therefore examined the role of Id-1 in the regulation of the effects of WIN-55,212-2 on the proliferation of P-STS cells. We treated lentiviral-transfected P-STS cells, which were either Id-1 silenced or were overexpressing Id-1, with 5 µM WIN-55,212-2 and calculated the response in terms of cell count upon treatment.

Treatment with WIN-55,212-2 led to a reduced cell count of the wild-type P-STS cells, which we used as control. Interestingly, this effect was increased by 27.97% on average in Id-1 silenced P-STS cells compared to the wild type. In contrast, the effect of WIN-55,212-2 on cell count was decreased in Id-1 overexpressing cells. This indicates that Id-1 might play a protective role against the effects of cannabinoids on P-STS cells. The role of Id-1 in mediating the anti-proliferation effect of cannabinoids is well supported by other studies.(49,50)

The cell viability was assessed every 24 hours upon treatment with WIN-55,212-2 by performing WST-1 Assays. Over the course of 3 days, the cell viability was decreased significantly at concentrations between 1 and 10 µM WIN-55,212-2, except at the concentration of 2 µM, where there was no significant effect.

To assess whether Id-1 also has a protective function against WIN-55,212-2 induced reduction of cell viability, we performed WST-1 Assays on Id-1 silencing and overexpressing cells after treatment with WIN-55,212-2.

WIN-55,212-2 increased the cell viability in Id-1 silenced cells and had almost no effect on Id-1 overexpressing cells, contradicting the results regarding cell count mentioned above. This would indicate that Id-1 increases the susceptibility to cannabinoids of P-STS cells. An increased cell viability and proliferation through downregulation of Id-1 is, however, not well supported by the literature. The reason for this result in cell viability could also be the poor quality of the WST-1 Assay, as the respective absorbance was very low on day 2 and day 3, possibly altering the results. This indicates that the results regarding cell count might be more reliable than the results of cell viability.

The Ki67 labelling index is a score commonly used to assess proliferation in tumours. We calculated this index for cells treated with 5 µM WIN-55,212-2 for 72 hours and compared it to the Ki67 index of untreated P-STS cells. Treatment with WIN-55,212-2 decreased the Ki67 labelling index by 38.38%, confirming the inhibitory effect of WIN-55,212-2 on cell proliferation.

To determine whether this effect on proliferation is not only limited to cell culture conditions, but also applies *in vivo*, we performed Ki67 immunofluorescence staining on treated P-STS cell xenografts and compared them to untreated xenografts. The tissue sections of xenografts treated with 5 µM WIN-55,212-2 showed a lower level

of Ki67 expression than sections of untreated xenografts. Additionally, the nuclei had a more heterogeneous morphology and the tumour growth appeared to be less dense compared to untreated xenografts. In treated xenografts, the tumour cells were organised in clusters with larger intercellular spaces compared to the rather compact growth pattern in untreated xenografts.

4.2 WIN-55,212-2 and apoptosis

Several pathways have been discovered through which cannabinoids play a role in the induction of apoptosis. For example, a study found that Δ_9–THC induces apoptosis in PC-3 cells via the PI3K/Akt pathway with sequential involvement of Raf-1/ERK1/2 and induction of nerve growth factor.(34) The PI3K/ERK pathway is one of the most common pro-apoptotic pathways known to be induced by cannabinoids.(99)

Another pro-apoptotic pathway is the inhibition of FAAH (fatty acid amide hydrolase), an enzyme that regulates the levels of anandamide, which leads to the activation of the nuclear factor erythroid 2-related factor (Nrf2)/antioxidant responsive element (ARE) pathway and the induction of heme oxidase-1 (HO-1).(28)

It has also been shown that WIN-55,212-2 induces a cannabinoid receptor mediated apoptosis in mantle cell lymphoma, a malignant b-cell lymphoma.(100)

In this study, we assessed the effect of treatment with WIN-55,212-2 on apoptosis of P-STS cells. We measured Caspase 3/7 activity and DNA fragmentation as parameters for apoptosis *in vitro* and we performed TUNEL assays on treated xenografts to assess apoptosis *in vivo*.

We measured the caspase activity with Caspase-Glo® 3/7 Assays every 24 hours upon treatment with the respective concentrations of WIN-55,212-2 (1–10 µM).
Caspases are a family of enzymes that belong to the cysteine proteases. They play a crucial role during apoptosis, cleaving a variety of proteins. This process is used by the caspase assay to quantify apoptosis.(101)

Caspase activity was increased significantly at all concentrations and at all time points, except for the population treated with 1 µM WIN-55,212-2 after 24 hours. This indicates that treatment with WIN-55,212-2 induces apoptosis in P-STS cells.

Detecting DNA fragmentation, which occurs during apoptosis, is another way of quantifying apoptosis. This is done by using Br-dUTPs (bromolated deoxyuridine triphosphate nucleotides), which are incorporated into fragmented internucleosomal DNA strands. Once incorporated, Br-dUTP can be made visible with a fluorescence labelled anti-BrdU monoclonal antibody.

Macroscopically, more cells were Br-dUTP positive in the population treated with 5 µM WIN-55,212-2. Additionally, treated cells had far more polymorph and smaller nuclei than untreated cells. Further analysis revealed that the percentage of Br-dUTP positive cells was increased by 25.51% in the treated population. This supports the results of our caspase assays, suggesting that WIN-55,212-2 induces apoptosis in P-STS cells.

To determine whether WIN-55,212-2 also induces apoptosis *in vivo*, we performed *in situ* hybridisation TUNEL assays on tissue sections of xenografts treated with 5 and 10 µM WIN-55,212-2, and compared them to sections of untreated xenografts. Br-dUTP uptake did not differ macroscopically between tissue sections of untreated xenografts and tissue sections of xenografts treated with 5 µM WIN-55,212-2, indicating that no changes in apoptosis occurred upon treatment with WIN-55,212-2. The reason for this could also, however, be unsuccessful staining, as the positive control was only borderline positive and the negative control had a high background signal. The Br-dUTP uptake of the tissue sections treated with 10 µM WIN-55,212-2 was increased compared to the control. This effect could be caused by the additional cytotoxic effect, seen in the proliferation experiments, rather than by a pro-apoptotic effect of WIN-55,212-2.

4.3 WIN-55,212-2 and tumour growth

The effect of WIN-55,212-2 on proliferation and apoptosis *in vitro* and on proliferation *in vivo* suggests that the treatment might also cause changes in macroscopical tumour morphology.

We assessed the changes induced by treatment with WIN-55,212-2 in terms of tumour morphology by scoring the tumours according to their macroscopical appearance, by measuring the tumour dimensions of xenograft tissue sections and by measuring the tumour surface area.

We scored the macroscopical tumour appearance according to various criteria that we determined. The tumours were then either assigned to the solid growth pattern group or to the diffuse growth pattern group. The untreated P-STS cell xenografts formed 33.33% more tumours with solid growth pattern than xenografts treated with 5 µM WIN-55,212-2 and 54.76% more than xenografts treated with 10 µM WIN-55,212-2.

To find evidence of this effect on tumour morphology at a microscopical level, we cut through the entire tumour, creating 6 µm-thick tissue sections. We then chose the section with the greatest tumour dimensions and measured tumour length and height with the CellSensDimension software. The ratio of height/depth of treated xenograft tissue sections was then compared to the ratio of untreated tumour sections. The mean height/depth ratio was 0.66 in untreated xenograft sections, indicating a round tumour shape, which corresponds to the fact that the solid growth pattern was more frequent in untreated xenografts. In contrast, sections of treated xenografts were flatter, with a mean ratio under 0.35.

We also measured the tumour surface area of xenografts with the CellSensDimensions software while they were still on the chorioallantoic membrane. The surface area was increased upon treatment with concentrations higher than 5 µM WIN-55,212-2. Taking into consideration the fact that the tumour height of tissue sections was smaller in treated xenografts, the greater surface area of treated tumours does not imply that they also had a greater mass, but rather confirms the diffuse growth pattern of treated P-STS cell tumours. Additionally, treated tumours showed a much slower mean day-to-day surface area reduction. This could indicate that WIN-55,212-2 also has effects on cell migration or adhesion, which is supported by similar effects shown in other studies.(46–48) It has been shown that cannabinoids inhibit cytoskeletal focal adhesion in the cell line MDA-MB-231 via the ERK signalling pathway (46) and inhibit migration of the same cell line via the inhibition of the cAMP-dependent protein kinase A.(45)

4.4 WIN-55,212-2 and tumour invasiveness

It has been shown that cannabinoids can inhibit the invasion of A549 cells (human lung cancer) both *in vitro* and *in vivo*. This effect is accompanied by upregulation of the tissue inhibitor of matrix metalloproteinase-1 (TIMP-1) and decreased

expression of plasminogen activator inhibitor-1 (PAI-1).(47,48) Furthermore, the invasion of 4T1 (mammary metastatic cell line) cells can be inhibited by CBD via downregulation of Id-1 and inhibition of ROS.(21)

In this study, we assessed the extent to which P-STS cell xenografts invaded the chorioallantoic membrane. We measured the tumour-free tissue depth of the chorioallantoic membrane as a parameter for tumour invasion. The depth was not significantly changed in xenografts treated with 1 and 10 µM WIN-55,212-2, although the reason for the lack of an effect at 10 µM might have been poor tissue section quality. In contrast, treatment at 5 µM led to an increase in the depth of the tumour-free tissue by 546.45 µm, marking a significant effect on tumour invasiveness at this concentration.

4.5 WIN-55,212-2 and neoangiogenesis

It has been shown that cannabinoids inhibit neoangiogenetic factors such as VEGF and Ang2 and therefore reduce tumour neoangiogenesis significantly.(102)

The synthetic cannabinoids LYR-7 and LYR-8 for example, inhibit VEGF-mediated neoangiogenesis signalling in MCF-7 and tamoxifen-resistant MCF-7 cells.(42) In skin cancer, treatment of WIN-55,212-2 caused a reduced tumour vascularisation and decreased expression of neoangiogenetic factors such as VEGF, placental growth factor and angiopoietin-2.(43)

In this study, we assessed neoangiogenesis with CAM Assays. We examined the neoangiogenetic effect of factors in tumour cell suspension supernatant, measured the number of blood vessels converging to the xenograft, and scored vascular density and vascular branching as parameters for tumour neoangiogenesis.

We assessed the neoangiogenetic effect of factors in the supernatant of tumour cell suspension by placing meshes with a collagen and tumour cell suspension supernatant onto the chorioallantoic membrane. The induced neoangiogenesis was assessed by calculating the percentage of vascularised squares after 72 hours of incubation. The supernatant of treated tumour cells induced an increase of vascularisation by 47.38% compared to the control. This indicates that cannabinoids enhance tumour neoangiogenesis and production angiogenetic factors under *in vitro* conditions.

We also assessed three different macroscopical parameters of tumour neoangiogenesis with CAM assays. P-STS cells were xenografted onto the chorioallantoic membrane and treated every 24 hours over the course of three days. The neoangiogenesis parameters were also measured every 24 hours.

As the first parameter, we measured the number of vessels converging to the tumours. An effect of WIN-55,212-2 on neoangiogenesis could only be seen on day 3. Then number of blood vessels converging to the tumour was decreased in tumours treated with concentrations higher than 5 µM WIN-55,212-2.

As the second macroscopical parameter for tumour neoangiogenesis, we assessed the vascular density in the proximity of the graft site. The score assigns values from 0–5 to different levels of density. (98) In practice, we applied the score to the same xenografts examined for the number of vessels converging to the graft, in order to have an additional parameter for neoangiogenesis. The density of the vascular network was decreased in xenografts treated with WIN-55,212-2 concentrations higher than 5 µM after 48 and 72 hours. The results of this experiment are therefore in line with the results of the first macroscopical neoangiogenesis parameter described above.

As the third macroscopical parameter for tumour neoangiogenesis, we assessed the branching patterns in the proximity of the graft site. The score assigns different values according to the branching patterns of vessels close to the xenograft. (98) The branching score was significantly decreased in xenografts treated with WIN-55,212-2 at concentrations higher than 5 µM after 72 hours, consistent with the other macroscopical parameters we assessed.

4.6 WIN-55,212-2 and Id-1

Several studies have shown that Id-1, a helix-loop-helix transcription factor inhibiting protein, mediates cannabinoid signalling in breast cancer.(49,50) It has also been shown that Id-1 is an oncogene and plays a role in angiogenesis, cell growth, cell survival and cellular senescence.(56,65,67,76,77,80)

In this study, we measured the level of Id-1 expression upon treatment with WIN-55,212-2 by performing real-time qPCRs.

We found that treatment with WIN-55,212-2 led to a downregulation of Id-1 at concentrations higher than 2 µM. This indicates that Id-1 might be part of a signalling pathway through which cannabinoids affect the various anti-tumorigenic parameters we assessed in this study, such as proliferation, apoptosis and angiogenesis.

4.7 Conclusion

In summary, our experiments provide strong evidence that WIN-55,212-2 inhibits tumour cell growth of the small intestine neuroendocrine cancer cell line P-STS *in vitro* and suggest that this effect also occurs *in vivo*. This is also supported by various other studies performed on different cancer types, such as breast and prostate cancer.(29–31,33,39,40,42,49) Additionally, Id-1 downregulation might mediate the effect of WIN-55,212-2 on P-STS cells and might also play a protective role against the inhibitory effect of WIN-55,212-2 treatment on cell count. In contrast, Id-1 overexpression seems to have the opposite effect on cell viability, increasing the effect of WIN-55,212-2 on Id-1 overexpressing P-STS cells.

Regarding apoptosis, our experiments provide strong evidence that treatment with WIN-55,212-2 induces apoptosis in the small intestine neuroendocrine cell line P-STS *in vitro*. The experiments provide no evidence that this effect also occurs *in vivo*, although increased DNA fragmentation could be seen in the tissue sections of xenografts treated with 10 µM WIN-55,212-2. This might be caused by cytotoxicity rather than by pro-apoptotic effects. The induction of apoptosis by cannabinoids is supported by various studies that show the same effect in a variety of different cancer types.(21,37,39,41)

We further showed that treatment with WIN-55,212-2 induces morphological changes of P-STS cell xenografts, both at a macroscopical and a microscopical level. Treated tumours were more diffuse and flat, whereas untreated tumours had a more solid and round morphology. We also showed that WIN-55,212-2 might induce changes in cell migration and adhesion.

There were also changes in tumour invasiveness of treated tumours. This is supported by various studies that also demonstrate the inhibitory effect of cannabinoids on invasion in other tumour types. (21,47,48)

Our experiments regarding neoangiogenesis provide contradictory evidence. On the one hand, the CAM assay with tumour cell suspension supernatant showed that tumour cells treated with WIN-55,212-2 *in vitro* produce angiogenetic factors, while on the other hand, the three *in vivo* assessments of tumour neoangiogenesis showed that WIN-55,212-2 reduces neoangiogenesis in treated tumours. However, the macroscopical neoangiogenesis analyses and scores might be a better method to evaluate neoangiogenesis, since those CAM assays resemble *in vivo* conditions more closely than the CAM assay with supernatant retrieved *in vitro*. This discrepancy between *in vitro* and *in vivo* conditions could be caused by the difference of cell growing in a suspension as in cell culture conditions and of cells growing as tumour tissue, allowing interactions between cells, and between cells and the surrounding tissue. Additionally, the inhibitory effect of cannabinoids on neoangiogenesis is supported by the literature (21,28,40,42,43,47), while the increase of neoangiogenesis is not.

Treatment with WIN-55,212-2 downregulated Id-1. As Id-1 regulates normal cell proliferation by initiating DNA synthesis and the G1 to S phase progression, this might indicate that the effects of WIN-55,212-2 regarding cell proliferation might be mediated by the downregulations of Id-1.(70,71) Additionally, we showed that Id-1 overexpression decreases the susceptibility to WIN-55,212-2 in terms of cell growth, which means that Id-1 plays a protective role against cannabinoid treatment in P-STS cells. This effect only applied to cell growth and not to cell viability.

Although our study demonstrates that WIN-55,212-2 has a variety of anticarcinogenic effects on the small intestine neuroendocrine cancer cell line P-STS, further studies are needed to investigate cannabinoids as a therapeutic approach in neuroendocrine cancer. On the one hand, we need to explore the effects of other cannabinoids and their derivatives on P-STS cells, while on the other hand, it is necessary to confirm the results in other NET cell lines. Furthermore, studies with different *in vivo* tumour models need to be carried out to verify these effects.

5 References

1. Gustafsson BI, Kidd M, Modlin IM. Neuroendocrine tumors of the diffuse neuroendocrine system. Curr Opin Oncol [Internet]. 2008 [cited 2016 Mar 6];20(1):1–12. Available from: http://www.ncbi.nlm.nih.gov/pubmed/18043250
2. Langley K. The neuroendocrine concept of today. Ann N Y Acad Sci [Internet]. 1994;15(733):1–17. Available from: http://www.ncbi.nlm.nih.gov/pubmed/?term=7978856
3. Day R, Salzet M. Neuroendocrine phenotype, cellular plasticity and the search for genetic switches : Rede fi ning the diffuse neuroendocrine system. Neuroendocrinol Lett Nos Neuroendocrinol Lett [Internet]. 2002 [cited 2016 Mar 6];23(2356):447–51. Available from: http://www.ncbi.nlm.nih.gov/pubmed/?term=12500170
4. DeLellis RA. The neuroendocrine system and its tumors: an overview. [Internet]. American Journal of Clinical Pathology. 2001 [cited 2016 Mar 7]. p. S5–16. Available from: http://www.ncbi.nlm.nih.gov/pubmed/11993690
5. Berge T, Linell F. Carcinoid tumours. Frequency in a defined population during a 12-year period. Acta Pathol Microbiol Scand A [Internet]. 1976 Jul [cited 2016 Mar 7];84(4):322–30. Available from: http://www.ncbi.nlm.nih.gov/pubmed/961424
6. Zikusoka MN, Kidd M, Eick G, Latich I, Modlin IM. The molecular genetics of gastroenteropancreatic neuroendocrine tumors [Internet]. Cancer. 2005 [cited 2016 Mar 8]. p. 2292–309. Available from: http://www.ncbi.nlm.nih.gov/pubmed/16258976
7. Öberg K, Castellano D. Current knowledge on diagnosis and staging of neuroendocrine tumors. Cancer Metastasis Rev [Internet]. 2011 Mar [cited 2016 Mar 8];30(SUPPL. 1):3–7. Available from: http://www.ncbi.nlm.nih.gov/pubmed/21311954
8. Oberg K. Neuroendocrine gastrointestinal tumors-a condensed overview of diagnosis and treatment. Ann Oncol [Internet]. 1999 [cited 2016 Mar 10];10 Suppl 2:S3–8. Available from: http://www.ncbi.nlm.nih.gov/pubmed/10399026
9. Niederle B, Pape U-F, Costa F, Gross D, Kelestimur F, Knigge U, et al. ENETS Consensus Guidelines Update for Neuroendocrine Neoplasms of the Jejunum and Ileum. Neuroendocrinology [Internet]. 2016 [cited 2016 Apr 1];103(2):125–38. Available from: http://www.ncbi.nlm.nih.gov/pubmed/26758972
10. Reubi JC, Waser B. Concomitant expression of several peptide receptors in neuroendocrine tumours: molecular basis for in vivo multireceptor tumour targeting. Eur J Nucl Med Mol Imaging [Internet]. 2003 May [cited 2016 Mar 10];30(5):781–93. Available from: http://www.ncbi.nlm.nih.gov/pubmed/12707737
11. Modlin IM, Latich I, Kidd M, Zikusoka M, Eick G. Therapeutic options for gastrointestinal carcinoids. Clin Gastroenterol Hepatol [Internet]. 2006 May [cited 2016 Mar 10];4(5):526–47. Available from: http://www.ncbi.nlm.nih.gov/pubmed/16630755
12. Bruns C, Lewis I, Briner U, Meno-Tetang G, Weckbecker G. SOM230: A novel somatostatin peptidomimetic with broad somatotropin release inhibiting factor

(SRIF) receptor binding and a unique antisecretory profile. Eur J Endocrinol [Internet]. 2002 May [cited 2016 Mar 10];146(5):707–16. Available from: http://www.ncbi.nlm.nih.gov/pubmed/11980628
13. Schupak K, Wallner K. The role of radiation therapy in the treatment of locally unresectable or metastatic carcinoid tumors. Int J Radiat Oncol [Internet]. 1991 Mar [cited 2016 Mar 10];20(1991):489–95. Available from: http://www.ncbi.nlm.nih.gov/pubmed/1995534
14. Kwekkeboom DJ, Mueller-Brand J, Paganelli G, Anthony LB, Pauwels S, Kvols LK, et al. Overview of results of peptide receptor radionuclide therapy with 3 radiolabeled somatostatin analogs. J Nucl Med [Internet]. 2005 Jan [cited 2016 Mar 10];46 Suppl 1:62S – 6S. Available from: http://www.ncbi.nlm.nih.gov/pubmed/15653653
15. Deiana S. Medical use of cannabis. Cannabidiol: A new light for schizophrenia? [Internet]. Drug Testing and Analysis. 2013 [cited 2016 Mar 13]. p. 46–51. Available from: http://www.ncbi.nlm.nih.gov/pubmed/23109356
16. Matsuda LA, Lolait SJ, Brownstein MJ, Young AC, Bonner TI. Structure of a cannabinoid receptor and functional expression of the cloned cDNA. Nature [Internet]. 1990 Aug 9 [cited 2016 Mar 13];346(6284):561–4. Available from: http://www.ncbi.nlm.nih.gov/pubmed/2165569
17. Mackie K. Distribution of cannabinoid receptors in the central and peripheral nervous system. Handb Exp Pharmacol [Internet]. 2005 [cited 2016 Mar 13];168(168):299–325. Available from: http://www.ncbi.nlm.nih.gov/pubmed/16596779
18. Munro S, Thomas KL, Abu-Shaar M. Molecular characterization of a peripheral receptor for cannabinoids. Nature [Internet]. 1993 Sep 2 [cited 2016 Mar 13];365(6441):61–5. Available from: http://www.ncbi.nlm.nih.gov/pubmed/7689702
19. Sun Y, Alexander SP, Garle MJ, Gibson CL, Hewitt K, Murphy SP, et al. Cannabinoid activation of PPAR alpha; a novel neuroprotective mechanism. Br J Pharmacol [Internet]. 2007 Nov [cited 2016 Mar 13];152(5):734–43. Available from: http://www.ncbi.nlm.nih.gov/pubmed/17906680
20. Adams R. Marihuana. Bull N Y Acad Med [Internet]. 1942 Jan [cited 2016 Mar 13];18(1):705–30. Available from: http://www.ncbi.nlm.nih.gov/pubmed/?term=19312292
21. Chakravarti B, Ravi J, Ganju RK. Cannabinoids as therapeutic agents in cancer: current status and future implications. Oncotarget [Internet]. 2014 Aug 15 [cited 2016 Mar 13];5(15):5852–72. Available from: http://www.ncbi.nlm.nih.gov/pubmed/25115386
22. Di Marzo V, Melck D, De Petrocellis L, Bisogno T. Cannabimimetic fatty acid derivatives in cancer and inflammation [Internet]. Prostaglandins and Other Lipid Mediators. 2000 [cited 2016 Mar 13]. p. 43–61. Available from: http://www.ncbi.nlm.nih.gov/pubmed/10785541
23. Christie MJ, Vaughan CW. Neurobiology Cannabinoids act backwards. Nature [Internet]. 2001 Mar 29 [cited 2016 Mar 13];410(6828):527–30. Available from: http://www.ncbi.nlm.nih.gov/pubmed/11279473
24. Devane W, Hanus L, Breuer A, Pertwee R, Stevenson L, Griffin G, et al. Isolation and structure of a brain constituent that binds to the cannabinoid receptor. Science (80-) [Internet]. 1992 Dec 18 [cited 2016 Mar 13];258(5090):1946–9. Available from: http://www.ncbi.nlm.nih.gov/pubmed/1470919

25. Mechoulam R, Ben-Shabat S, Hanus L, Ligumsky M, Kaminski NE, Schatz AR, et al. Identification of an endogenous 2-monoglyceride, present in canine gut, that binds to cannabinoid receptors. Biochem Pharmacol [Internet]. 1995 Jun 29 [cited 2016 Mar 13];50(1):83–90. Available from: http://www.ncbi.nlm.nih.gov/pubmed/7605349
26. Xian XS, Park H, Choi MG, Park JM. Cannabinoid receptor agonist as an alternative drug in 5-fluorouracil-resistant gastric cancer cells. Anticancer Res [Internet]. 2013 Jun [cited 2016 Mar 22];33(6):2541–7. Available from: http://www.ncbi.nlm.nih.gov/pubmed/23749906
27. Xian XS, Park H, Cho YK, Lee IS, Kim SW, Choi MG, et al. Effect of a synthetic cannabinoid agonist on the proliferation and invasion of gastric cancer cells. J Cell Biochem [Internet]. 2010 May 15 [cited 2016 Mar 22];110(2):321–32. Available from: http://www.ncbi.nlm.nih.gov/pubmed/20336665
28. Ranger JJ, Levy DE, Shahalizadeh S, Hallett M, Muller WJ. Identification of a Stat3-dependent transcription regulatory network involved in metastatic progression. Cancer Res [Internet]. 2009 Sep 1 [cited 2016 Mar 13];69(17):6823–30. Available from: http://www.ncbi.nlm.nih.gov/pubmed/19690134
29. De Petrocellis L, Melck D, Palmisano A, Bisogno T, Laezza C, Bifulco M, et al. The endogenous cannabinoid anandamide inhibits human breast cancer cell proliferation. Proc Natl Acad Sci U S A [Internet]. 1998 Jul 7 [cited 2016 Mar 13];95(14):8375–80. Available from: http://www.ncbi.nlm.nih.gov/pubmed/9653194
30. Melck D, De Petrocellis L, Orlando P, Bisogno T, Laezza C, Bifulco M, et al. Suppression of nerve growth factor Trk receptors and prolactin receptors by endocannabinoids leads to inhibition of human breast and prostate cancer cell proliferation. Endocrinology [Internet]. 2000 Jan [cited 2016 Mar 13];141(1):118–26. Available from: http://www.ncbi.nlm.nih.gov/pubmed/10614630
31. Melck D, Rueda D, Galve-Roperh I, De Petrocellis L, Guzmán M, Di Marzo V. Involvement of the cAMP/protein kinase A pathway and of mitogen-activated protein kinase in the anti-proliferative effects of anandamide in human breast cancer cells. FEBS Lett [Internet]. 1999 Dec 17 [cited 2016 Mar 13];463(3):235–40. Available from: http://www.ncbi.nlm.nih.gov/pubmed/10606728
32. Caffarel MM, Moreno-Bueno G, Cerutti C, Palacios J, Guzman M, Mechta-Grigoriou F, et al. JunD is involved in the antiproliferative effect of Delta9-tetrahydrocannabinol on human breast cancer cells. Oncogene [Internet]. 2008 Aug 28 [cited 2016 Mar 13];27(37):5033–44. Available from: http://www.ncbi.nlm.nih.gov/pubmed/18454173
33. Qamri Z, Preet A, Nasser MW, Bass CE, Leone G, Barsky SH, et al. Synthetic cannabinoid receptor agonists inhibit tumor growth and metastasis of breast cancer. Mol Cancer Ther [Internet]. 2009 Nov [cited 2016 Mar 13];8(11):3117–29. Available from: http://www.ncbi.nlm.nih.gov/pubmed/19887554
34. Nithipatikom K, Endsley MP, Isbell MA, Falck JR, Iwamoto Y, Hillard CJ, et al. 2-Arachidonoylglycerol: A novel inhibitor of androgen-independent prostate cancer cell invasion. Cancer Res [Internet]. 2004 Dec 15 [cited 2016 Mar 14];64(24):8826–30. Available from: http://www.ncbi.nlm.nih.gov/pubmed/15604240
35. Sarfaraz S, Afaq F, Adhami VM, Mukhtar H. Cannabinoid receptor as a novel

target for the treatment of prostate cancer. Cancer Res [Internet]. 2005 Mar 1 [cited 2016 Mar 14];65(5):1635–41. Available from: http://www.ncbi.nlm.nih.gov/pubmed/15753356
36. Velasco L, Ruiz L, Sánchez MG, Díaz-Laviada I. Δ9-tetrahydrocannabinol increases nerve growth factor production by prostate PC-3 cells: Involvement of CB1 cannabinoid receptor and Raf-1. Eur J Biochem [Internet]. 2001 Dec 22 [cited 2016 Mar 14];268(3):531–5. Available from: http://www.ncbi.nlm.nih.gov/pubmed/?term=11168391
37. Sarfaraz S, Afaq F, Adhami VM, Malik A, Mukhtar H. Cannabinoid receptor agonist-induced apoptosis of human prostate cancer cells LNCaP proceeds through sustained activation of ERK1/2 leading to G1 cell cycle arrest. J Biol Chem [Internet]. 2006 Dec 22 [cited 2016 Mar 14];281(51):39480–91. Available from: http://www.ncbi.nlm.nih.gov/pubmed/17068343
38. Sánchez MG, Sánchez AM, Ruiz-Llorente L, Díaz-Laviada I. Enhancement of androgen receptor expression induced by (R)-methanandamide in prostate LNCaP cells. FEBS Lett [Internet]. 2003 [cited 2016 Mar 14];555(3):561–6. Available from: http://www.ncbi.nlm.nih.gov/pubmed/?term=14675774
39. Mimeault M, Pommery N, Wattez N, Bailly C, Hénichart J-P. Anti-proliferative and apoptotic effects of anandamide in human prostatic cancer cell lines: implication of epidermal growth factor receptor down-regulation and ceramide production. Prostate [Internet]. 2003 Jun 15 [cited 2016 Mar 14];56(1):1–12. Available from: http://www.ncbi.nlm.nih.gov/pubmed/12746841
40. Olea-Herrero N, Vara D, Malagarie-Cazenave S, Díaz-Laviada I. Inhibition of human tumour prostate PC-3 cell growth by cannabinoids R(+)-Methanandamide and JWH-015: involvement of CB2. Br J Cancer [Internet]. 2009 Sep 15 [cited 2016 Mar 14];101(6):940–50. Available from: http://www.ncbi.nlm.nih.gov/pmc/articles/PMC2743360/
41. Sreevalsan S, Joseph S, Jutooru I, Chadalapaka G, Safe SH. Induction of Apoptosis by Cannabinoids in Prostate and Colon Cancer Cells Is Phosphatase Dependent. [cited 2016 Mar 14]; Available from: http://www.ncbi.nlm.nih.gov/pmc/articles/PMC3280884/
42. Thapa D, Lee JS, Heo SW, Lee YR, Kang KW, Kwak MK, et al. Novel hexahydrocannabinol analogs as potential anti-cancer agents inhibit cell proliferation and tumor angiogenesis. Eur J Pharmacol [Internet]. 2011 Jan 10 [cited 2016 Mar 14];650(1):64–71. Available from: http://www.ncbi.nlm.nih.gov/pubmed/20950604
43. Blazquez C, Carracedo A, Barrado L, Real PJ, Fernandez-Luna JL, Velasco G, et al. Cannabinoid receptors as novel targets for the treatment of melanoma. FASEB J [Internet]. 2006 Dec [cited 2016 Mar 14];20(14):2633–5. Available from: http://www.ncbi.nlm.nih.gov/pubmed/17065222
44. Massi P, Vaccani A, Bianchessi S, Costa B, Macchi P, Parolaro D. The non-psychoactive cannabidiol triggers caspase activation and oxidative stress in human glioma cells. Cell Mol Life Sci [Internet]. 2006 Sep [cited 2016 Mar 14];63(17):2057–66. Available from: http://www.ncbi.nlm.nih.gov/pubmed/16909207
45. Takeda S, Okajima S, Miyoshi H, Yoshida K, Okamoto Y, Okada T, et al. Cannabidiolic acid, a major cannabinoid in fiber-type cannabis, is an inhibitor of MDA-MB-231 breast cancer cell migration. Toxicol Lett [Internet]. 2012 Nov 15 [cited 2016 Mar 14];214(3):314–9. Available from: http://www.ncbi.nlm.nih.gov/pubmed/22963825

46. Hall A. The cytoskeleton and cancer [Internet]. Cancer and Metastasis Reviews. 2009 [cited 2016 Mar 14]. p. 5–14. Available from: http://www.ncbi.nlm.nih.gov/pubmed/19153674
47. Massi P, Solinas M, Cinquina V, Parolaro D. Cannabidiol as potential anticancer drug. Br J Clin Pharmacol [Internet]. 2013 Feb [cited 2016 Mar 14];75(2):303–12. Available from: http://doi.wiley.com/10.1111/j.1365-2125.2012.04298
48. Ramer R, Hinz B. Inhibition of cancer cell invasion by cannabinoids via increased expression of tissue inhibitor of matrix metalloproteinases-1. J Natl Cancer Inst [Internet]. 2008 Jan 2 [cited 2016 Mar 14];100(1):59–69. Available from: http://www.ncbi.nlm.nih.gov/pubmed/18159069
49. McAllister SD, Murase R, Christian RT, Lau D, Zielinski AJ, Allison J, et al. Pathways mediating the effects of cannabidiol on the reduction of breast cancer cell proliferation, invasion, and metastasis. Breast Cancer Res Treat [Internet]. 2011 Aug [cited 2016 Mar 14];129(1):37–47. Available from: http://www.ncbi.nlm.nih.gov/pubmed/20859676
50. McAllister SD, Christian RT, Horowitz MP, Garcia A, Desprez P-Y. Cannabidiol as a novel inhibitor of Id-1 gene expression in aggressive breast cancer cells. Mol Cancer Ther [Internet]. 2007 Nov [cited 2016 Mar 14];6(11):2921–7. Available from: http://www.ncbi.nlm.nih.gov/pubmed/18025276
51. Gustafsson SB, Wallenius A, Zackrisson H, Popova D, Plym Forshell L, Jacobsson SOP. Effects of cannabinoids and related fatty acids upon the viability of P19 embryonal carcinoma cells. Arch Toxicol [Internet]. 2013 Nov [cited 2016 Mar 14];87(11):1939–51. Available from: http://www.ncbi.nlm.nih.gov/pubmed/23552853
52. Wong Y-C, Wang X, Ling M-T. Id-1 expression and cell survival. Apoptosis [Internet]. 2004 [cited 2016 Mar 14];9(3):279–89. Available from: http://www.ncbi.nlm.nih.gov/pubmed/15258459
53. Olson EN, Klein WH. bHLH factors in muscle development: Dead lines and commitments, what to leave in and what to leave out [Internet]. Genes and Development. 1994 [cited 2016 Mar 14]. p. 1–8. Available from: http://www.ncbi.nlm.nih.gov/pubmed/8288123
54. Kadesch T. Consequences of heteromeric interactions among helix-loop-helix proteins. Cell Growth Differ [Internet]. 1993 Jan [cited 2016 Mar 14];4(1):49–55. Available from: http://www.ncbi.nlm.nih.gov/pubmed/8424906
55. Benezra R, Davis RL, Lockshon D, Turner DL, Weintraub H. The protein Id: A negative regulator of helix-loop-helix DNA binding proteins. Cell [Internet]. 1990 Apr 6 [cited 2016 Mar 14];61(1):49–59. Available from: http://www.ncbi.nlm.nih.gov/pubmed/2156629
56. Perk J, Iavarone A, Benezra R. Id family of helix-loop-helix proteins in cancer. Nat Rev Cancer [Internet]. 2005 Aug [cited 2016 Mar 14];5(8):603–14. Available from: http://www.ncbi.nlm.nih.gov/pubmed/16034366
57. Norton JD, Deed RW, Craggs G, Sablitzky F. Id helix-loop-helix proteins in cell growth and differentiation [Internet]. Trends in Cell Biology. 1998 [cited 2016 Mar 14]. p. 58–65. Available from: http://www.ncbi.nlm.nih.gov/pubmed/9695810
58. Pesce S, Benezra R. The loop region of the helix-loop-helix protein Id1 is critical for its dominant negative activity. Mol Cell Biol [Internet]. 1993 [cited 2016 Mar 14];13(12):7874–80. Available from:

http://www.ncbi.nlm.nih.gov/pubmed/8247002
59. López-Rovira T, Chalaux E, Massagué J, Rosa JL, Ventura F. Direct binding of Smad1 and Smad4 to two distinct motifs mediates bone morphogenetic protein-specific transcriptional activation of Id1 gene. J Biol Chem [Internet]. 2002 Feb 1 [cited 2016 Mar 14];277(5):3176–85. Available from: http://www.ncbi.nlm.nih.gov/pubmed/11700304
60. Cubillo E, Diaz-Lopez A, Cuevas EP, Moreno-Bueno G, Peinado H, Montes A, et al. E47 and Id1 Interplay in Epithelial-Mesenchymal Transition. Ballestar E, editor. PLoS One [Internet]. 2013 Mar 26 [cited 2016 Mar 14];8(3):e59948. Available from: http://dx.plos.org/10.1371/journal.pone.0059948
61. Korchynskyi O, Ten Dijke P. Identification and functional characterization of distinct critically important bone morphogenetic protein-specific response elements in the Id1 promoter. J Biol Chem [Internet]. 2002 Feb 15 [cited 2016 Mar 14];277(7):4883–91. Available from: http://www.ncbi.nlm.nih.gov/pubmed/11729207
62. Hollnagel A, Oehlmann V, Heymer J, Rüther U, Nordheim A. Id genes are direct targets of bone morphogenetic protein induction in embryonic stem cells. J Biol Chem [Internet]. 1999 Jul 9 [cited 2016 Mar 14];274(28):19838–45. Available from: http://www.ncbi.nlm.nih.gov/pubmed/10391928
63. Kleinegger F. Role of ID-1 in “cancer stem-cell-ness” of the gastroenteropancreatic neuroendocrine tumor cell line P-STS. Technische Universität Graz; 2015.
64. Valdimarsdottir G, Goumans MJ, Rosendahl A, Brugman M, Itoh S, Lebrin F, et al. Stimulation of Id1 expression by bone morphogenetic protein is sufficient and necessary for bone morphogenetic protein-induced activation of endothelial cells. Circulation [Internet]. 2002;106(17):2263–70. Available from: http://www.ncbi.nlm.nih.gov/pubmed/12390958
65. Ruzinova MB, Benezra R. Id proteins in development, cell cycle and cancer. Trends Cell Biol [Internet]. 2003 Aug [cited 2016 Mar 14];13(8):410–8. Available from: http://www.ncbi.nlm.nih.gov/pubmed/12888293
66. Kebebew E, Treseler P a, Duh QY, Clark OH. The helix-loop-helix transcription factor, Id-1, is overexpressed in medullary thyroid cancer. Surgery [Internet]. 2000;128(6):952–7. Available from: http://www.ncbi.nlm.nih.gov/pubmed/11114629
67. Goldstein S. Replicative senescence: the human fibroblast comes of age. Science [Internet]. 1990 Sep 7 [cited 2016 Mar 14];249(4973):1129–33. Available from: http://www.ncbi.nlm.nih.gov/pubmed/2204114
68. Hara E, Smith R, Parry D, Tahara H, Stone S, Peters G. Regulation of p16CDKN2 expression and its implications for cell immortalization and senescence. Mol Cell Biol [Internet]. 1996 Mar [cited 2016 Mar 14];16(3):859–67. Available from: http://www.ncbi.nlm.nih.gov/pubmed/8622687
69. McConnell BB, Starborg M, Brookes S, Peters G. Inhibitors of cyclin-dependent kinases induce features of replicative senescence in early passage human diploid fibroblasts. Curr Biol [Internet]. 1998 Mar 12 [cited 2016 Mar 14];8(6):351–4. Available from: http://www.ncbi.nlm.nih.gov/pubmed/9512419
70. Tang J, Gordon GM, Müller MG, Dahiya M, Foreman KE. Kaposi’s sarcoma-associated herpesvirus latency-associated nuclear antigen induces expression of the helix-loop-helix protein Id-1 in human endothelial cells. J Virol [Internet]. 2003 May [cited 2016 Mar 14];77(10):5975–84. Available from:

http://www.ncbi.nlm.nih.gov/pubmed/12719589
71. Nickoloff BJ, Chaturvedi V, Bacon P, Qin JZ, Denning MF, Diaz MO. Id-1 delays senescence but does not immortalize keratinocytes. J Biol Chem [Internet]. 2000 Sep 8 [cited 2016 Mar 14];275(36):27501–4. Available from: http://www.ncbi.nlm.nih.gov/pubmed/10908559
72. Ouyang XS, Wang X, Ling M-T, Wong HL, Tsao SW, Wong YC. Id-1 stimulates serum independent prostate cancer cell proliferation through inactivation of p16(INK4a)/pRB pathway. Carcinogenesis [Internet]. 2002 May [cited 2016 Mar 14];23(5):721–5. Available from: http://www.ncbi.nlm.nih.gov/pubmed/12016143
73. Ling M-T, Wang X, Ouyang X-S, Lee TKW, Fan T-Y, Xu K, et al. Activation of MAPK signaling pathway is essential for Id-1 induced serum independent prostate cancer cell growth. Oncogene [Internet]. 2002 Dec 5 [cited 2016 Mar 14];21(55):8498–505. Available from: http://www.nature.com/doifinder/10.1038/sj.onc.1206007
74. Kim D, Peng XC, Sun XH. Massive apoptosis of thymocytes in T-cell-deficient Id1 transgenic mice. Mol Cell Biol [Internet]. 1999 Dec [cited 2016 Mar 23];19(12):8240–53. Available from: http://www.ncbi.nlm.nih.gov/pubmed/10567549
75. Parrinello S, Lin CQ, Murata K, Itahana Y, Singh J, Krtolica A, et al. Id-1, ITF-2, and Id-2 Comprise a Network of Helix-Loop-Helix Proteins That Regulate Mammary Epithelial Cell Proliferation, Differentiation, and Apoptosis. J Biol Chem [Internet]. 2001 Oct 19 [cited 2016 Mar 23];276(42):39213–9. Available from: http://www.ncbi.nlm.nih.gov/pubmed/11498533
76. Ling M-T, Wang X, Ouyang X-S, Xu K, Tsao S-W, Wong Y-C. Id-1 expression promotes cell survival through activation of NF-kappaB signalling pathway in prostate cancer cells. Oncogene [Internet]. 2003 Jul 17 [cited 2016 Mar 23];22(29):4498–508. Available from: http://www.ncbi.nlm.nih.gov/pubmed/12881706
77. Desprez PY, Lin CQ, Thomasset N, Sympson CJ, Bissell MJ, Campisi J. A novel pathway for mammary epithelial cell invasion induced by the helix-loop-helix protein Id-1. Mol Cell Biol [Internet]. 1998 Aug [cited 2016 Mar 23];18(8):4577–88. Available from: http://www.ncbi.nlm.nih.gov/pubmed/9671467
78. Lyden D, Young AZ, Zagzag D, Yan W, Gerald W, O'Reilly R, et al. Id1 and Id3 are required for neurogenesis, angiogenesis and vascularization of tumour xenografts. Nature [Internet]. 1999 Oct 14 [cited 2016 Mar 23];401(October):670–7. Available from: http://www.ncbi.nlm.nih.gov/pubmed/10537105
79. Lyden D, Hattori K, Dias S, Costa C, Blaikie P, Butros L, et al. Impaired recruitment of bone-marrow-derived endothelial and hematopoietic precursor cells blocks tumor angiogenesis and growth. Nat Med [Internet]. 2001 Nov [cited 2016 Mar 23];7(11):1194–201. Available from: http://www.ncbi.nlm.nih.gov/pubmed/11689883
80. Volpert O V, Pili R, Sikder HA, Nelius T, Zaichuk T, Morris C, et al. Id1 regulates angiogenesis through transcriptional repression of thrombospondin-1. Cancer Cell [Internet]. 2002 Dec [cited 2016 Mar 23];2(6):473–83. Available from: http://www.ncbi.nlm.nih.gov/pubmed/12498716
81. Ruzinova MB, Schoer RA, Gerald W, Egan JE, Pandolfi PP, Rafii S, et al. Effect of angiogenesis inhibition by Id loss and the contribution of bone-

marrow-derived endothelial cells in spontaneous murine tumors. Cancer Cell [Internet]. 2003 Oct [cited 2016 Mar 23];4(4):277–89. Available from: http://www.ncbi.nlm.nih.gov/pubmed/14585355
82. Pfragner R, Behmel A, Höger H, Beham A, Ingolic E, Stelzer I, et al. Establishment and characterization of three novel cell lines - P-STS, L-STS, H-STS - Derived from a human metastatic midgut carcinoid. Anticancer Res [Internet]. 2009;29(6):1951–61. Available from: www.ncbi.nlm.nih.gov/pubmed/19528452
83. Tocris. WIN-55,212-2 mesylate [Internet]. 2006 [cited 2016 Mar 5]. Available from: https://www.tocris.com/dispprod.php?ItemId=1995
84. Sigma Aldrich. TRI reagent protocol [Internet]. User manual - sigma aldrich. 2014 [cited 2016 Mar 5]. Available from: http://www.sigmaaldrich.com/technical-documents/protocols/biology/tri-reagent.html
85. Lee JTY, Cheung KMC, Leung VYL. Extraction of RNA from tough tissues with high proteoglycan content by cryosection, second phase separation and high salt precipitation. J Biol Methods [Internet]. 2015 Jun 21 [cited 2016 Mar 5];2(2):20. Available from: http://www.jbmethods.org/jbm/article/view/40
86. Locklin RM, Riggs BL, Hicok KC, Horton HF, Byrne MC, Khosla S. Assessment of gene regulation by bone morphogenetic protein 2 in human marrow stromal cells using gene array technology. J Bone Miner Res [Internet]. 2001 Dec [cited 2016 Mar 25];16(12):2192–204. Available from: http://www.ncbi.nlm.nih.gov/pubmed/11760832
87. Hölzl M. Identification and characterisation of neuroendocrine cancer stem cells in P-STS cell line. Technische Universität Graz; 2014.
88. Scarfe System. CASY Cell Counters and Analyzer Systems [Internet]. 2003 [cited 2016 Mar 5]. Available from: http://www.rjmsales.com/casy.htm
89. GmbH RD. Cell Proliferation Reagent WST-1 [Internet]. Journal of Chemical Information and Modeling. Mannheim; 2013. Available from: http://www.sigmaaldrich.com/content/dam/sigma-aldrich/docs/Roche/Bulletin/1/cellprorobul.pdf
90. Cooperation P. Caspase Glo 3/7 assay [Internet]. Technical bulletin. 2015 [cited 2016 Mar 5]. Available from: https://at.promega.com/~/media/files/resources/protocols/technical bulletins/101/caspase-glo 3 7 assay protocol.pdf
91. Lopez F, Belloc F, Lacombe F, Dumain P, Reiffers J, Bernard P, et al. Modalities of synthesis of Ki67 antigen during the stimulation of lymphocytes. Cytometry [Internet]. 1991 [cited 2016 Mar 5];12(1):42–9. Available from: http://www.ncbi.nlm.nih.gov/pubmed/1999122
92. Abcam. Direct vs indirect immunofluorescence [Internet]. 2014 [cited 2016 Mar 5]. Available from: http://www.abcam.com/secondary-antibodies/direct-vs-indirect-immunofluorescence
93. abcam. In situ BrdU-Red DNA Fragmentation (TUNEL) Assay Kit [Internet]. abcam instruction manual. 2014 [cited 2016 Mar 5]. Available from: http://www.abcam.com/ps/products/66/ab66110/documents/ab66110 In situ BrdU_Red DNA Fragmentation Assay Kit Protocol v5 (website).pdf
94. R&D Systems. TACS-XL in situ apoptosis detection kit [Internet]. [cited 2016 Mar 5]. Available from: https://www.rndsystems.com/products/tacs-xl-in-situ-apoptosis-detection-kit--tacs-blue_4828-30-bk
95. Leng T, Miller JM, Bilbao K V, Palanker D V, Huie P, Blumenkranz MS. The

chick chorioallantoic membrane as a model tissue for surgical retinal research and simulation. Retina [Internet]. 2004 [cited 2016 Mar 5];24(3):427–34. Available from: http://www.ncbi.nlm.nih.gov/pubmed/15187666
96. Azoitei N, Becher A, Steinestel K, Rouhi A, Diepold K, Genze F, et al. PKM2 promotes tumor angiogenesis by regulating HIF-1α through NF-κB activation. Mol Cancer [Internet]. 2016 [cited 2016 Mar 5];15(1):3. Available from: http://www.ncbi.nlm.nih.gov/pubmed/26739387
97. Deryugina EI, Quigley JP. Chapter 2 Chick Embryo Chorioallantoic Membrane Models to Quantify Angiogenesis Induced by Inflammatory and Tumor Cells or Purified Effector Molecules [Internet]. Methods in Enzymology. 2008 [cited 2016 Mar 5]. p. 21–41. Available from: http://www.ncbi.nlm.nih.gov/pubmed/19007659
98. Ribatti D, Nico B, Vacca A, Presta M. The gelatin sponge-chorioallantoic membrane assay. Nat Protoc [Internet]. 2006 [cited 2016 Mar 5];1(1):85–91. Available from: http://www.ncbi.nlm.nih.gov/pubmed/17406216
99. Ellert-Miklaszewska A, Kaminska B, Konarska L. Cannabinoids down-regulate PI3K/Akt and Erk signalling pathways and activate proapoptotic function of Bad protein. Cell Signal [Internet]. 2005 Jan [cited 2016 Mar 17];17(1):25–37. Available from: http://www.ncbi.nlm.nih.gov/pubmed/15451022
100. Gustafsson K, Christensson B, Sander B, Flygare J. Cannabinoid receptor-mediated apoptosis induced by R(+)-methanandamide and Win55,212-2 is associated with ceramide accumulation and p38 activation in mantle cell lymphoma. Mol Pharmacol [Internet]. 2006 Nov [cited 2016 Mar 23];70(5):1612–20. Available from: http://www.ncbi.nlm.nih.gov/pubmed/16936228
101. Promega. Caspase-Glo 3/7 Assay [Internet]. 2015 [cited 2016 Mar 23]. Available from: https://ita.promega.com/~/media/files/resources/protocols/technical bulletins/101/caspase-glo 3 7 assay protocol.pdf
102. Blázquez C, Casanova ML, Planas A, Gómez Del Pulgar T, Villanueva C, Fernández-Aceñero MJ, et al. Inhibition of tumor angiogenesis by cannabinoids. FASEB J [Internet]. 2003 Mar [cited 2016 Mar 23];17(3):529–31. Available from: http://www.ncbi.nlm.nih.gov/pubmed/12514108

6 Appendix

6.1 Buffer recipes

1x PBS (pH 7,4)	
NaCl	8 g
KCl	0.3 g
KH_2PO_4	2 mg
Na_2HPO_4•2 H_2O	10 mg

1x TBS-T (pH 7.4)	
NaCl	8.8 g
KCl	0.2 g
TRIS base	3.0 g
Tween® 20	1 ml

6.2 Anticarcinogenic effects of cannabinoids

Cannabinoids	**Anticarcinogenic effect and its mechanism of action**
Anandamide	1)Breast cancer: (blocks G1 - S phase transition)-Regulates Raf- 1/ERK/MAP pathway, Wnt/β catenin signalling 2)Prostate cancer: Regulates EGFR pathway
THC	1)Breast cancer: (block G2 - M phase transition)- Activates the transcription factor JunD Anti-tumor action in MMTV-neu mice via inhibition of AKT Anti-invasive effect-modulate MMP-2/MMP-9 pathway 2)Prostate cancer:PI-3/AKT and Raf-1/ERK1/2 pathway Mitogenic effect at low doses. 3)Lung cancer: ERK1/2, JNK and AKT pathway Mitogenic effect at low doses.

Cannabinoids	Anticarcinogenic effect and its mechanism of action
	4)Glioma: MMP-2pathway, ER stress mediated autophagy 5)Lymphoma: MAPK/ERK pathway
2-AG	1)Breast cancer: Suppression of nerve growth factor Trk receptors and prolactin receptors Prostate cancer: NF-κB/cyclin D and cyclin E, Suppression of nerve growth factor Trk receptors and prolactin receptors. 2)Glioma: Inhibition Ca(2+) influx 3)Bone cancer: Attenuates mechanical hyperalgesia
HU120	1)Prostate cancer: AKT pathway
WIN-55,212-2	1)Breast cancer: Regulates COX-2/PGE2 signalling pathway 2)Prostate cancer: Sustained activation of ERK1/2 3)Skin cancer: Inhibits pro-angiogenic growth factor, AKT and pRB pathway 4)Glioma: Ceramide and NF-Kb pathway 5)Lymphoma: Ceramide and p38 pathway
R-(+)-MET	1)Breast cancer: decreased phosphorylation of focal adhesion–associated protein kinase and Src and tyrosine kinases involved in migration and adhesion 2)Prostate cancer: mitogenic effect at low dose
JWH-133	1)Breast cancer: inhibition of AKT-Regulate COX-2/PGE2 signalling pathway 2)Lung cancer: MMPs pathway 3)Skin cancer: G1 arrest-AKT pathway

Cannabinoids	Anticarcinogenic effect and its mechanism of action
Met-F-AEA	1)Breast cancer: S phase cell cycle arrest Regulates FAK/Src and RhoA-ROCK pathways
JWH-015	1)Breast cancer: CXCR-4/CXCL12 pathway 2)Prostate cancer: JNK/AKT signalling pathway
Δ^9-THC	1)Breast cancer: mitogenic effect in cells expressing low levels of CB1/CB2 receptors. 2)Prostate cancer: PI3K/Akt and Raf-1/ERK1/2 pathway Mitogenic at low doses 3)Lung cancer: EGFR/ERK1/2, c-Jun-NH2-kinase1/2, and Akt pathway. Mitogenic at low doses 4)Glioma: MMP-2 pathway
CBD	1)Breast cancer: ER stress/ERK and reactive oxygen species (ROS) pathways 2)Prostate cancer: ERK1/2 and AKT pathways 3)Lung cancer: upregulation of TIMP-1 Cox-2 and PPAR-γ regulation 4)Cervical cancer: Upregulation of TIMP1
CBDA	1)Breast cancer: PKA/RhoA pathway
AME1241	1)Bone cancer: Anti-nociception

Table 13: Overwiev of anticarcinogenic effects of various cannabinoids.(21)